8-2005

An Investigation on Phase Behavior and Orientation Factor of Electrospun Nanofibers

Kai Feng
University of Tennessee - Knoxville

To the Graduate Council:

I am submitting herewith a thesis written by Kai Feng entitled "An Investigation on Phase Behavior and Orientation Factor of Electrospun Nanofibers." I have examined the final electronic copy of this thesis for form and content and recommend that it be accepted in partial fulfillment of the requirements for the degree of Master of Science, with a major in Polymer Engineering.

Kevin M. Kit, Major Professor

We have read this thesis and recommend its acceptance:

Bin Hu, Joseph. E. Spruiell

Accepted for the Council:
Carolyn R. Hodges

Vice Provost and Dean of the Graduate School

(Original signatures are on file with official student records.)

To the Graduate Council:

I am submitting herewith a thesis written by Kai Feng entitled "An investigation on phase behavior and orientation factor of electrospun nanofibers". I have examined the final electronic copy of this thesis for form and content and recommend that it be accepted in partial fulfillment of the requirements for the degree of Master of Science, with a major in Polymer Engineering.

Kevin M. Kit

Major Professor

We have read this thesis and recommend its acceptance:

Bin Hu

Joseph. E. Spruiell

Accepted for the Council:

Anne Mayhew

Vice Chancellor and
Dean of Graduate Studies

(Original signatures are on file with official student records.)

An investigation on phase behavior and orientation factor of electrospun nanofibers

A Thesis Presented for the Master of Science Degree

The University of Tennessee, Knoxville

Kai Feng

August 2005

Dedicated to

My parents

Feng, Guoren and Yao, Yuanyong

Acknowledgements

The author wishes to express a sincere gratitude to his major advisor, Dr. Kevin M. Kit for his continuous encouragement, support and guidance throughout the course of this project. The gratitude is also extended to his committee advisors: Dr. Bin Hu and Dr. Joseph E. Spruiell.

The author also thanks Greg Jones and Dr. Dunlop for their help in handling of SEM and TEM. The author also thanks Luo, Xiaoyu and Chris Stephens for their help in handling of FTIR. The author also thanks each one in Material Science and Engineering department for their support at different stages of this project. This project submitted as thesis work for Master of Science diploma was funded in part by Dupont Textiles and Tnteriors.

Abstract

Electrospinning is a straightforward method to produce polymer nanofibers (10-500nm in diameter) from polymer solutions and melts. When the applied electrical force at the surface of polymer solution or polymer melt overcomes its surface tension, a charged jet is ejected, which travels towards a grounded target. Solvent evaporates and nanofibers form on the target surface. In this thesis, an investigation on phase behavior of the nanofibers electrospun from polymer blends and orientation factors within nanofibers electrospun from both single polymer solution and polymer blends were conducted.

Single-phase nanofibers were produced by electrospinning blends of polycarbonate (PC) and polyvinylchloride (PVC) dissolved in a mixture of tetrahydrofuran (THF) and N,N-dimethylformamide (DMF). The phase behavior of the as-spun fibers was determined by a dynamic mechanical analyzer (DMA). Only one glass transition temperature was obtained which indicates single-phase structure. The surface morphology of the as-spun fibers was observed by scanning electron microscopy (SEM). The as-spun fibers were annealed for different times and same type of DMA test was performed on the fibers and there appeared two separate glass transition temperatures, which demonstrated phase separation. The annealed fibers were also stained by ruthenium tetroxide (RuO4). The resulting phase morphology of the fiber was examined by transmission electron microscopy (TEM). The TEM images demonstrated that by controlling the annealing of the as-spun fibers, a specific fiber surface morphology could be accessed.

Nanofiber mats were produced by directly electrospinning nylon 66 dissolved in formic acid and PVC and PVC blend dissolved in a solvent mixture of THF and DMF onto a rotating metal wheel. SEM and FTIR were used to investigate the orientation of the sample. In order to determine molecular orientation within the fibers with respect to the fiber axis, molecular orientation with respect to fiber winding direction obtained by FTIR was divided by fiber orientation measured manually from the SEM pictures. The relationship between the molecular orientation of the electrospun nanofibers and three electrospinning process parameters were determined. The molecular orientation will increase if the wheel speed increases due to the increase of the mechanical tensile drawing force when the nanofibers hit the rotating wheel. The molecular orientation decreases if the applied voltage increases due to the decrease of the same mechanical tensile drawing force. High molecular weight polymers had higher molecular orientation when electrospun into nanofibers because the higher molecular polymers have greater relaxation time to preserve more orientation obtained. The mechanical properties of the oriented non-woven nanofibers mats were studied by DMA. It seems that the mechanical properties follows the same trend of the overall orientation with respect to fiber winding direction, not just the molecular orientation within the fiber and with respect to fiber axis. The information available in the literature was considered together with the experimental results to explain the phase behavior of the nanofiber electrospun from polymer blends and molecular orientation factors within the nanofibers.

Table of Contents

List of Tables

List of Figures

Chapter 1 Introduction

1.1 History

The fundamental idea of the term "electrospinning" has existed in the literature for more than 60 years. Formhals set up an experiment for producing polymer filaments using electrostatic force and gained a series of patents from year 1934 to 1944. [**1-3**] A polymer solution was introduced to the electrical field by placing one electrode into solution and the other onto a collector. Thus, charged polymer solution jets ejected out of a metal spinnerette and evaporated and formed fibers onto the collector.

In the 1950s, Vonnegut and Neubauer succeeded in making approximately 0.1 mm electrified droplet streams by simple self-invented apparatus. Variable ac or dc potentials (5-10 Kv) were applied to water or liquids in capillaries and monodisperse aerosols were formed. [**4**] Three years later, by the similar experiment setup used by Vonnegut and Neubauer, Drozin found out that under certain conditions (high electrical potential and suitable solution viscosity), water and 12 other pure liquids could form aerosols consisting of uniform fine droplets from a capillary. Different stages of the dispersion were also captured. [**5**]

In the middle 1960s, Simons obtained a patent by using the electrical spinning process to produce lightweight, patterned, and textured non-woven polyurethane resin fabrics. The

negative electrode was connected to a grounded metal plate where fibers formed, while the positive one was immersed into the polyurethane in ketone solutions. [**6**]

Later, acrylic fibers with diameters in sub-micron range were electrospun by Baumgarten. The experiment setup started to mature and was used by later scientists and engineers. A high voltage was connected to a stainless steel capillary tube and the spinning drop was suspended from the capillary. Fibers were collected on the grounded metal screen.[**7**]

With a surging interest in nanotechnology since the 1980s, electrospinning, an efficient method to produce polymer nanofibers (10-500nm in diameter) from polymer solutions and melts, has gained much more attention. Those nanofibers possess some amazing characteristic like large surface area to volume ratio, flexibility in surface functionalities, and superior mechanical properties. The electrospinning process has advantages over traditional nanofiber fabrications like drawing, template sythesis, phase separation, and self assembly, one of which is the possibility to develop one-by-one continuous nanofibers from various polymers for mass production[**8**]. Because of these two reasons, electrospinning has found important applications in filtration and protective clothing [**9**], composite reinforcement [**10, 11**], sensors [**12-15**], electronic devices [**16**], and medical researches [**17-21**]. Application fields of US patents on electrospun nanofibers and potential applications of electrospun polymer nanofibers are illustrated in Figure 1.1 and Figure 1.2, respectively.

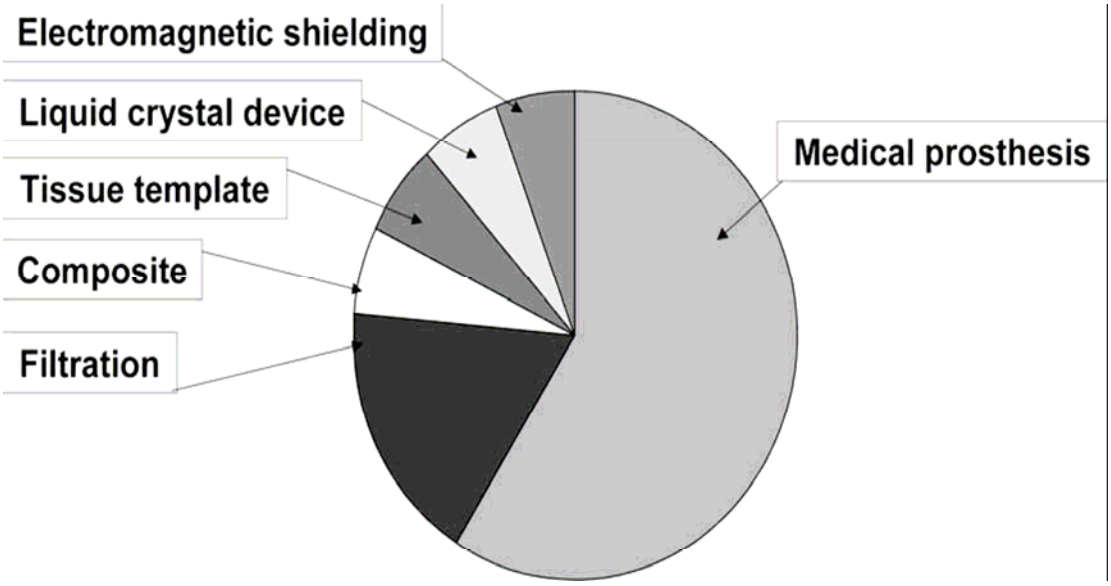

Figure 1.1 Application fields of US patents on elelctrospun nanofibers [**8**]

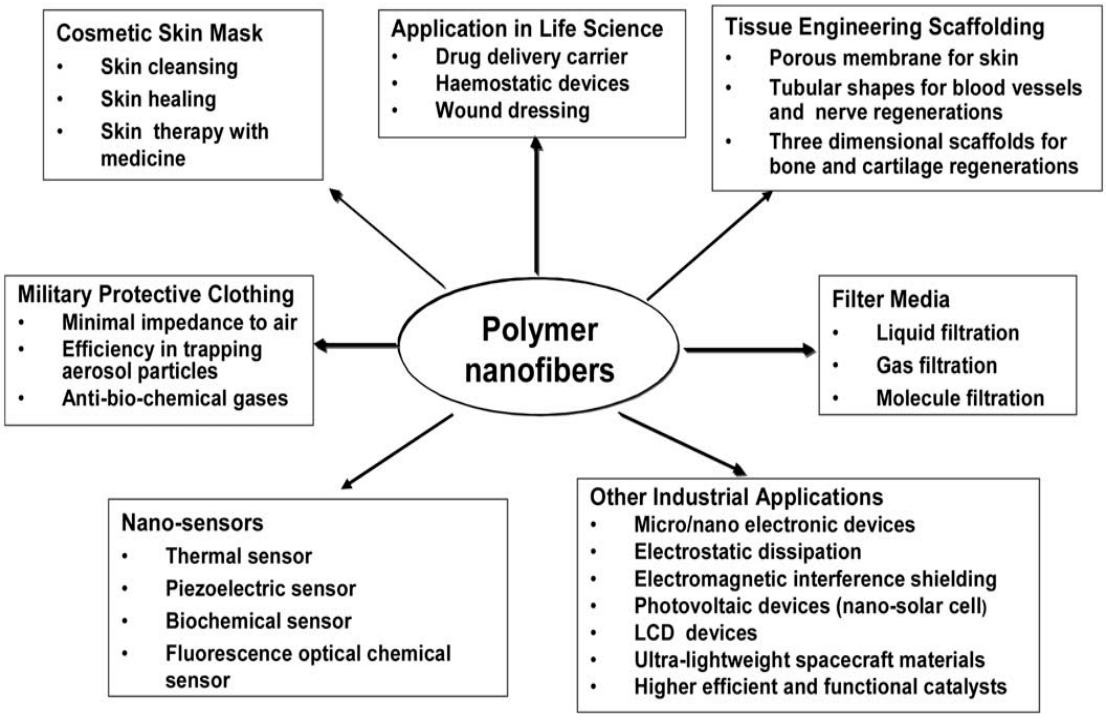

Figure 1.2 Potential applications of electrospun polymer nanofibers [**8**]

1.2 Objective

Today, many single polymer solutions or melts have been investigated to be electrospun to form nanofibers, but only a few polymer blends have been electrospun for investigation. [**22-24**] Polymer blends are an ideal low cost alternative to the synthesis of entirely new macromolecules and a bicomponent system can possess properties that are a combination of the two polymeric components. In addition, little information has been reported on aligning the electrospun fibers and measurement of its molecular orientation within the nanofibers in recent electrospinning research.

Hence, the two main objectives of this project are to investigate (1) phase behavior of polymer nanofibers electrospun from polymer blends and (2) molecular orientation within the polymer nanofibers produced by electrospinning of single polymer solution.

Chapter 2 Literature Review

2.1 Electrospinning process

Electrospinning is a straightforward method to produce nanofibers from polymer solution and melts. The process is complex and involves physics, fluid mechanics, polymer science, and rheology. In general, the basic experimental setup of electrospinning includes: (1) applied voltage (2) grounded target collector (3) polymer reservoir with a spinneret. The process involves three stages: (1) jet initiation and extension in a straight line, (2) growth of bending instability of the jet, (3) Solidification of the jet and formation of nanofibers.

In stage 1, with increasing applied voltage, the charged polymer solution or melt forms a cone shape pendent drop at the tip of the spinneret, which is called a "Taylor's cone". [**25**] Once the applied electrical force overcomes the surface tension of the polymer solution or melt, a charged jet will form from the Taylor's cone, whose semi-vertex angle is calculated as 49.3º. [**26**]

After initiation, the path of the jet travels in a straight line for a certain distance. Then, an electrically driven bending instability grows at the bottom end of the straight jet, which causes the jet to bend and follow a whipping and spiraling path. The electrically driven bending instability appears in a self-cycled fashion. Each cycle is similar but smaller than the previous one and has three steps. The three steps in each cycle are: (1) straight

segment develops an array of bends, (2) The bends become a series of spiraling loops as the segment of jet in each bend elongates, (3) The diameters of the loops become smaller and smaller as the each loop grows longer and step 1 developed again along each loop.

In the final stage, the solution jet evaporates and solidifies and is collected as an interconnected web of small nanofibers. [**27**] The collectors are grounded and can be either a stationary target or a rotating target. The electrospinning process is demonstrated in Figure 2.1.

In the literature, there are more than fifty different polymers that have been electrospun into ultra fine fibers successfully, most of which were dissolved in solvents before electrospinning. A summary of nylon 66 and polycarbonate and polyvinylchloride, three polymers used in this thesis is listed in table 2.1

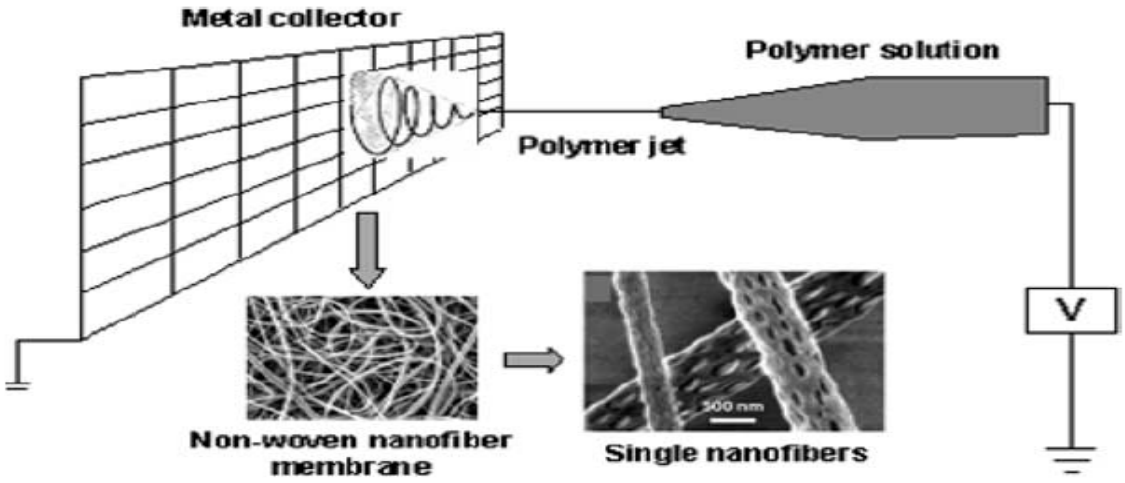

Figure 2.1 Electrospinning process representation [**8**]

Table 2.1 Summary of electrospining of nylon 66 and polycarbonate and polyvinylchloride in their solution form

Polymer	Nylon 66	Polycarbonate	polyvinylchloride
Reference	[**31**]	[**31, 32**] [**33-35**]	[**14, 36**]
Solvent	Formic acid	(1)Tetrahydrofuran/ dimethylformamide =1:1 (2)Chloroform, tetrahydrofuran	Tetrahydrofuran/ Dimethylformamide =100/0,80/20,60/40,50/50, 40/60,20/80,0/100 (vol.%)
Concentration	10 wt%	10-20 wt%	10-15 wt%
Applications	Protective clothing	Protective clothing, Sensor, Filter	Optical sensor

Fewer polymer melts at high temperature have been electrospun into nanofibers. In this case, the polymer melt is introduced into a capillary tube and the electrospinning process has to be performed in a vacuum condition. [**28-30**] Table 2.2 summarizes the polymers that have been successfully electrospun into nanofibers in their melt forms.

2.2 Processing parameter effects on fiber morphology

Several parameters will influence the morphology of the nanofibers electrospun from polymer solutions. Fiber diameter and bead formation are the two morphology characters

Table 2.2 Summary of electrospining of polymers in their melt form

Polymer	Reference	Processing Temperature (°C)
kPolyethylene	[**28, 30, 37, 38**]	200-220
Polypropylene	[**28, 30, 37, 38**]	220-240
Nylon 12	[**29**]	220
Polyethylene terephthalate	[**37, 39**]	270
Polyethylene naphthalate	[**37-39**]	290
PET/PEN blends	[**39**]	290

that have been mostly studied. These influential parameters can be included into three categories: (1) Solution properties including viscosity, concentration, conductivity, and surface tension. (2) Controlled variables including electric potential at the tip, gap distance and solution feed rate. (3) Ambient parameters including temperature, humidity, and air velocity in the electrospinning chamber. [**40**]

2.2.1 Effect of solution properties

Solution properties have an important role in fiber formation in the electrospinning process. In order to obtain nanofibers electrospun from polymer solution, the solution viscosity should be in a suitable range. That viscosity range varies from one polymer system to another. At higher viscosity, electrospinning will be prohibited due to the flow

instability caused by the high cohesiveness of the solution. At lower viscosity, droplets will form instead of fibers. [41, 42] The solution viscosity is a function of the polymer concentration, so these two solution properties are actually related once a polymer is choosen. Researches have found that the higher the polymer concentration the larger the resulting nanofiber diameter will be. Deitzel et al. believed the fiber diameter increased with solution concentration through a power law relationship. [43] Demir et al. believed that the fiber diameter was proportional to the cube of the polymer concentration. [44]

Research has found that higher polymer concentration (high viscosity) resulted in fewer beads, which are spherical or spindle-like defects in the electrospun nanofibers. The existing beads at higher concentration have larger diameter than beads formed at lower concentrations. The shape of the beads changed from spherical to spindle like with the increase of concentration. The influence of viscosity and concentration on bead formation is illustrated in Figure 2.2.

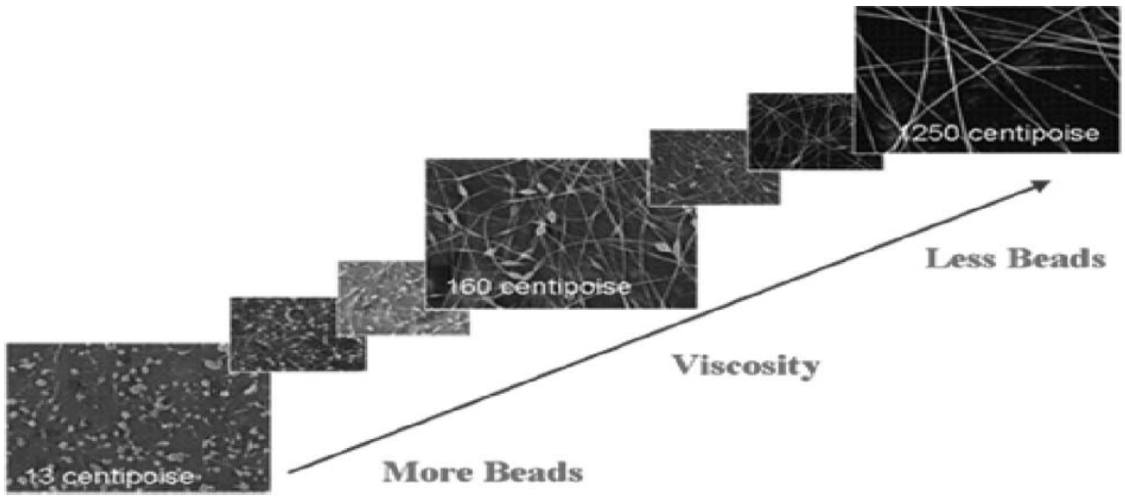

Figure 2.2 SEM images of electrospun nanofibers from different concentration of styrene-butadiene-styrene triblock copolymer solutions. [**45**]

Researches found out that by reducing surface tension of a polymer solution, fibers can be obtained bead free. Surface tensions depend on the choice of solvents. [**40**] Researches also found out that increasing the conductivity of the polymer solution by the addition of salts will result in smaller bead and thinner fiber diameters. [**46**] The addition of the salts will increase electric charges in the jet, which will increase the elongational forces imposed on the jet by the applied voltage. So, the fibers will become thinner and the bead formation is prevented.

2.2.2 Effect of controlled variables

Nanofibers are produced by electrospinning process only if the applied voltage is above the given critical value required to overcome the surface tension of the solution. Above that voltage value, the voltage determines the amount of polymer reaching the collection target. Researches found out that with the increase of the applied voltage, the resulting nanofibers will have smaller diameters and higher bead density, which is demonstrated in Figure 2.3. With the increase of the electrospinning voltage, the shape of the droplet from which the jet originates will change. The volume of the droplet will decrease and the Taylor cone will recede or even disappear, leaving the jet to initiate from a liquid surface within the syringe tip or even inside the syringe needle, which will cause an increase in the instability of the jet and finally result in an increased number of bead defects forming along the electrospun fibers. [**43**] The influence of applied voltage on bead densities is shown in Figure 2.4.

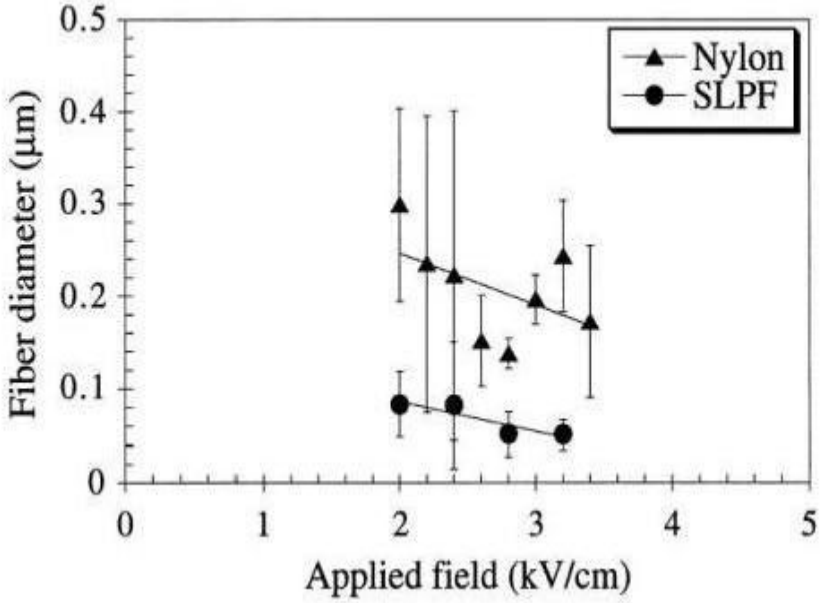

Figure 2.3 Fiber diameters decreases with increasing voltage for nylon 6,6 and silk-like protein polymer (SLPF) in formic acid [**43**]

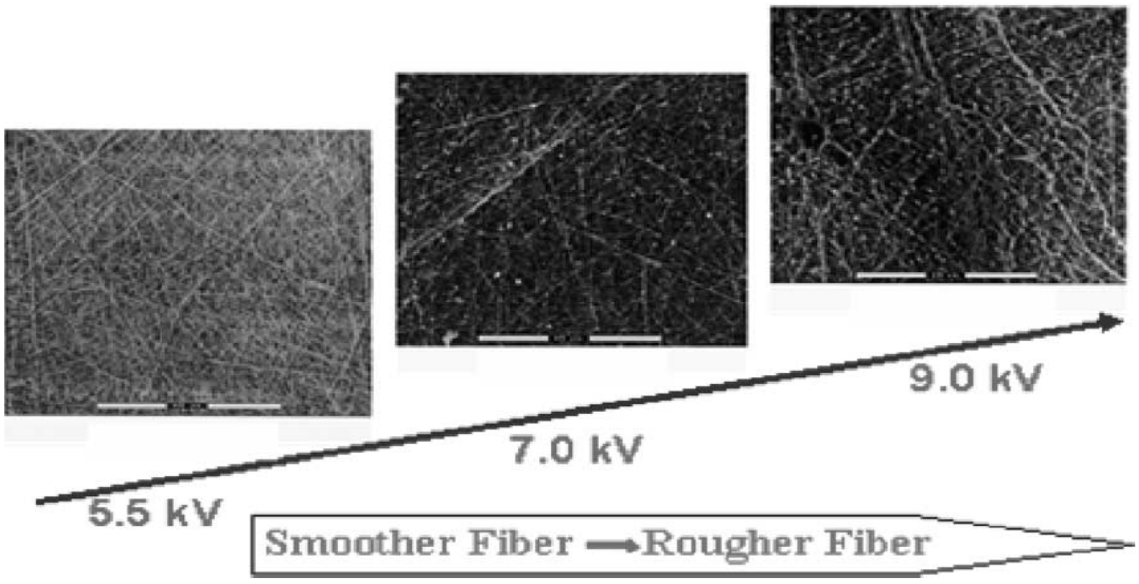

Figure 2.4 SEM photographs of PEO nanofibers electrospun under different voltages [**43**]

It was found that the feed rate at which the polymer solution is pumped into the capillary tip would change the fiber morphology. The higher the feed rate, the larger the fiber diameter and lower bead density will be found in these fibers. The effects of feed rate on fiber diameter and bead density are shown in Figure 2.5 and 2.6 respectively. [**47**]

It was also found that the gap distance between the syringe tip or capillary and the collector target played an important role in the fiber diameter and morphology. The greater the gap distance, the smaller fiber diameter and lower bead density will be found. The effect of gap distance on fiber diameter and bead density is shown in Figure 2.7 [**47**]

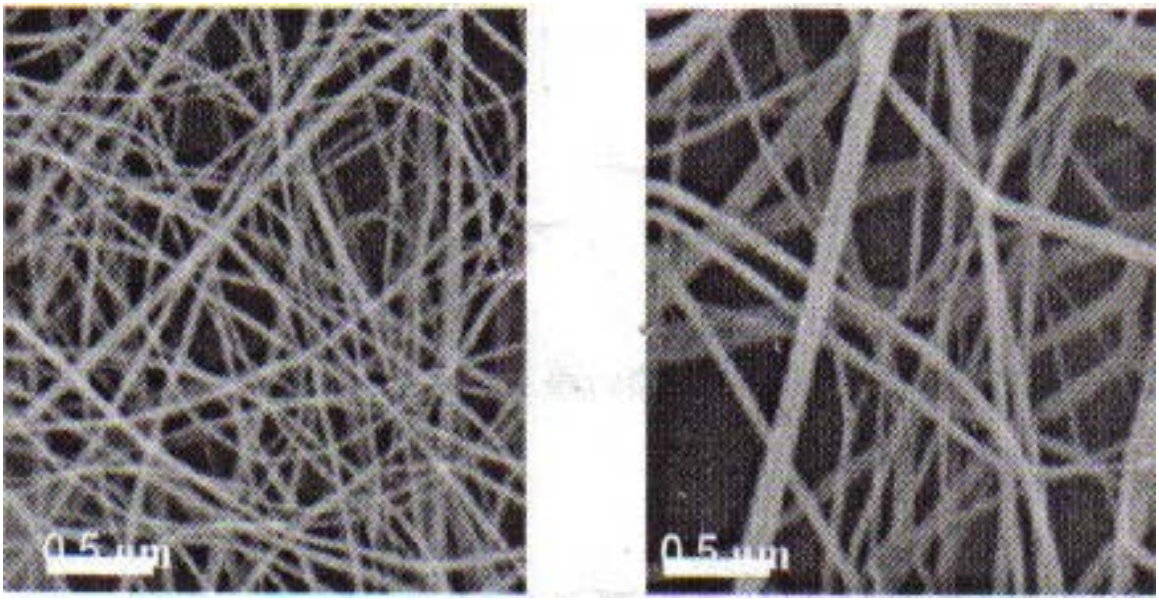

Figure 2.5 SEM images of polycarbonate nanofibers electrospun at 0.05 (right) and 0.1 (left) ml/min [**47**]

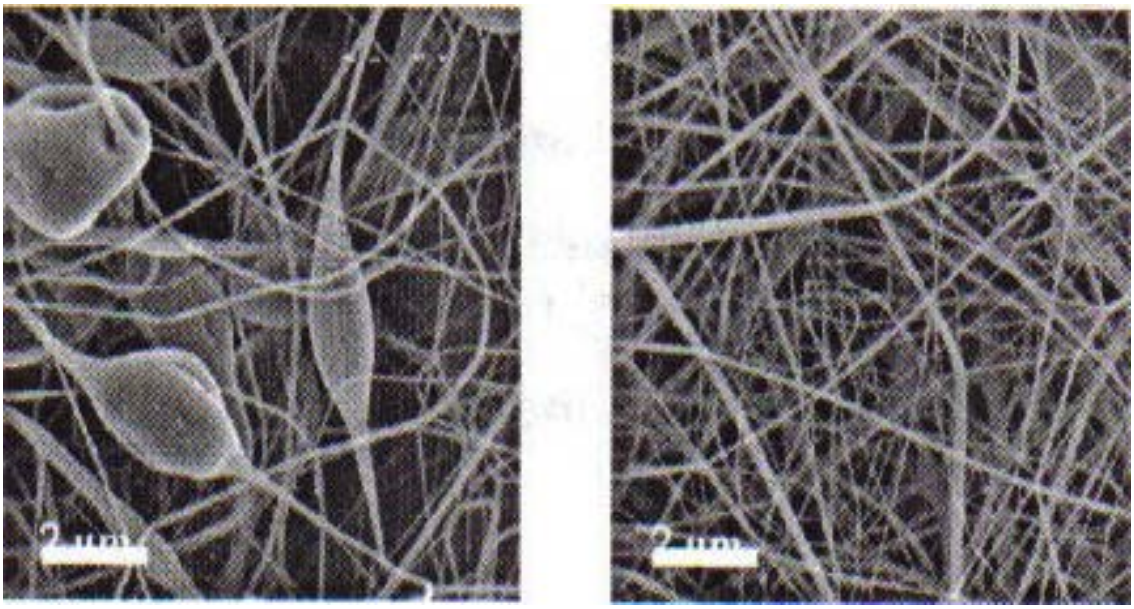

Figure 2.6 SEM images of polycarbonate nanofibers electrospun at 0.05 (right) and 0.1 (left) ml/min [**47**]

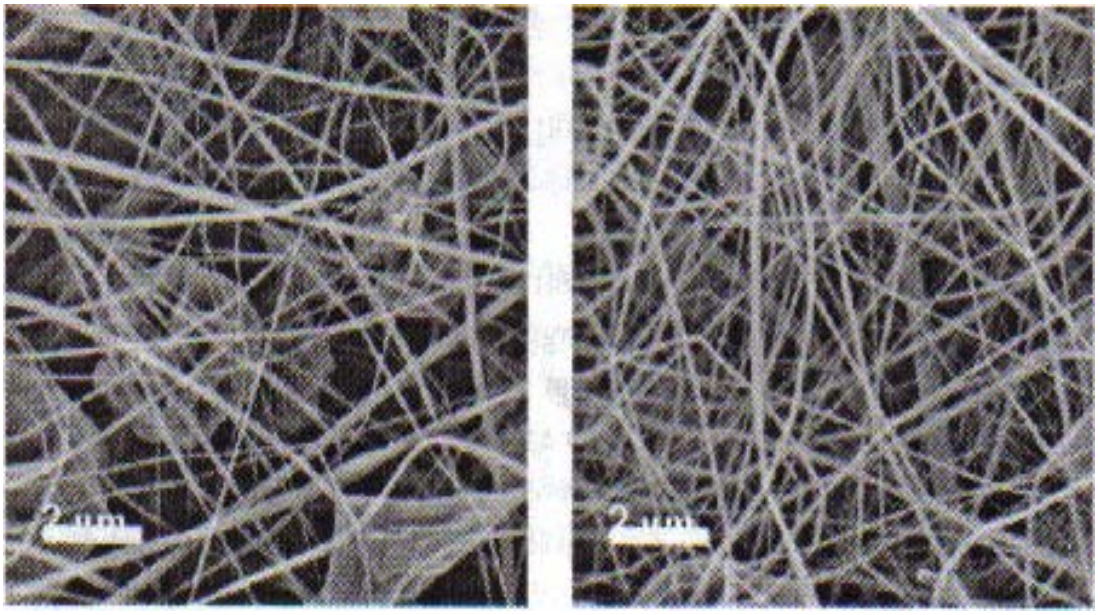

Figure 2.7 SEM images of polycarbonate nanofibers electrospun at 8 inches (left) and 6 inches (right) gap distance [**47**]

2.2.3 Effect of ambient parameters

It was discovered that fiber diameters obtained from a polyurethane solution were much more uniform at higher temperatures than those obtained at low room temperatures. [**44**] It was also reported that the average fiber diameters would increase with the increase of temperature due to the higher drying rate of the solution resulting in a high jet viscosity of the jet stream. **[48]**

Some researches have also been done on the effect of temperature and airflow rate on the fiber formation capability in electrospinning process by introducing hot air blowing. The approved electrospinning process is called Electro-Blowing by the authors. **[48]** They found out that by increasing the air blowing rate, the capacity of fiber formation was caused by the air blowing. The effect of blowing rate is shown in Figure 2.8. They also found out that by increasing blowing air temperature, the capacity of fiber formation in electro-blowing was improved due to the rapid solvent evaporation rate. The effect of temperature is shown in Figure 2.9.

Research has been done on the effect of humidity on the electrospun nanofiber morphology. [**49**] It is reported that humidity affect fiber surface morphology. Increasing humidity will increase the number, diameter of pores in the electrospun nanofibers' surface. The trend is demonstrated by FESEM images shown in Figure 2.10. The reason behind this phenomenon is complex. The author believes that it is the combination of breath figure formation and phase separation. [**49**] Breath figure formation is a process

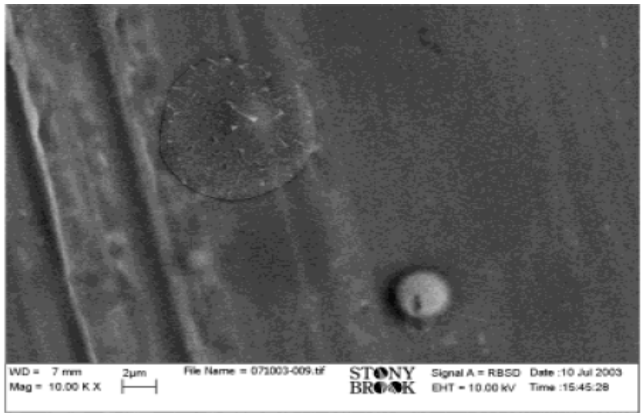

(a)

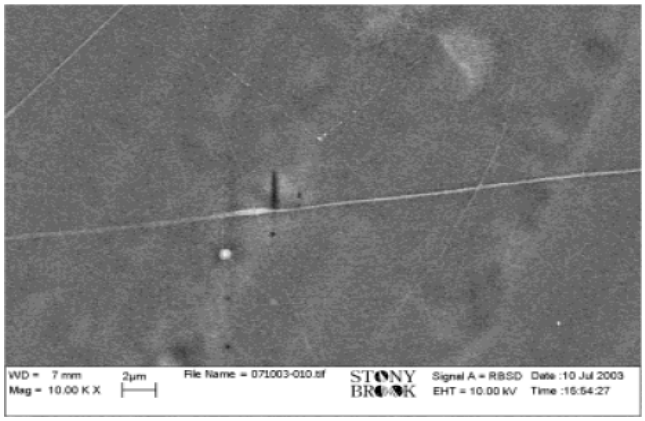

(b)

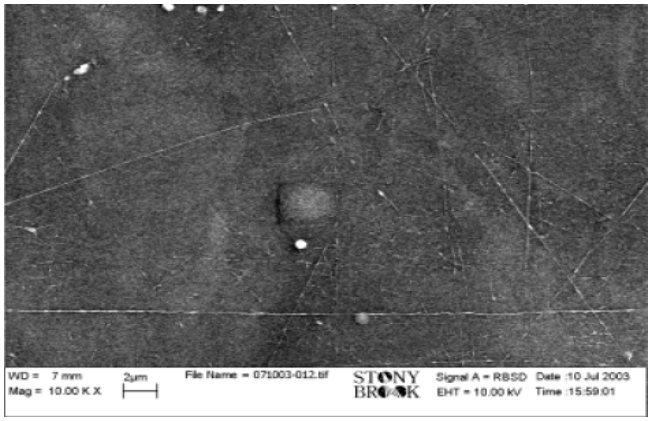

(c)

Figure 2.8 SEM microgaphs of electro-blown hyaluronic acid (HA) with room temperature of air blown at blow rates: (a) 0 ft^3/hr, (b) 70 ft^3/hr, (c) 150 ft^3/hr [**48**]

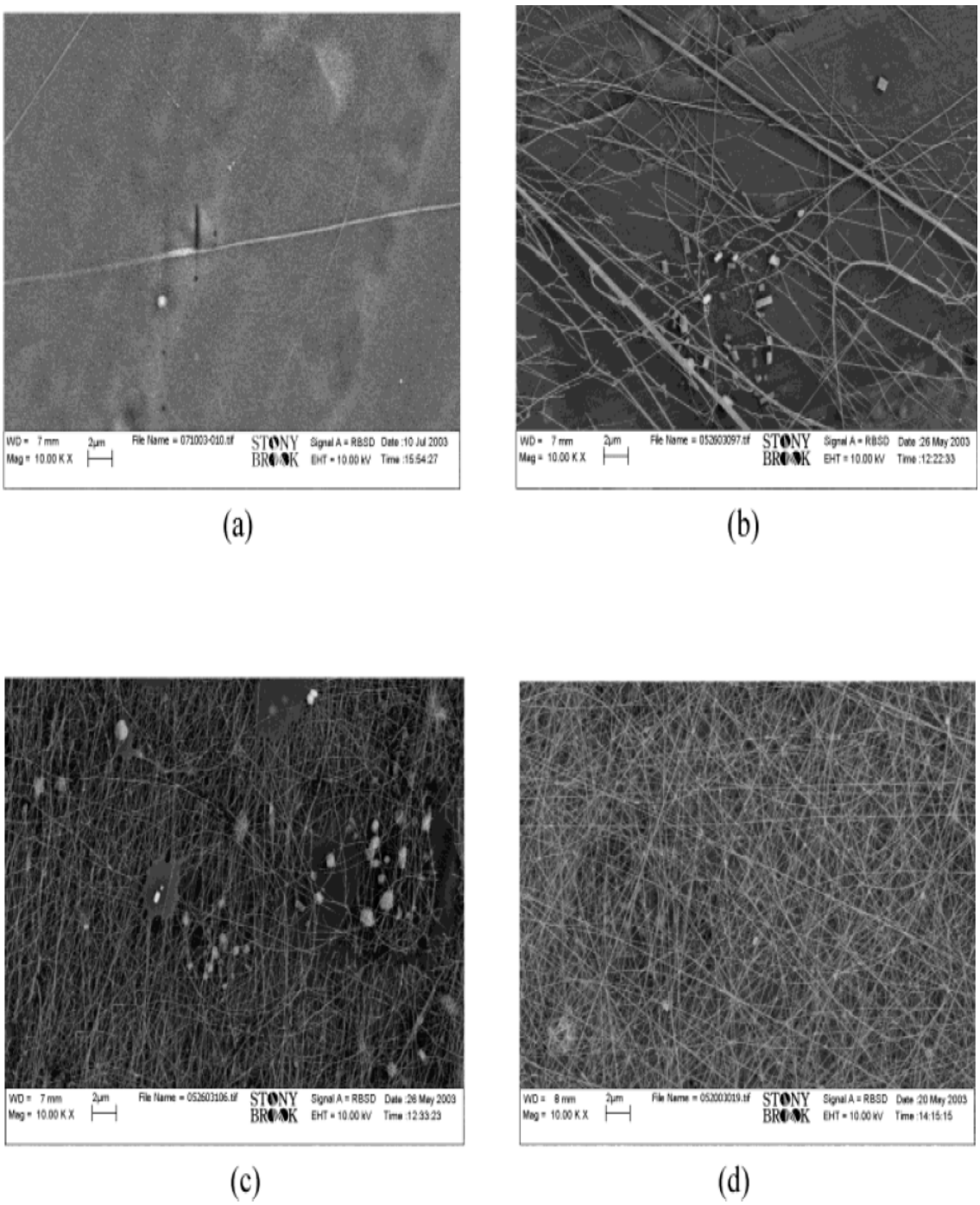

Figure 2.9 Effect of air blow temperature in the electro-blowing process of 2.5 w/v% HA-C solution: (a) 25 °C (b) 39 °C (c) 47 °C (d) 57 °C. [**48**]

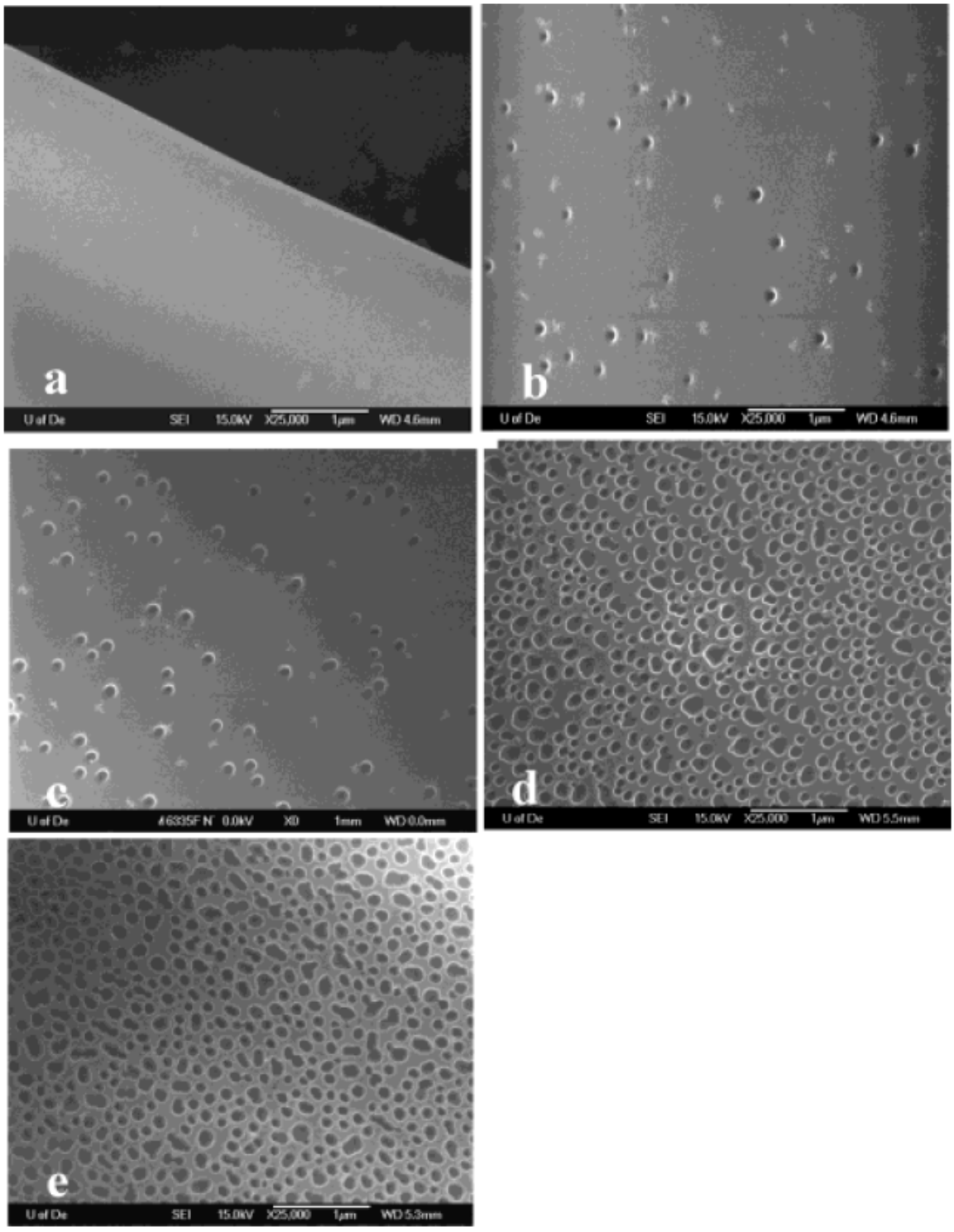

Figure 2.10 FESEM micrographs of 190 000 g/mol PS/THF fibers electrospun under varying humidity: (a) <25%, (b) 31-38%, (c) 40-45%, (d) 50-59%, (e) 60-72%. [**49**]

when the surface of the jet cools due to the rapid evaporation of the solvent; water in the air condenses on the fiber surface and leaves an imprint later when the fiber dries. [**35**] Phase separation is due to the thermodynamic instability caused by decreasing temperature, loss of solvent, or increase in nonsolvent. [**49**]

2.3 Nanofibers electrospun from polymer blends

2.3.1 Study on nanofibers electrospun from polymer blends

Today, many single polymer solutions or melts have been investigated to be electrospun to form nanofibers, but only a few polymer blends have been electrospun for investigation. [**50, 51**] Polymer blends are an ideal low cost alternative to the synthesis of entirely new macromolecules [**52**] and may create a bicomponent system whose properties are the combination of the two polymeric components. For example, one of the polymers can contribute to the mechanical properties while the other can have some desired chemical, optical or biomedical function. Some successful attempts have been made in this area. Electronically conducting polyaniline (PANI) has been blended with campor sulphonic acid (CSA) and poly (methyl methacrylate) (PMMA). The blends have been successfully electrospun into nanofibers and the SEM images of those nanofibers are shown in Figure 2.11. [**22**] The phase behavior of the two polymers inside the electrospun nanofibers was investigated and will be shown in section 2.3.2. Hard and stiff material poly(vinylchloride) PVC has been blended with a very widely used thermoplastic polyurethane PU and the blend electrospun into nanofibers. [**53**] In this

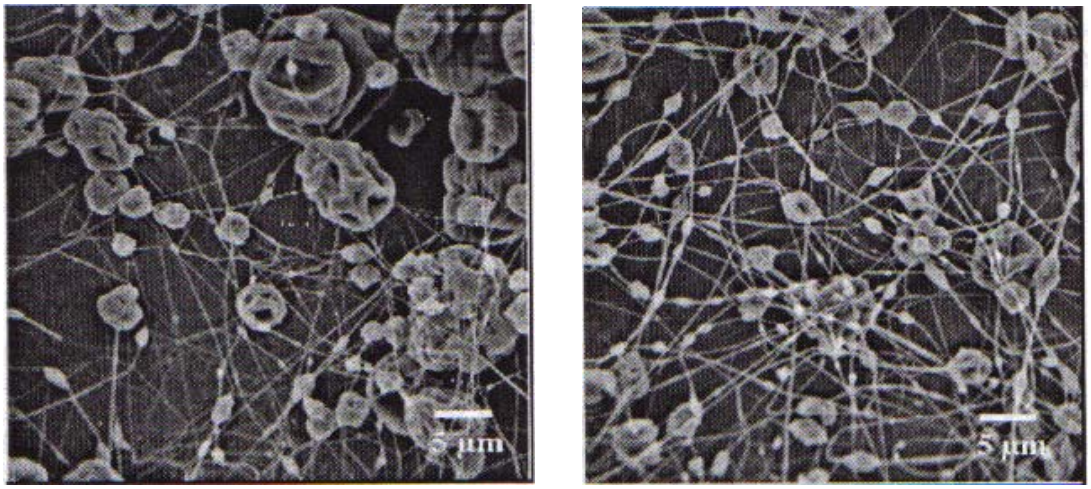

Figure 2.11 SEM images of electrospun nanofibers of 8 wt% PANI-CSA-12 wt% PMMA blends at 20 kV (left) and 25 kV (right). [**22**]

paper, the mechanical properties of these nanofiber were studied, but the phase behavior of the two polymers inside the nanofibers is not addressed. The SEM images of nanofibers electrospun from those blends are shown in Figure 2.12.

Some researches have been conducted on the potential expansion of the scope of polymer blend electrospinning. Polymers can be blended with water-soluble small molecules or macromolecules like DNA, drugs, enzymes, which will be encapusulated as aqueous domains within thin polymer fibers produced by electrospinning process.[**51**] Later, those domains can swell and burst due to osmotic pressure to release the small molecules or macromolecules inside in a controlled way, which will be very useful in drug delivery or other biomedical research. Figure 2.13 shows electrospun poly (ethylene-co-vinyl acetate) EVA fiber encapsulating bovine serum albumin (BSA, MW-66kDa) domains. Figure 2.14 shows those BSA domains in Figure 2.13 swell in water in a controlled manner.

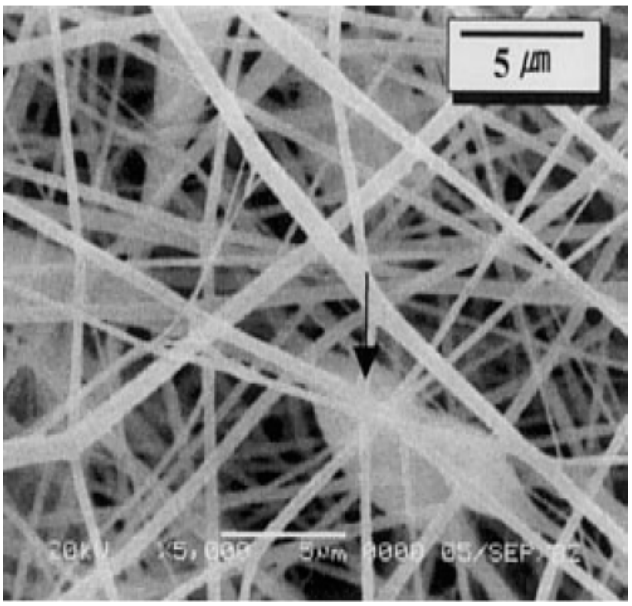

(a)

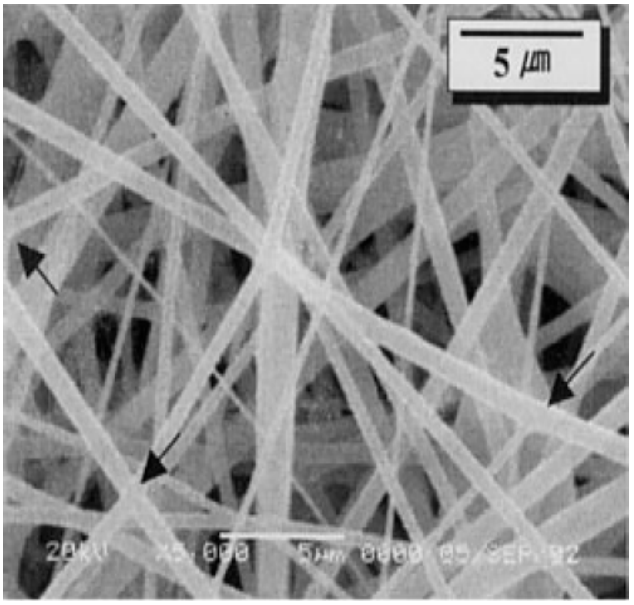

(b)

Figure 2.12 SEM images of fibers electrospun from a 13 wt% solution of PVC/PU polyblends: (a) 75/25(b) 50/50 and (c) 25/75 (arrow means point-bonded structure) [**53**]

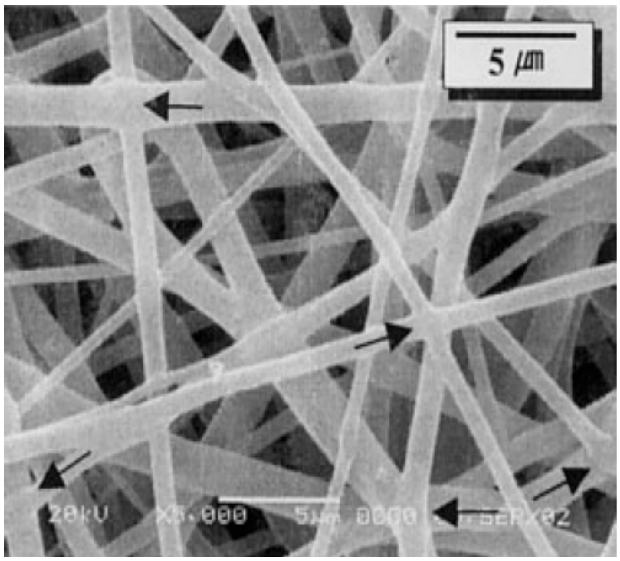

(c)

Figure 2.12 continued

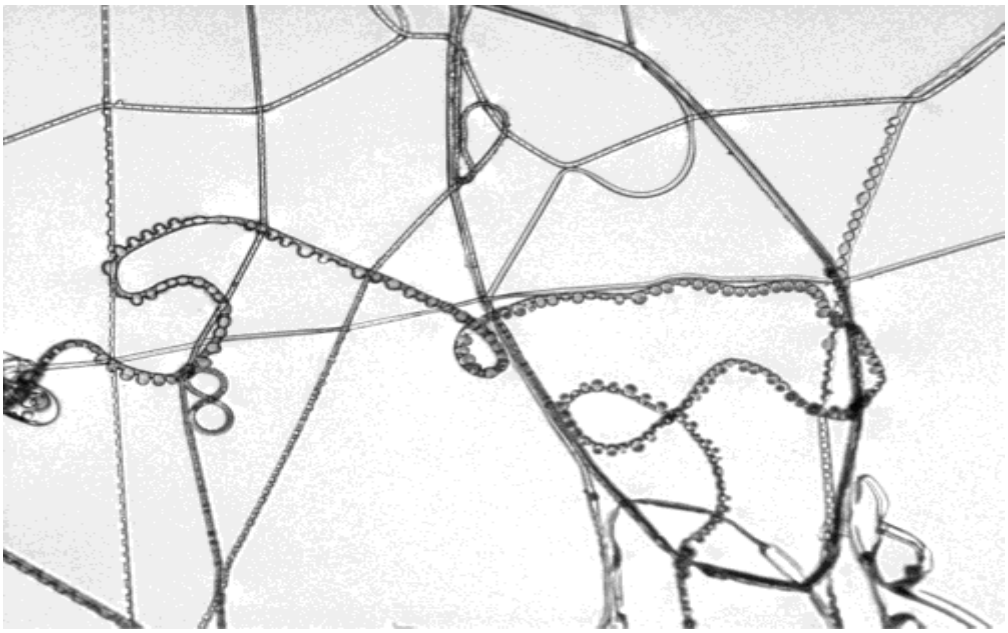

Figure 2.13 Electrospun EVA fibers showing extensive strings of swollen microencapsulated aqueous BSA domains. [**51**]

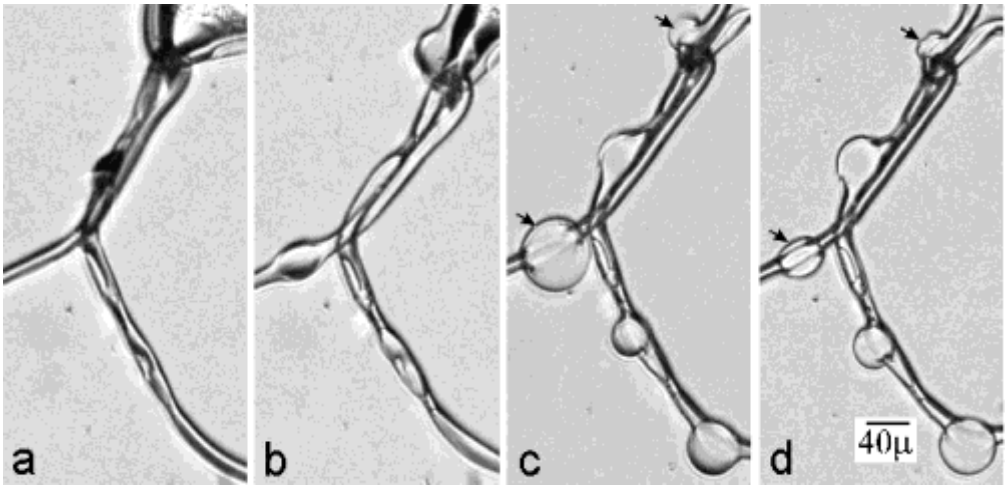

Figure 2.14 Swelling of aqueous BSA domains due to osmotic pressure: (a) 0 min. (b) 6 min, (c) 32 min, (d) 115 min, arrows indicate domains that deflated. [**51**]

Also, electrospinning polymer/enzyme blends into nanofibers can be used as an efficient and viable method to immobilizing enzyme to provide means for them to be used repetitively. Lipasa has been blended with polymer (not specified in the paper) and electrospun into nanofiber mats. [**54**] Figure 2.15 shows electrospun fibrous membranes from 10% polymer/lipase solution.

2.3.2 Phase behavior of the polymers inside the nanofibers electrospun from polymer blends

In general, the mixing entropy of polymers is very small, so the free energy of mixing of a polymer mixture is usually positive, which means immiscibility occurs and the blends

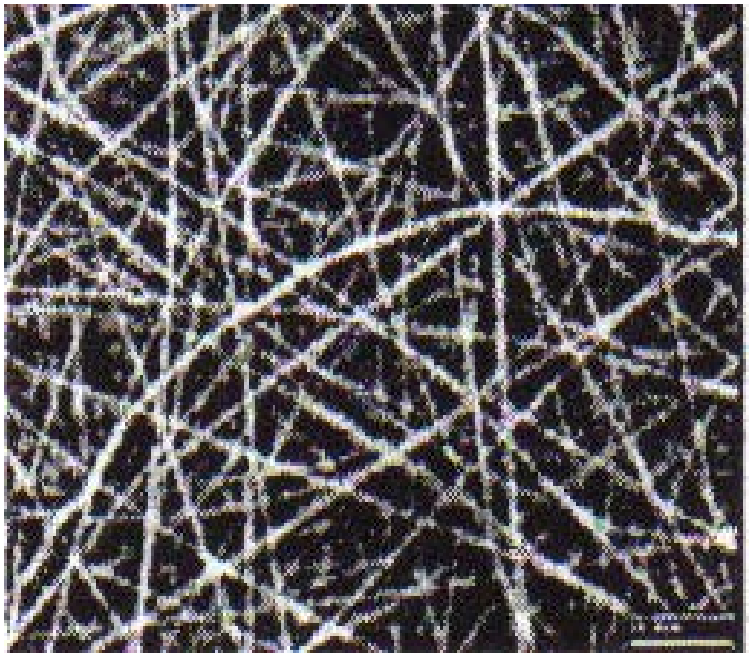

Figure 2.15 Electrospun fibrous membrane from 10% polymer/Lipase solution (bar=10μm). [**54**]

are multiphased in most cases. Generally speaking, the properties of immiscible blends are dependent on their phase size and connectivity. Few reports have addressed the phase behavior of the polymers in the nanofibers electrospun from polymer blends. Phase separation is common in those researches on the nanofibers from electrospinning of polymer blends. [**22-24**]

It was discovered that by staining nanofibers electrospun from PANI-CSA-PMMA blends solutions with OsO_4, which will attack the amide bond in polyaniline, that phase contrast TEM images can be obtained. From Figure 2.16 and 2.17, it is very obvious that two phases exists with PANI being the dark phase domain.

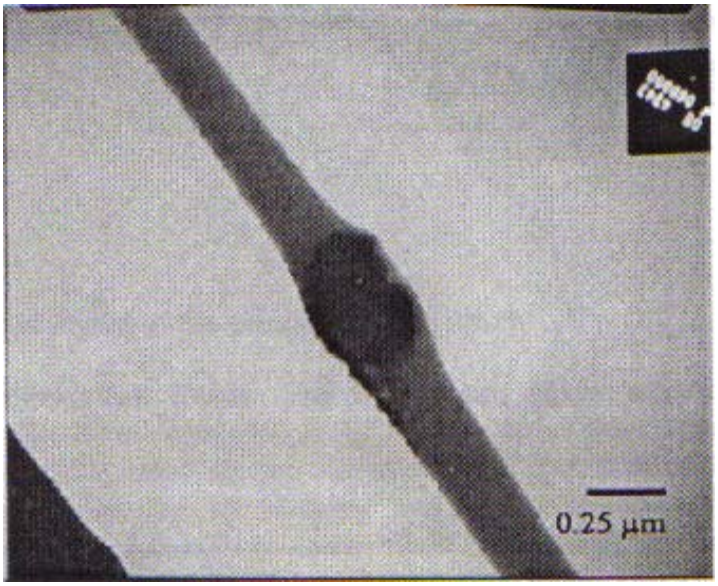

Figure 2.16 TEM micrograph of 4 wt% PANI-CSA-16 wt% PMMA fiber stained using OsO_4 [**22**]

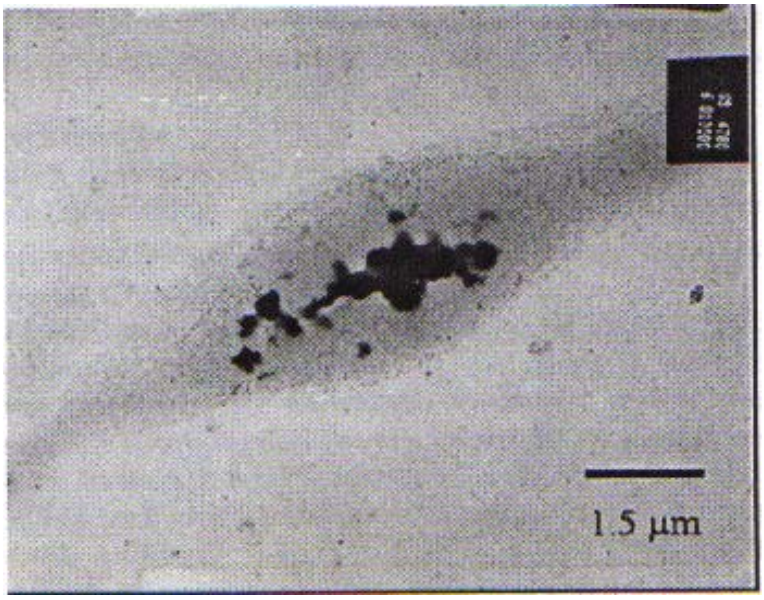

Figure 2.17 TEM micrograph of 8 wt% PANI-CSA-12 wt% PMMA fiber stained using OsO_4. [**22**]

Similar research has been done on the phase behavior of nanofibers electrospun from polyvinylpyrrolidone (PVP)/ polylactide (PLA) blends. PLA can be Poly-L-Lactide (PLLA), which is isotactic and semi-crystalline, or poly-D, L-lactide (PDLLA) which is atactic and amorphous. Selective removal of one component from fibers was used as a method to study the phase behavior of the two polymers inside the nanofibers. Annealing the fibers at high temperature will remove PLA component due to its low viscosity; on the contrary, subjecting the fibers to water will remove PVP by extraction. After selective removal, the fiber morphologies are observed by SEM and shown in Figure 2.18. From these SEM images, it is reasonable to conclude that phase separation is not suppressed in the electrospinning PVP/PLA blends despite the rapid evaporation of the solvent and the fiber solidification. Co-continuous phase morphologies are found within these fibers. [**24**] The phase structure of the PVP/PLA blend is shown in Figure 2.19.

2.3.3 Mechanical behavior of nanofiber mats electrospun from polymer blends

The mechanical properties of these nanofibers mats have been barely addressed before in literature. [**53, 55**] Research has been done on the mechanical properties of nanofibers mats electrospun from poly (vinyl chloride)/polyurethane blend solution.

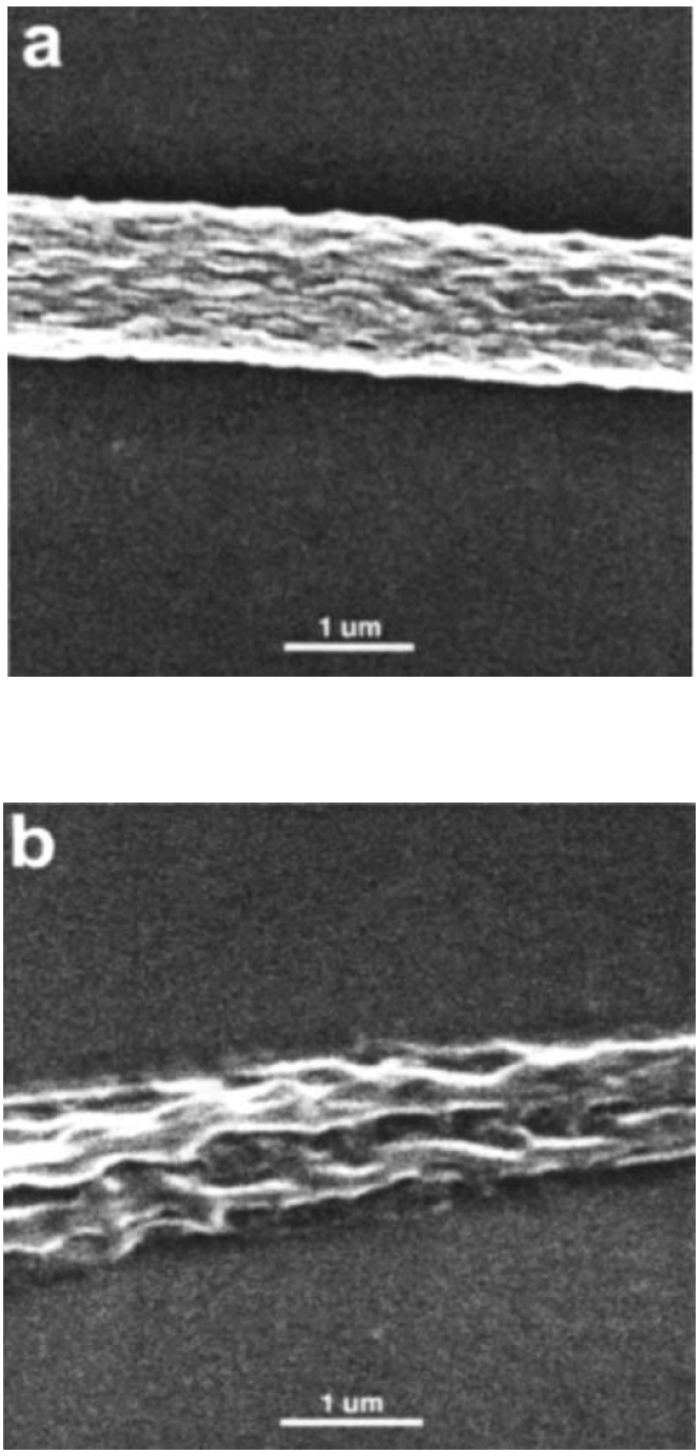

Figure 2.18 SEM images of PVP/PLA 1:1 fibers (a) residual PLLA fiber after selective removal of PVP; (b) residual PDLLA fiber after selective removal of PVP; and (c) Residual PVP fibers after selective removal of PLLA. [**24**]

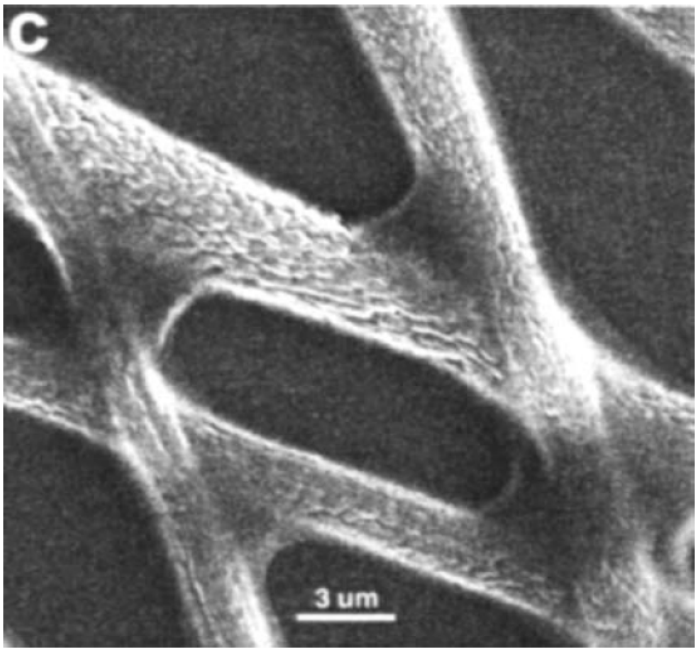

Figure 2.18 continued

Figure 2.19 Schematic representation of possible fiber morphologies of co-cotinuous phase morphologies with dimensions smaller than the fiber diameter. [**24**]

Various compositions of PVC/PU polyblends are dissolved in a mixture of tetrahydrofuran (THF) and N, N-dimethylformamide (DMF) at room temperature at fixed 13 wt%. Nanofiber mats were electrospun from those polyblends solutions and dried in a vacuum oven. The mechanical behavior of the fiber mats was examined with a universal testing machine with a crosshead speed of 10 mm/min. [**53**] The stress-strain behavior of electrospun polyblends (PVC/PU) fiber mats is illustrated in Figure 2.20. Mechanical properties of electrospun polyblend nonwovens are listed in Table 2.3.

From Figure 2.20 and Table 2.3, it is clear that the pure PVC nanofiber mat has low tensile strength and elongation. With the increase of PU composition, the elongation and tensile strength increases. The modulus first increases and reaches a maximum at composition of PVC/PU 50/50, then decreases. It is assumed that for pure PVC with low strength and elongation, a distinct elastic region was formed. PVC/PU 75/25 and 50/50,

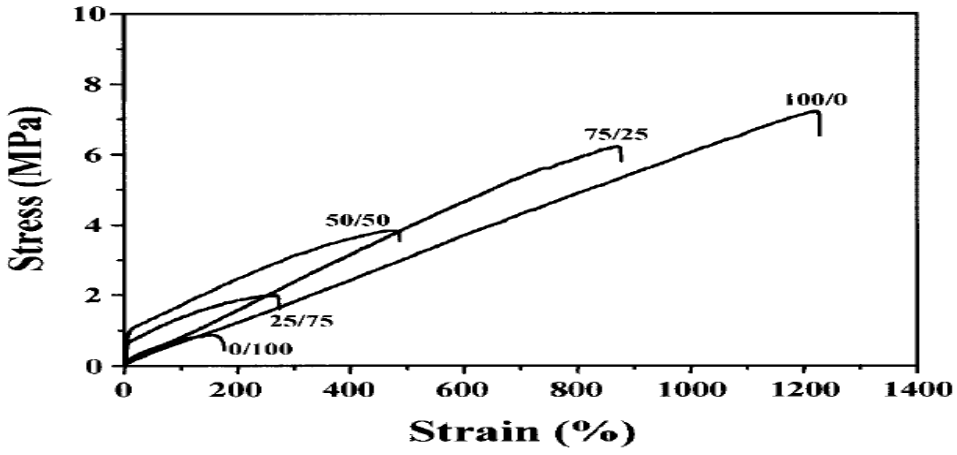

Figure 2.20 Stress-strain behavior of electrospun polyblends (PU/PVC) fiber mats, number indicates PU/PVC polyblends of weight ratio. [**53**]

Table 2.3 Mechanical properties of electrospun polyblend nonwovens [**53**]

PVC/PU (w/w)	Modulus (MPa)	Yield Stress (MPa)	Tensile Strength (MPa)	Elongation at Break (%)
100/0	3.75	0.13	0.90	153
75/25	8.94	0.68	1.97	245
50/50	11.80	1.03	3.73	465
25/75	0.78	—	6.30	905
0/100	0.62	—	7.04	1210

have a plastic or elastomeric behavior with an increased modulus, strength and elongation. For higher PU compositions (PVC/PU 25/75 and 0/100), the more elastomeric PU controlled the tensile behavior results in a linear elastic behavior up to fracture. The formation of a point-bonded structure of electrospun PU fibers is the reason behind these phenomena, which is shown in Figure 2.12. These point-bonded structures will hinder the slip of stiffer PVC fiber and increase load transfer to PVC fibers when PU concentration is low and will act as a load-bearing structure when PU concentration is high. [**53**]

2.4 Orientation of electrospun nanofibers

2.4.1 Methods to introduce orientation to electrospun nanofibers

So far, most nanofibers produced by electrospinning are in non-woven form. However, for some application, not only the electrospun nanofiber diameter and their intrinsic properties but also the fiber orientation and the molecular orientation inside nanofibers

matter as in traditional fiber and textile industry. In these cases, electrospun nanofibers should be in either continuous single nanofibers form or uniaxial fiber bundles form to be useful, which is a tough target to be achieved, since the polymer jet does not travel in a straight line but in a whipping way during the electrospinning process due to the bending instability. Still, great efforts have been made towards this goal. Until now, there are five basic methods reported in this area. [**8**]

1. A cylinder collector with high rotating speed.
2. An auxiliary electrode/electrical field.
3. A thin wheel with sharp edge
4. A frame collector
5. Multiple field technique

Researchers have found that by electrospinning nanofibers onto a rotating cylinder collector at a speed up to thousand of rpm (revolution per minute), orientation will be introduced into the nanofibers obtained. The speed of the rotating cylinder surface should match the alignment speed of the fiber, which is the speed of the solidified jet, in order to achieve a measure of orientation. Lower speed or much higher speed is not good. Figure 2.21 demonstrated the experiment setup and Figure 2.22 shows the oriented electrospun nanofibers obtained by this method.

Researchers have also found out that by employing an auxiliary electrical field the fiber alignment will be greatly improved. [**56**] [**57**] The electrospinning setup and the alignment effect are shown in Figure 2.23 and Figure 2.24 respectively.

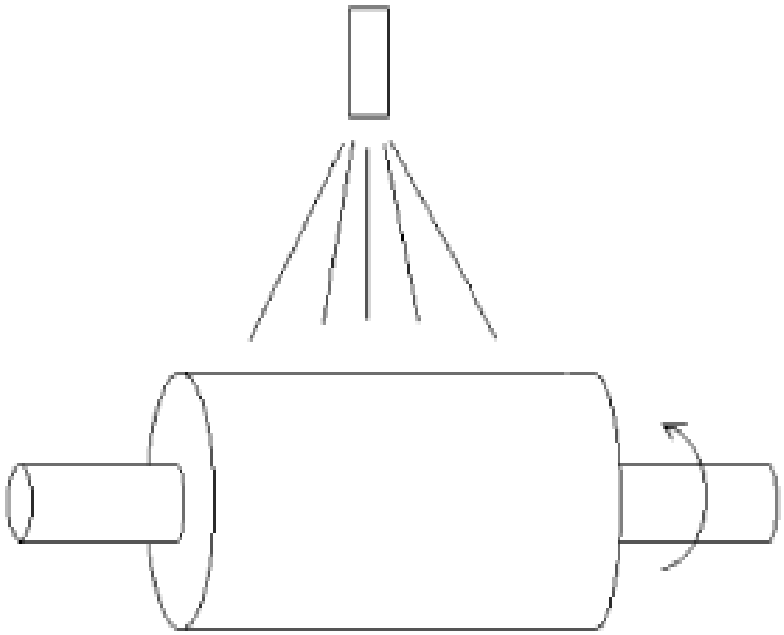

Figure 2.21 A schematic rotating collector for electrospun nanofibers. [**8**]

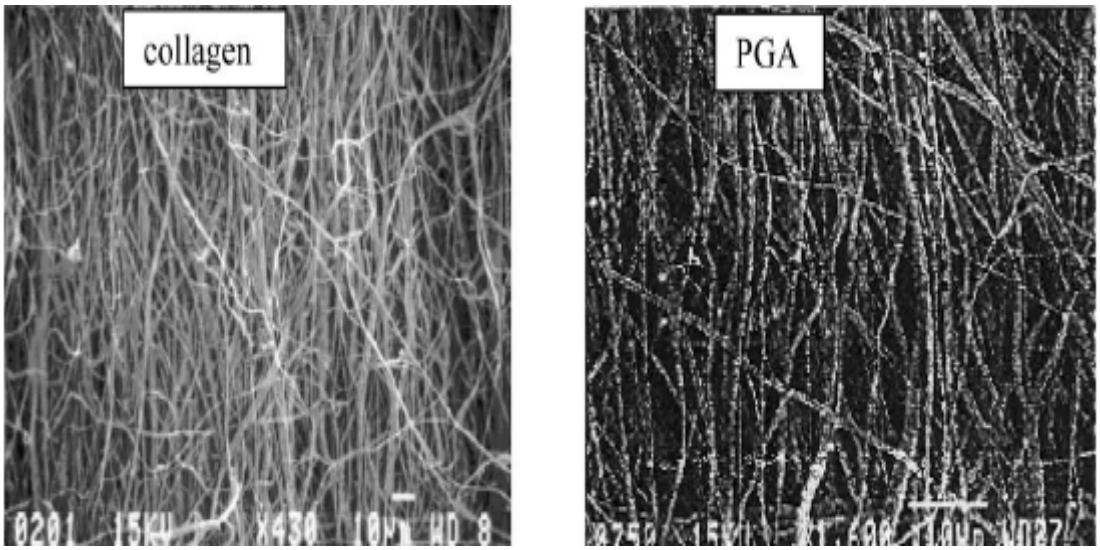

Figure 2.22 Aligned collagen [**58**]and PGA [**59**]electrospun nanofibers

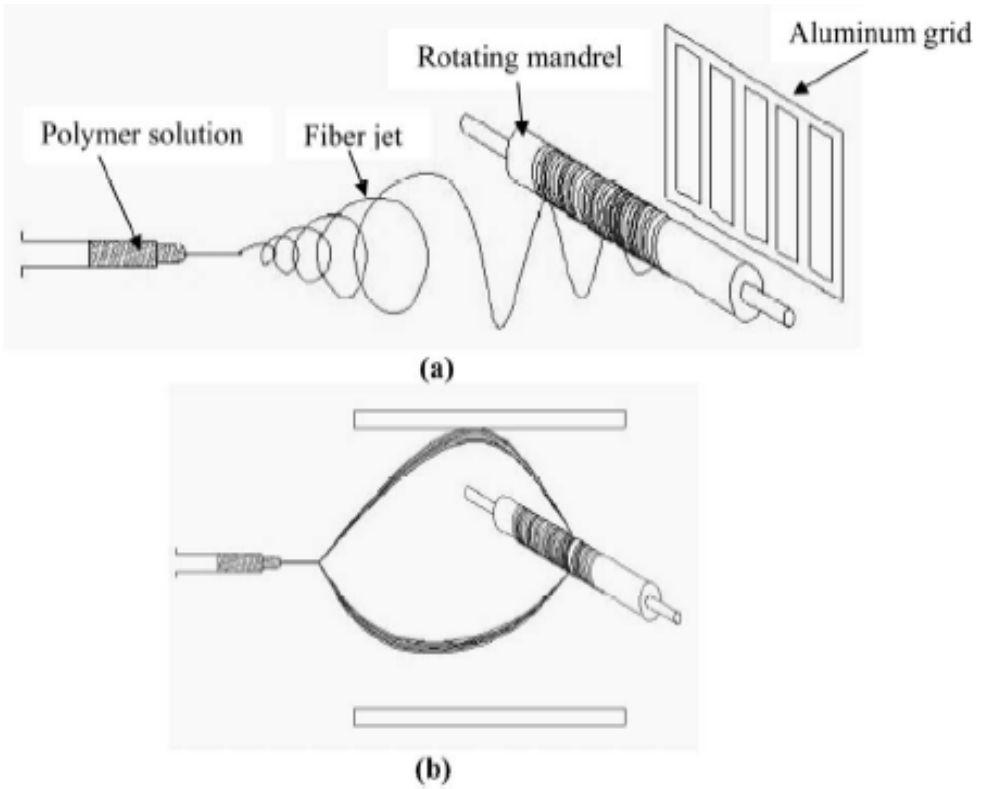

Figure 2.23 Aligning electrospun fibers with an auxiliary electrical field. [**8**]

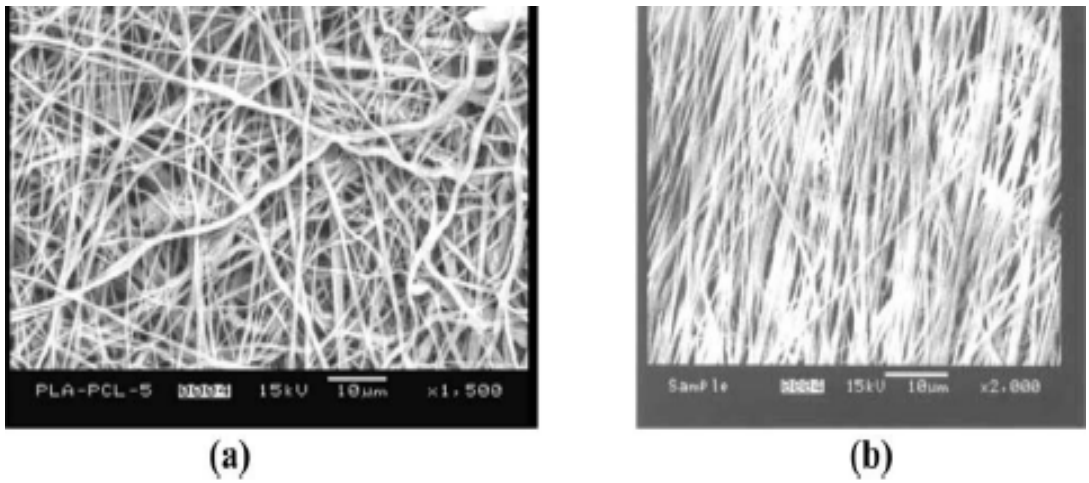

Figure 2.24 Comparison between polymer PLA-PCL (75:25) nanofiber: (a) without and (b) with an auxiliary electrical field [**8**]

Researchers have developed a novel approach to align nanofibers on a tapered and grounded wheel-like bobbin, which is a great advancement in collecting, aligned electrospun nanofibers. The as-spun nanofibers will be attracted to and be continuously oriented on the edge of the rotating wheel because of the electrical field concentration effect caused by edge's tip like feature. The experimental setup and aligned polyethylene oxide (PEO) nanofibers are shown in was shown in Figure 2.25. [**60**]

Placing a rectangular frame structure under the electrospinning jet can also introduce orientation into the electrospun nanofibers, which is a simple method. Different frame materials result in different fiber alignment. The experimental setup is shown in Figure 2.26 and optical microscopy images of aligned PEO nanofibers electrospun on both a wooden frame and an aluminum frame are shown in Figure 2.27. From the images, it is clear that aluminum frame favors better fiber alignments than a wooden frame. [**8**]

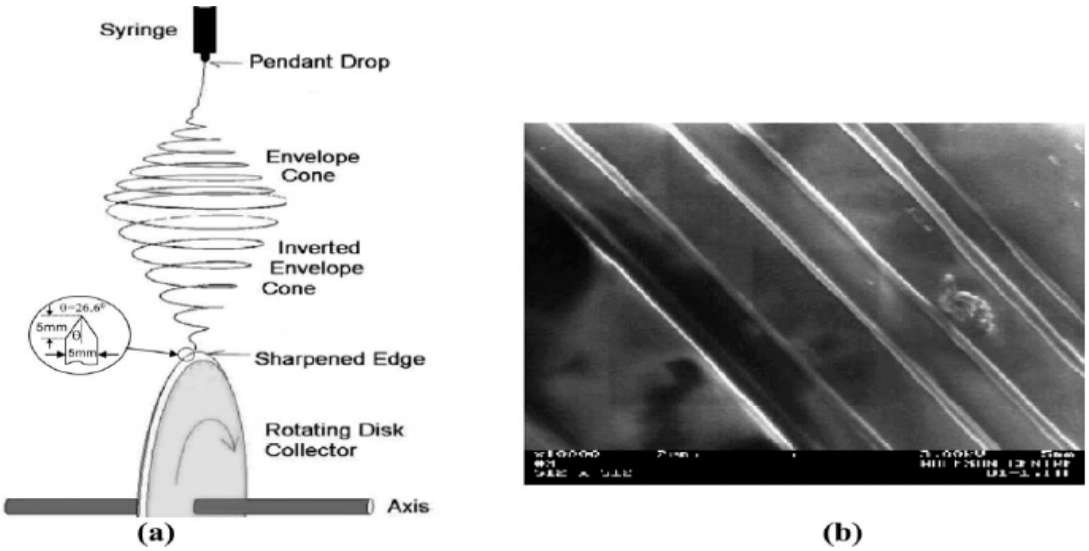

Figure 2.25 Experiment setup to collect uniaxial nanofibers by a thin wheel with sharp edge, (b) PEO fibers thus obtained [**60**]

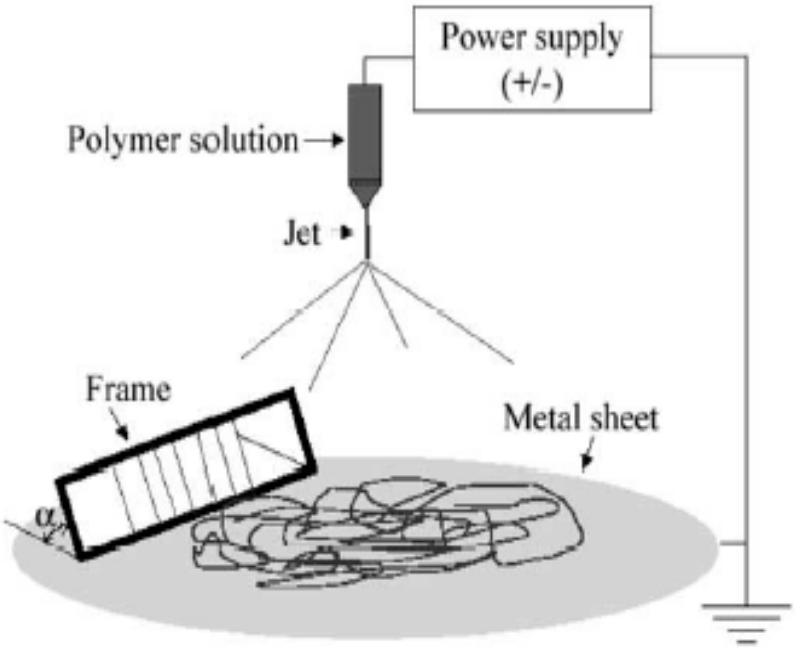

Figure 2.26 Experiment setup to collect uniaxial nanofibers by a frame method. [**8**]

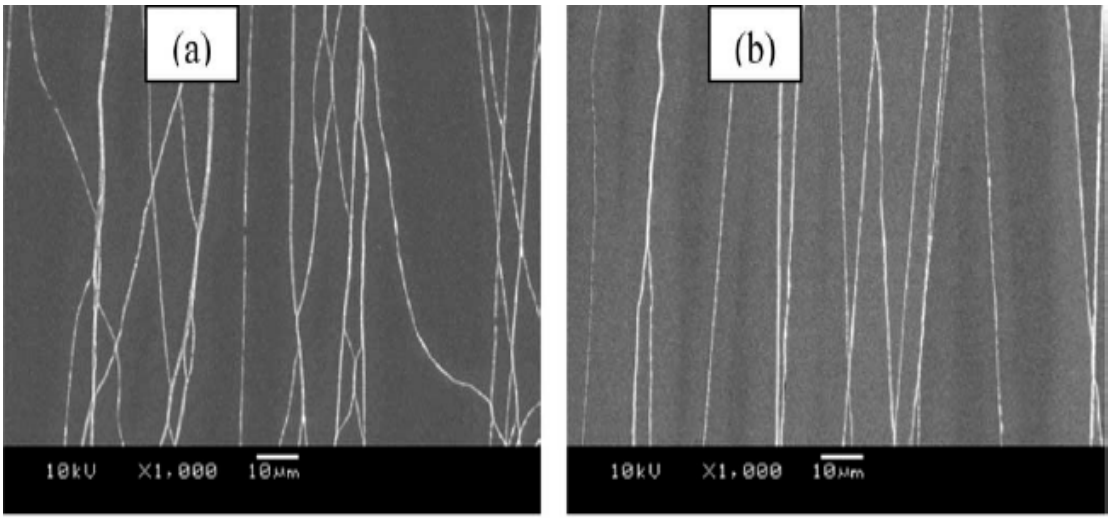

Figure 2.27 Comparison of fiber alignments between using (a) a wooden frame and (b) an aluminum frame. [**8**]

The last method to introducing orientation into electrospun nanofibers that appeared in the literature is using a multiple field technique. The basic principle behind this method is by using a multiple field to reduce the chaotic oscillating motion of the jet as it travels towards the collecting target. Thus, the jet can be straightened to some extent. [**27**] The experimental setup and the aligned PEO fiber yarns are shown in Figure 2.28.

2.4.2 Application of aligned nanofibers

Aligned electrospun nanofibers have found important applications in composite reinforcement [**61, 62**], sensors [**63**], and medical researches. [**64**] [**65**] For these

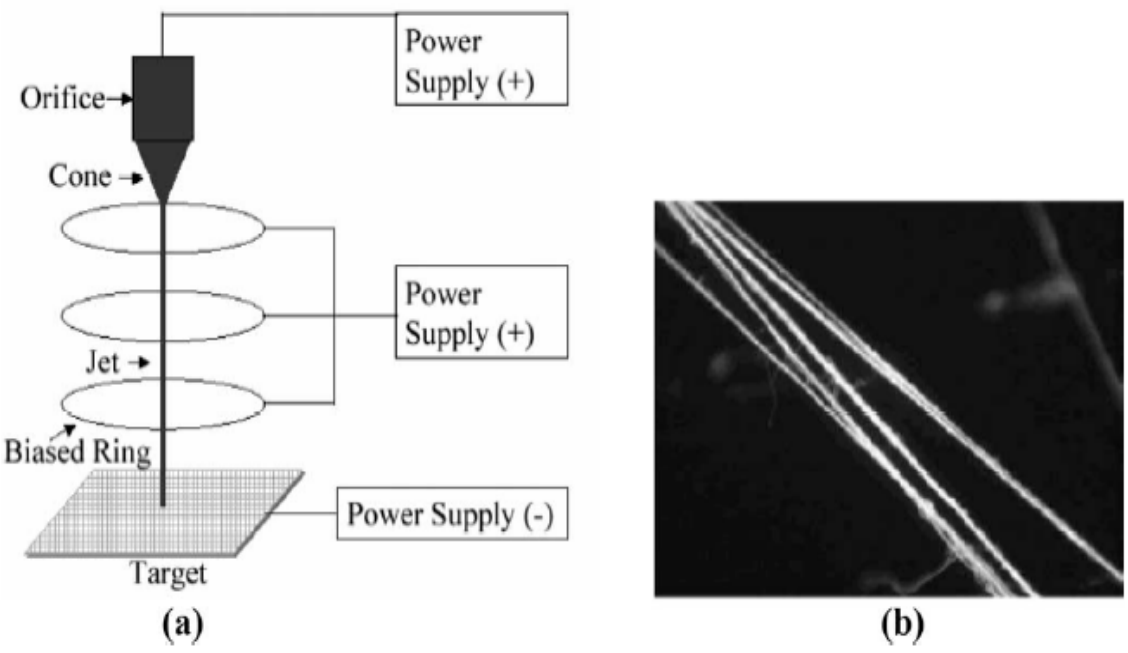

Figure 2.28 Experimental setup and the aligned PEO fiber yarns (a) a multiple field technique, and (b) aligned PEO fiber yarn obtained.[**27**]

applications, not only the fiber diameters and their intrinsic properties but also the fiber orientation and the molecular orientation inside nanofibers are important. For tissue engineering, well-aligned nanofibrous scaffold produced by electrospinning will better support cell culture and improve cell growth because of the fiber orientation. [**64**] [**65**] For composite reinforcement, carbon nanofibers widely used as fiber fillers can be produced from electrospun PAN precursor fibers, [**61, 62, 66**] and the molecular orientation of the precursor fiber will influence the mechanical properties of the carbon naofibers and the efficiency of the reinforcement effect.

2.4.3 Orientation factor quantification

Although orientation has been observed by electrospinning fibers directly onto a rotation object, very few papers have quantified it [**67**]. In this paper [**67**], nanofibers were electrospun from 10 wt% polyacrylonitrile (PAN) in dimethylformamide (DMF) solution onto a high speed rotating target at 16 kV. The orientation factors with respect to fiber winding direction of PAN nanofibers were determined by Fourier transform infrared spectrophotometer (FTIR) and wide angle x-ray diffraction (WAXD). WAXD patterns of those nanofiber bundles are shown in Figure 2.29. The orientation factors obtained by both FTIR and WAXD are shown in Figure 2.30. From Figure 2.29 and Figure 2.30, it is clear that with the increase of the rotating wheel speed, the orientation factor increases and reaches a maximum of 0.23 at a rotating speed between 8.1 and 9.8 m/s [**67**].

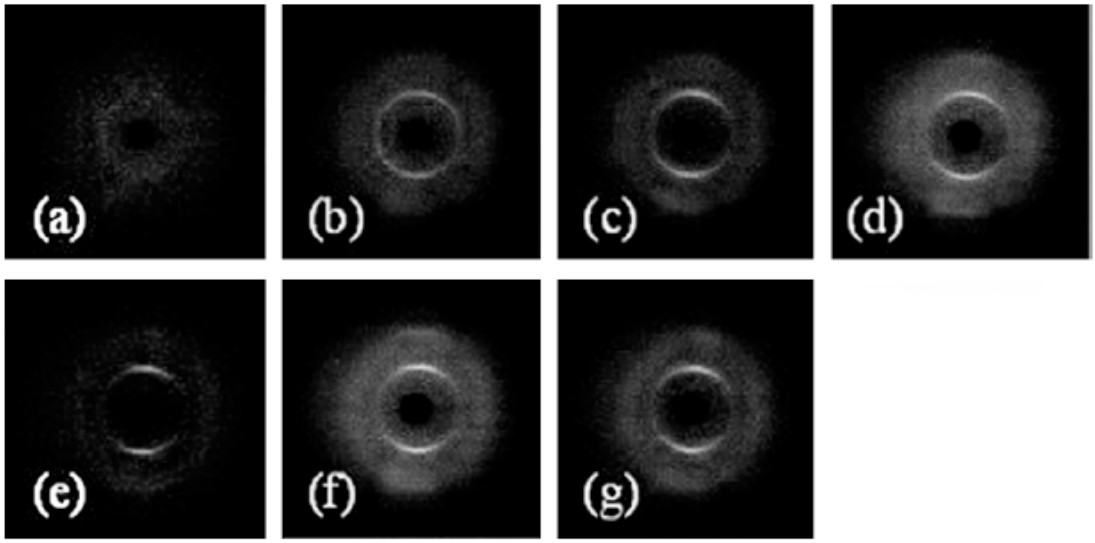

Figure 2.29 WAXD of bundles of fibers electrospun with an applied voltage of 16 kV onto a rotating target with a surface velocity of (a) 0 m/s, (b) 3.5 m/s, (c) 6.1 m/s, (d) 8.6 m/s, (e) 9.8 m/s, (f) 11.1 m/s, (g) 12.3 m/s. [**67**]

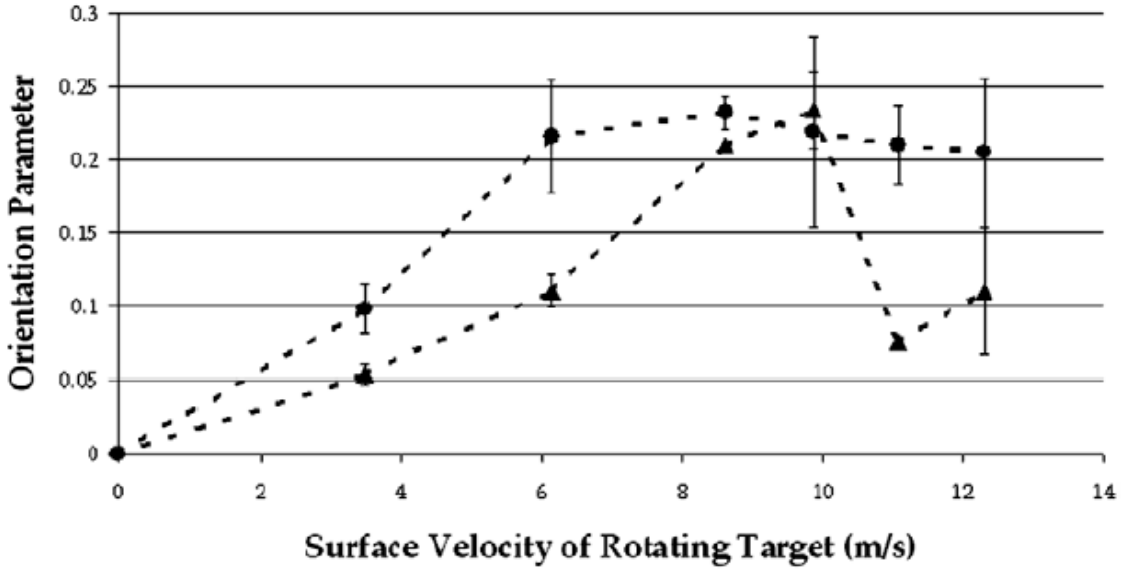

Figure 2.30 Orientation parameter versus surface velocity of the rotating target determined by WAXD of the 5.3 A ° equatorial peak (—○ -) and dichroism of nitrile-stretching vibration (- ▲ -). [**67**]

2.4.4 Mechanical properties of oriented electrospun nanofibers

The mechanical properties of polymer fibers depend on molecular orientation, degree of crystallinity, polarity of the polymer, and presence of plasticizer. Electrospinning nanofibers directly onto a rotating target will improve the mechanical properties of the nanofiber mats due to the increase of the orientation of fiber and molecular orientation within the fiber. Very few papers have been reported on the mechanical properties of oriented electrospun nanofibers. **[67, 68]** It is found that the nanofiber mats electrospun on a rotating drum will have different properties in different directions. **[14, 36]** A stress-strain curve of a parallel polylactide (PLA) nanofiber mat is shown in Figure 2.31.

The mechanical characterization of an individual nanofiber is rare due to its very small dimension. The tenacity of a single electrospun polyacrylonitrile (PAN) nanofiber was measured by a cantilever technique [**69**].

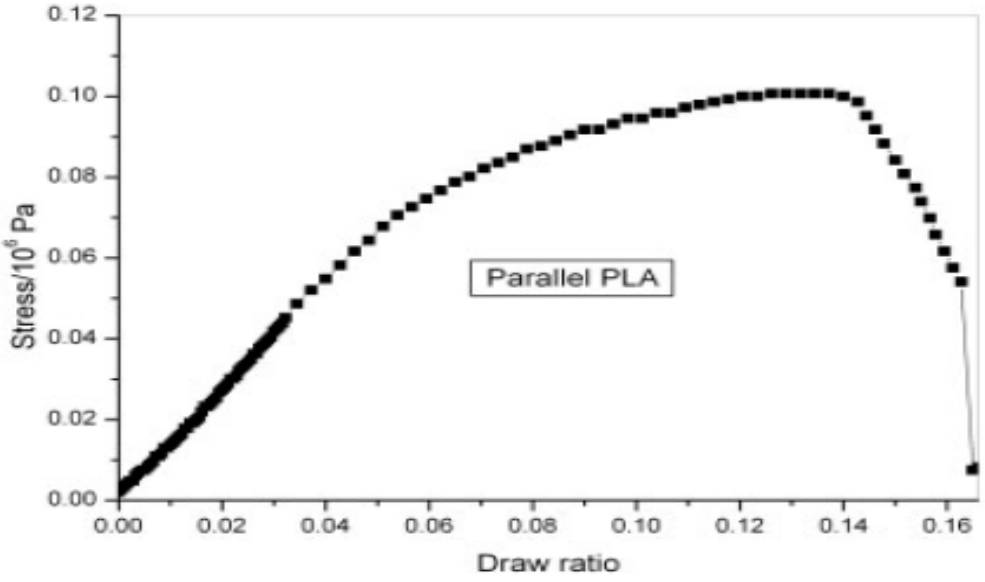

Figure 2.31 Stress-strain curves of sets of parallel PLA fibers [**68**]

Chapter 3 Experimental Procedures

3.1 Materials

The polymers used in this project were obtained from Dupont Textiles & Interiors and Scientific Polymer Products Inc. Acros Organic and Fisher Scientific provided the solvents. The salt was purchased from Structure Probe, Inc. The polymers and solvents used are listed below:

a. Nylon 66 (Mn: 12,600 g/mol, Mw: 36,150 g/mol) from Dupont

b. Polycarbonate – Poly(bisphenol-A carbonate) from Scientific Polymer Products Inc (Mw: 60,000 g/mol)

c. Polyvinyl chloride from Scientific Polymer Products Inc. (Mw: 120,000 g/mol)

e. Polyvinyl chloride form Scientific Polymer Products Inc. (Mw: 215,000 g/mol)

f. Formic acid 99% from Acros Organic

g. Tetrahydrofuran (certified) from Fisher Scientific

h. N,N-Dimethyl-formamide 99% from Acros Organic

i. Ruthenium Oxide Hydrated (RuO_2*2H_2O) from Structure Probe, Inc

j. Sodium Periodate ($NaIO_4$) from Structure Probe, Inc

3.2 Electrospinning process

The polymers used in this project for electrospinning are nylon 66 (Mn: 12,600 g/mol, Mw: 36,150 g/mol); polycarbonate (Mw 60,000 g/mole); polyvinyl chloride blends (Mw: 215,000 g/mol and Mw: 120,000 g/mol); polyvinyl chloride (Mw: 215,000 g/mol) and polycarbonate (Mw: 60,000 g/mol) blends. Nylon 66 was dissolved in formic acid and the weight percentage of the polymer was 10%. Pure polyvinyl chloride and polycarbonate (10% by weight) were dissolved in a solvent mixture (90% by weight) with a weight ratio of THF/DMF 3/2. PC/PVC blends with weight ratio of 25/75, 50/50, 75/25 and PVC blend with a weight ratio of PVC (215,000 g/mol)/PVC (120,000 g/mol) 55/45 was also dissolved in the same THF/DMF solvent mixture. The solutions were prepared by stirring the polymers in solvent for about 4-5 hours till they dissolved completely.

After mixing, the polymer solution was placed in a 10 cc glass syringe from Fisher Scientific attached to a steel hypodermic needle (0.42 mm in diameter inside) and a syringe pump (Harvard apparatus Pump 11). A high voltage power supply (Gamma High Voltage Research) applied the potential to the needle. A grounded stationary copper plate or a 25 cm diameter, 6.35 mm thick stainless steel rotating disc was used as a target to collect nanofibers.

For the phase behavior study, the stationary copper plate was chosen as the target to collect nanofibers. Pure poly (vinyl chloride), polycarbonate, and PC/PVC blends were electrospun onto the copper plate. The applied voltage was 20 kV; the flow rate was 20 μl/min, and the distance between the needle tip and the target was 10 cm. Figure 3.1 (a) shows the electrospinning experimental setup for the phase behavior study.

For molecular orientation study, the stainless steel disc, which has a tapered edge machined to an angle of 64°, was used as both a stationary and rotating target to collect nanofibers. A Micromaster 420 variable frequency motor from Siemens controlled the disc rotating speed in the range of 5 Hz to 60 Hz which corresponds to the linear speed at the edge of the disc in a range of 233 to 2833 m/min. Nanofibers were electrospun directly onto the edge of the rotating disc to introduce orientation onto the nanofibers both in fiber and molecular level. The flow rate is 20 μl/min, the distance between the needle tip and the target was 10cm, the applied voltage is varied from 17.5 KV to 30 KV. The nylon 66 was electrospun onto the rotating disc to determine the relationship between the applied voltage and the molecular orientation within the nanofibers. Two rotating speed 20 Hz and 40 Hz was chosen to be constant and the applied voltage was varied from 17.5 KV to 30 KV. Pure PVC (215,000 g/mol) and PVC blends were electrospun onto the rotating disc to determine the relationship between the molecular weight and the molecular orientation within the nanofibers. The applied voltage was kept constant at 20 KV,

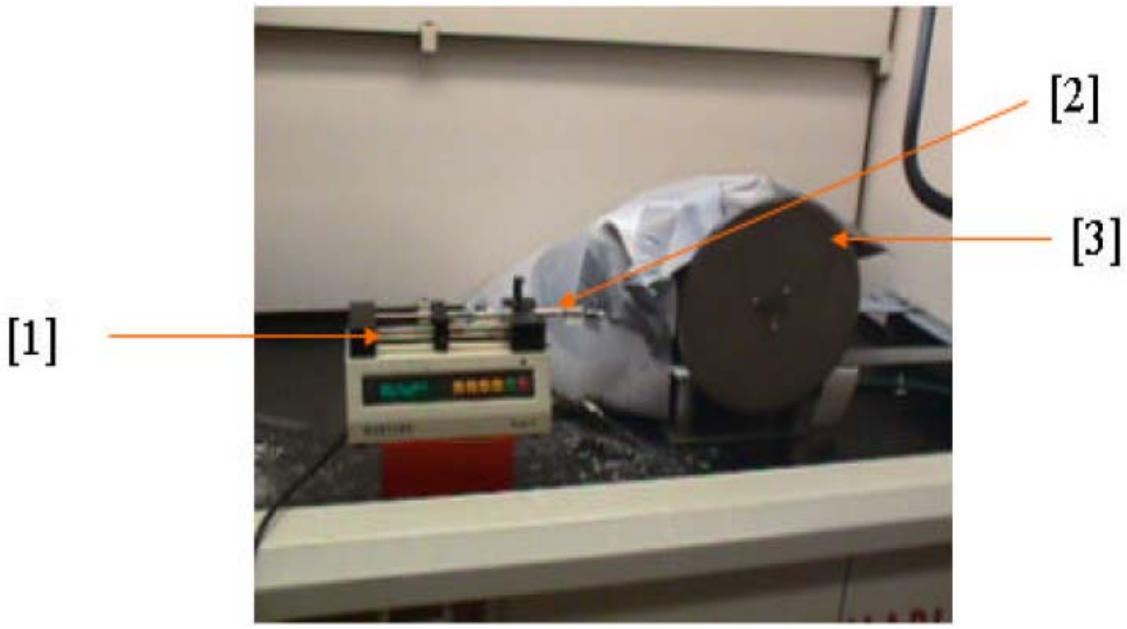

(a)

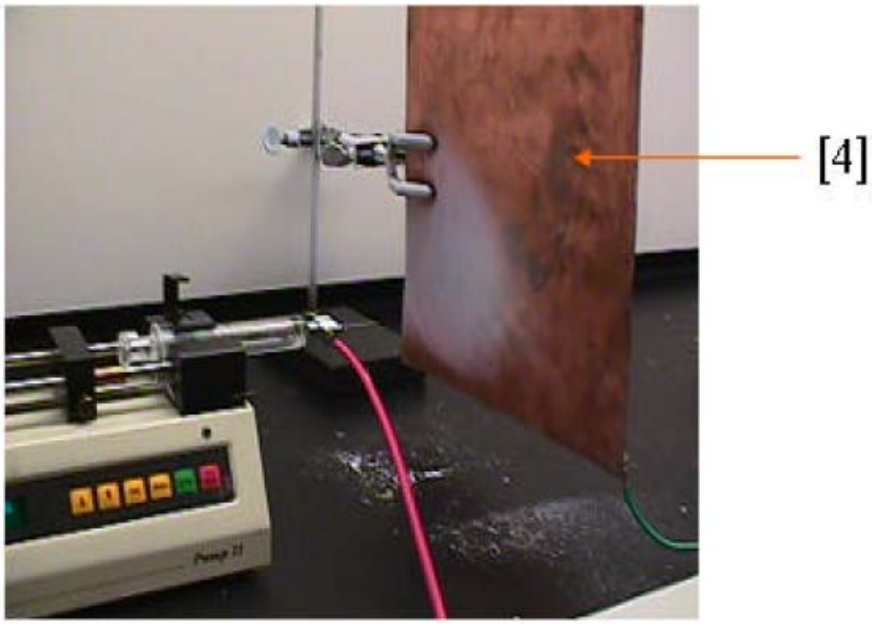

(b)

Figure 3.1 Electrospinning Experiment setup with rotating disc for orientation study (a) and with copper target for phase behavior study (b) [1] Displacement pump, [2] Glass Syringe, [3] Rotating Wheel, [4] Stationary Copper target.

the rotating speed was varied from 0 to 60 Hz. Figure 3.1 (b) shows the electrospinning experimental setup for phase behavior study.

3.3 Characterization methods

3.3.1 Fourier transform infrared spectroscopy (FTIR)

A Biorad FTS 6000 FTIR spectrometer (setting shown in Table 3.1) was used in this project to determine orientation factors. A polarizing filter was put between the sample and the incident beam to measure the dichroism ratio. The samples were cut from the non-woven nanofiber membrane as a small piece with 0.6 cm in diameter, 0.005 mm in thickness. Deuterated tri-glycine sulfate (DTGS) was used as detector, and potassium bromide as beam splitting crystal.

In order to calculate the dichroism ratio of the sample, the polarizer was placed in the optical bench, the polarizer was set to 0 or 90 degrees and separate backgrounds for

Table 3.1 Experimental setting of FTIR spectrometer

Speed	Filter	UDR	Resolution	Sensitivity
5 kHz	1.2	2	4 cm^{-1}	1 cm^{-1}
Scans to co-add	Save range	IR source	Beam	Detector
256	4000-400 cm^{-1}	Mid-IR	Internal	DTGS

parallel and perpendicularly polarized light were recorded. Then the sample was mounted onto the sample holder, loaded into the sample compartment and spectra were collected with both 0 and 90 degree setting of the polarizer. The computer calculated spectra using the background files obtained earlier. For nylon 66, N-H stretching band at 3303 cm^{-1} was used as the characteristic peak to calculate dichroism. For polyvinyl chloride, the C-Cl stretching bands at 613 and 639 cm^{-1} were used. The dichroism D, is calculated using the following equation:

$$\mathbf{D = A_{\|} / A-}$$

where $\mathbf{A_{\|}}$ is the measured absorbance of the characteristic peaks, when the polarization direction is parallel to the winding direction and A- is the measured absorbance when the polarization direction is normal to the winding direction. In this experiment, A|| and A- were calculated as the total area of the characteristic peak obtained by software when the polarizer was set to 0 and 90 degrees respectively.

The orientation function f (overall orientation including fiber orientation and molecular orientation within the fibers) for each sample was calculated from the dichroism ratio by the following equation:

$$f = \frac{C\,(D-1)}{(D+2)}$$

where

$$C = \frac{(2\cot^2\beta + 2)}{(2\cot^2\beta - 1)}$$

and **β** is the angle between the function group and the polymer backbone [**70**]. **β** is 90º for both C-Cl and N-H. Therefore, the above equation is simplified as follows:

$$f = \frac{-2\,(D-1)}{(D+2)}$$

The Biorad FTS6000 is shown in Figure 3.2.

3.3.2 Dynamic mechanical analysis

The Rheometrics DMTAV dynamic mechanical analyzer was used in this project. The fiber bunch was cut into a cylinder shape. The diameter for DMA test was estimated by

Figure 3.2 Fourier transform infrared spectrometer Bio Rad FTS 6000

the equation:

$$d = 2*(w/\rho\pi l)^{1/2}$$

where w is the weight of the fiber bunch, ρ is the density of the fibers in the bunch, 1.14 g/mol for nylon 66, 1.2 g/mol for polycarbonate, 1.4 g/mol for poly (vinyl chloride); l is the length of the fiber bunch. Two kinds of tests were performed on the sample: dynamic temperature ramp test and static strain rate test. The former was performed in tension on the as-spun nanofibers for the phase behavior study. The E', E", Tan δ data were obtained from room temperature to 200 °C with a heating rate of 1 °C/min, a frequency of 1 Hz and a strain amplitude of 0.1%. The latter was performed in tension on the as-spun nanofibers for orientation factor study. The stress and strain plot was obtained from room temperature with a constant stain rate of $2.5*10^{-4}$ (1/s). The tangent modulus was determined at 10% strain. The modulus gave information about the orientation comparison between the different fibers samples. The Rheometrics DMTAV dynamic mechanical analyzer is shown in Figure 3.3.

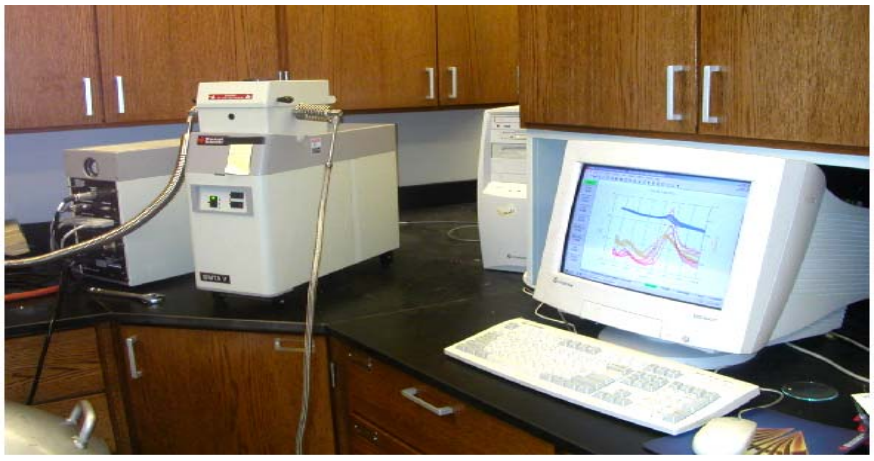

Figure 3.3 Rheometrics dynamic mechanical analyzer DMTA V

3.3.3 Scanning electron microscopy

Leo 1525 scanning electron microscope was used in this project to observe the polymer nanofibers' surface morphology and dimensions and to determine fiber orientation. Low emission voltage of 3 kV was used and the aperture size was kept at 60 mm. The as-spun fiber matrix was gold coated using a SPI Module™ sputter coater, with 20 mA current for 10 seconds, to avoid charging. The sample was placed on a carbon tape and attached to a sample stool that was placed on a sample holder to load into the vacuum chamber. After the vacuum is lowered to 1.5 x 10^{-5} Torr, SEM observation began. The images were prepared and focused using scanning speed 3, and were captured using scanning speed 5. The images were saved as TIFF file forms after stopping the scan. Leo 1525 scanning electron microscope is shown in Figure 3.4.

3.3.4 Transmission electron microscopy

Hitachi H-800 Transmission electron Microscope was used in this project to observe the phase behavior of the nanofibers. For the preparation of TEM samples, the as-spun fibers were electrospun directly on the carbon grids (0.25 cm in diameter) and underwent heat treatments. Then they were stained by RuO_4 vapor by suspending them over a RuO_4 solution for 1 hour. The staining RuO_4 solution was obtained by mixing 0.3g $NaIO_4$ and 0.15g RuO_2 to 25ml H_2O and RuO_4 was generated *in situ*. [**71**]

Figure 3.4 Scanning electron microscope Leo 1525

A transmission electron microscope studied the phase morphology of the nanofibers. The Hitachi H-800 Transmission electron Microscope is shown in Figure 3.5.

3.3.5 Manual measurement of orientation of fibers

The orientation factors of the fibers can be calculated by manual measurement of the fiber orientation distribution in the micrographs obtained by SEM using a protractor. Two lines were drawn, one of which was vertical and the other was horizontal on the SEM pictures. The angles of every fiber that intersected these two lines were measured with respect to the vertical line. Then a table that listed the angles ϕ and the number of the fibers that were oriented at these angles N (ϕ) was made. Then the angle at which N (ϕ) was a maximum was defined as ϕ=0 assuming this was the winding direction. The

Figure 3.5 Hitachi H-800 transmission electron microscope

average value of $<\cos^2\phi>$ is calculated from the equation below:

$$<\cos^2\phi> = \frac{\int_0^{2\pi} N(\phi)\cos^2\phi\, d\phi}{\int_0^{2\pi} N(\phi)\, d\phi}$$

The orientation factor measured for each speed of collection of fibers, was calculated using the Herman's Orientation function:

$$f = (\cos^2\phi - \sin^2\phi <\cos^2\theta>)$$

where θ is the angle between fiber axis and plane surface, in this case, θ is 0, so the equation is simplified and used as 2D Herman's orientation function:

$$f = 2 <\cos^2\phi> - 1$$

Chapter 4 Results and Discussion

4.1 Phase behavior study on electrospun nanofibers

4.1.1 Polymer system

Polycarbonate (PC) with molecular weight of 60,000 g/mol and polyvinylchloride (PVC) with molecular weight of 215,000 g/mol and their blends with weight ratio (PC/PVC) 25/75, 50/50, 74/25 were used to investigate the phase behavior of the nanofibers produced by electrospinning process. The electrospinning condition for all the polymer solutions is: 10wt% polymer solution concentration, 20 kV-applied voltage, 20 μL/min feed rate, 10cm gap distance. The clarity of the solution inside the syringe was checked before electrospinning. The polymer systems used were listed in Table 4.1.

Table 4.1 Polymer systems used to study the phase behavior of the fibers produced by the electrospinning process

Polymer (10wt%)	Solvent (90wt%)	Bulk solution clarity	Comments
PC/PVC (100/0)	THF/ DMF (3/2)	Clear	No phase separation
PC/PVC (75/25)	THF/ DMF (3/2)	Clear	No phase separation
PC/PVC (50/50)	THF/ DMF (3/2)	Clear	No phase separation
PC/PVC (25/75)	THF/ DMF (3/2)	A little Cloudy	Not Sure
PC/PVC (0/100)	THF/ DMF (3/2)	Clear	No phase separation

4.1.2 SEM observation on as-spun fibers

The as-spun nanofibers electrospun from pure PC, PVC and 3 PC/PVC blends were gold coated and underwent SEM observation. The surface morphology of the nanofibers is illustrated in Figure 4.1. From Figure 4.1, it is clear that fiber dimensions of the samples are not uniform. However, they are all in the range of 100-400 nm, and are not a significant function of blend composition.

4.1.3 Dynamic mechanical analysis

A dynamic temperature ramp test was used to determine the miscibility of the two polymers inside the nanofiber by investigating the variation of the glass transition temperature (Tg) of the nanofiber. Tan δ is plotted as a function of temperature for nanofibers electrospun from pure polymer solution and polymer blends in Figure 4.2. The temperatures of all the tan δ maximum are summarized in Table 4.2. For each of the PC/PVC blends, there was only one distinct tan δ peaks discernible. The glass transition temperatures of the blends are in good accordance to the Fox equation as illustrated in figure 4.3.

$$1/Tg=w_1/Tg_1+w_2/Tg_2.$$

where w_1, w_2 are the mass fraction of the two polymers (PC and PVC), and Tg_1, Tg_2 are the glass transition temperatures of the two pure polymers.

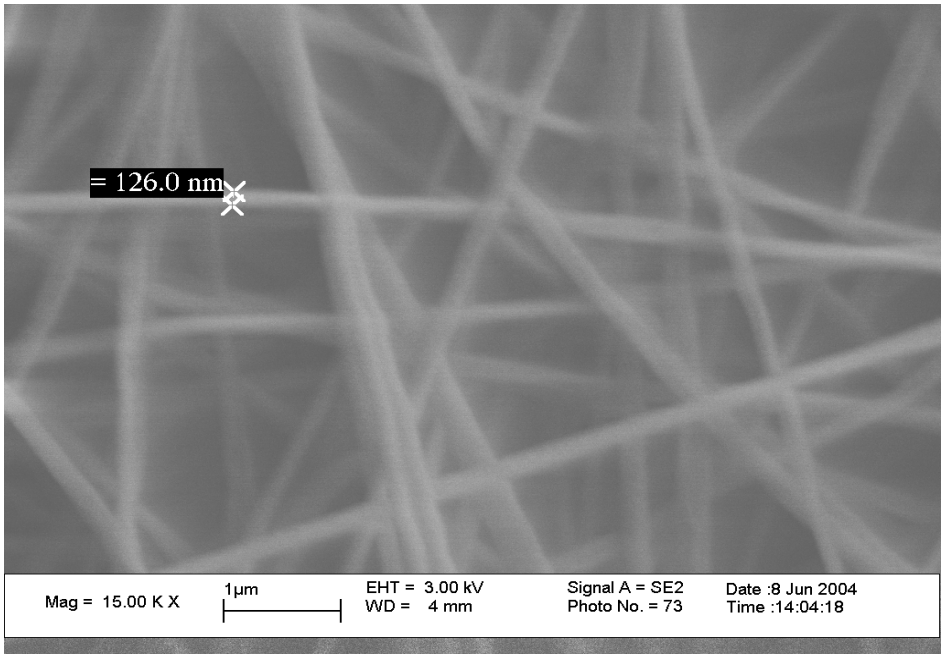

(a)

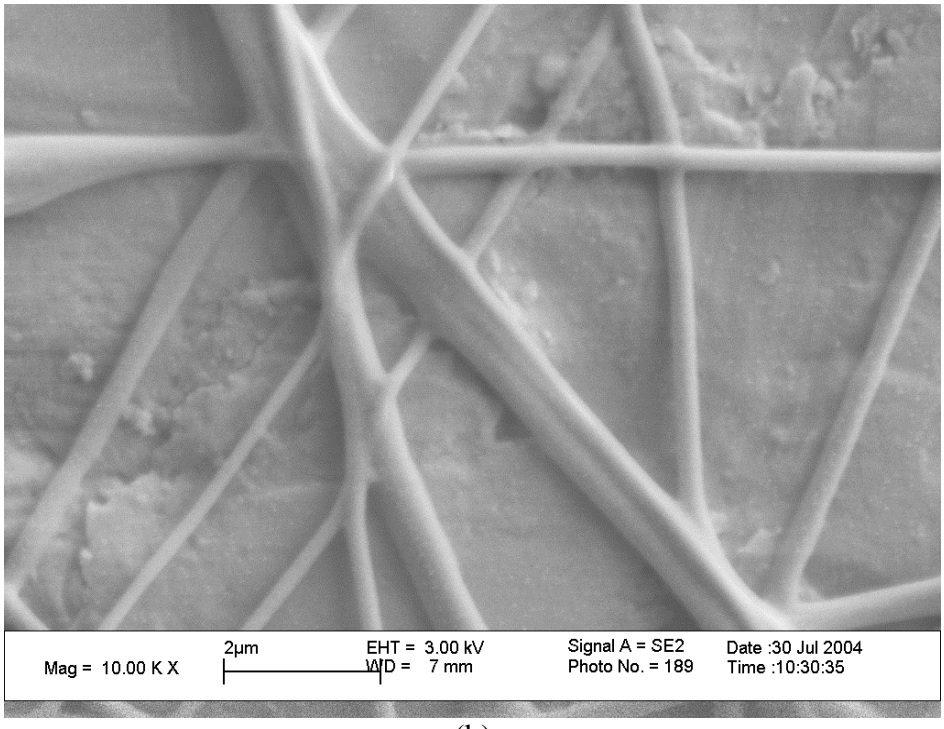

(b)

Figure 4.1 SEM images of nanofibers electrospun from (a) PVC (b) PVC/PC 75/25 (c) PVC/PC 50/50 (d) PVC/PC 25/75 (e) PC

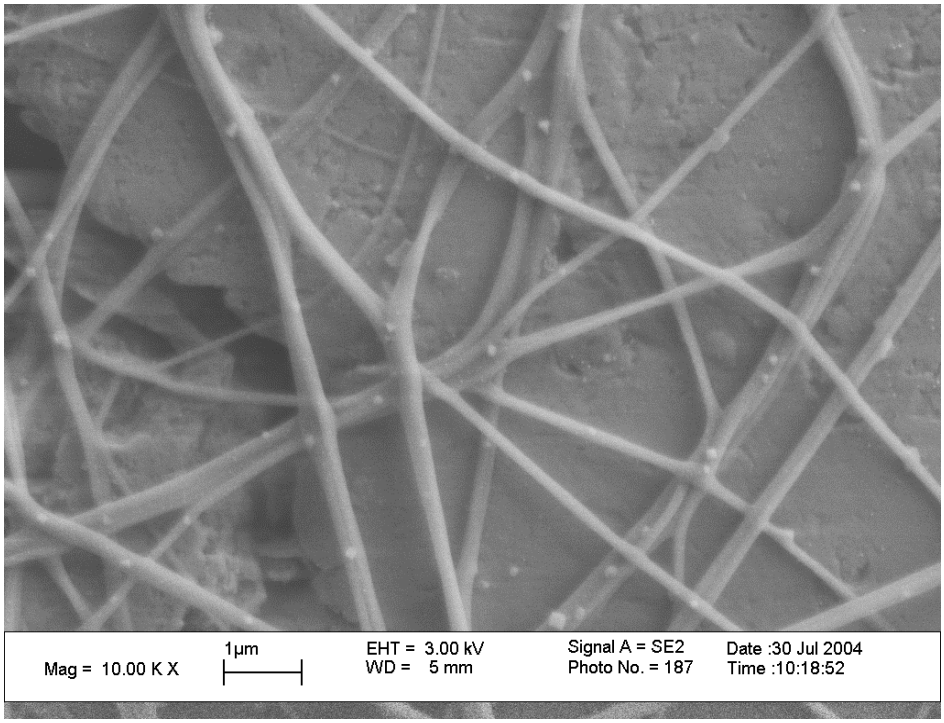

(c)

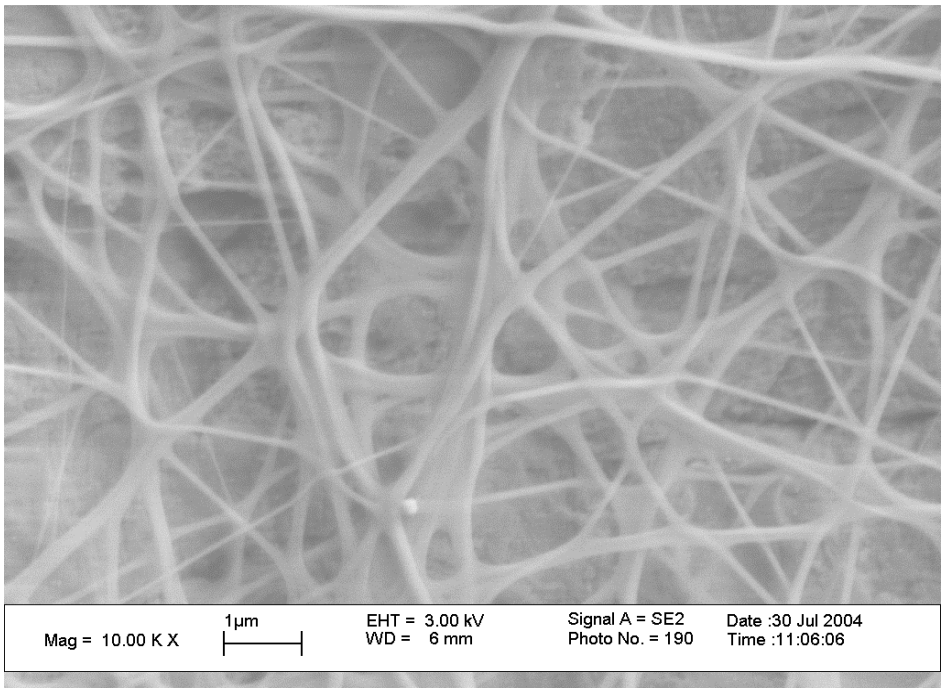

(d)

Figure 4.1 continued

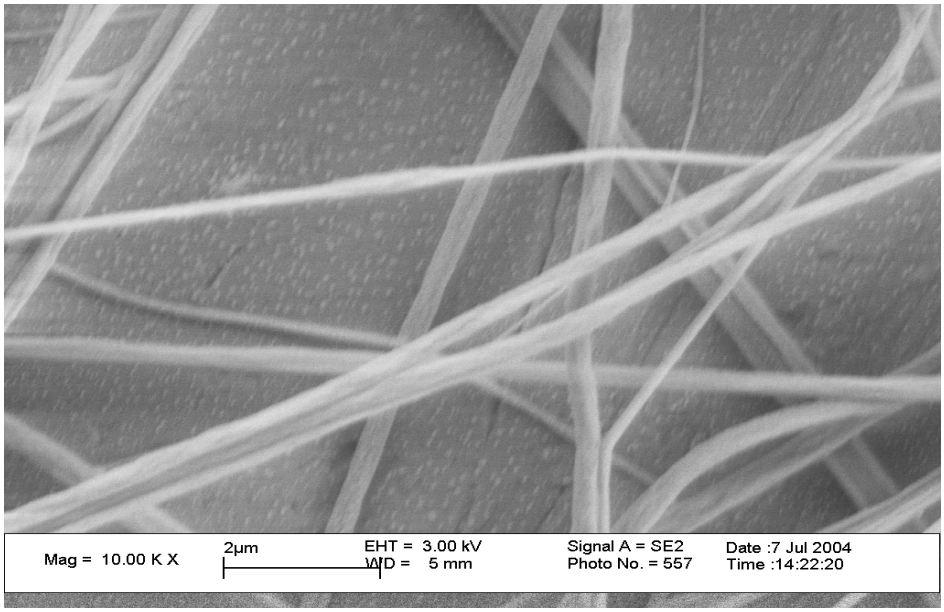

(e)

Figure 4.1 continued

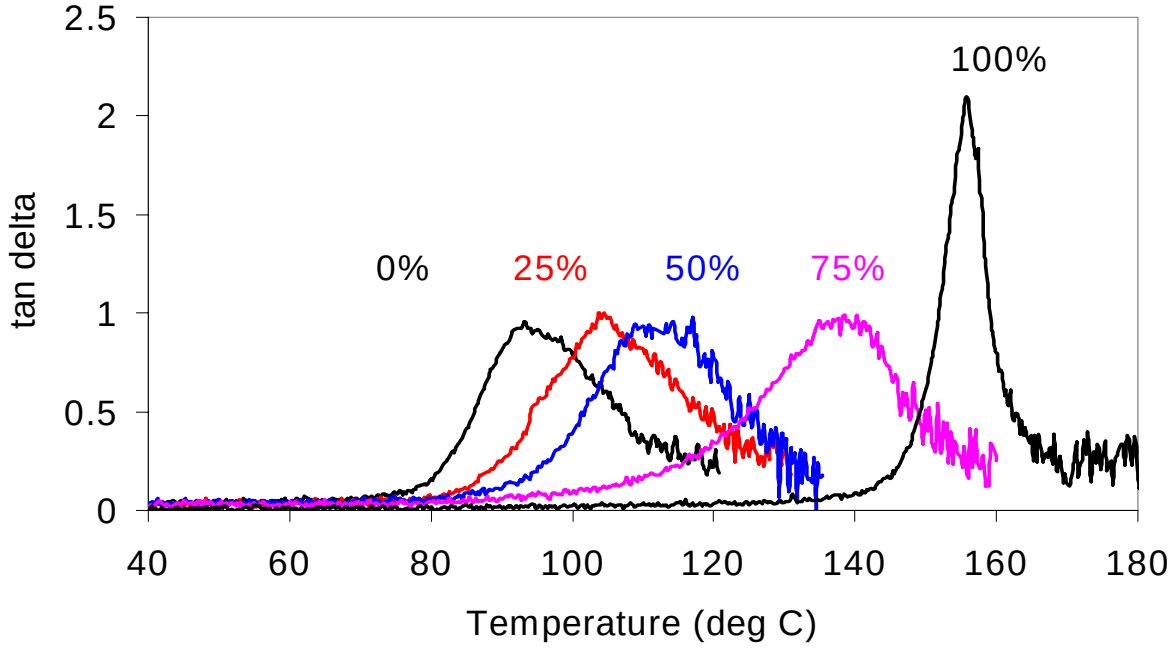

Figure 4.2 Tan delta vs. temperature for (a) pure PC (b) PC/PVC 75/25 (c) PC/PVC 50/50, (d) PC/PVC 25/75, (e) pure PVC. The percent showed in the figure indicates PC concentration.

Table 4.2 DMA results of pure polymer fibers and blends fibers.

Fiber composition (PC/PVC weight ratio)	Tg (DMA value) (° C)	Tg (Equation expectation) (° C)
0/100	95.1	
25/75	105.3	108.5
50/50	117	123
75/25	138.4	138.6
100/0	155.5	

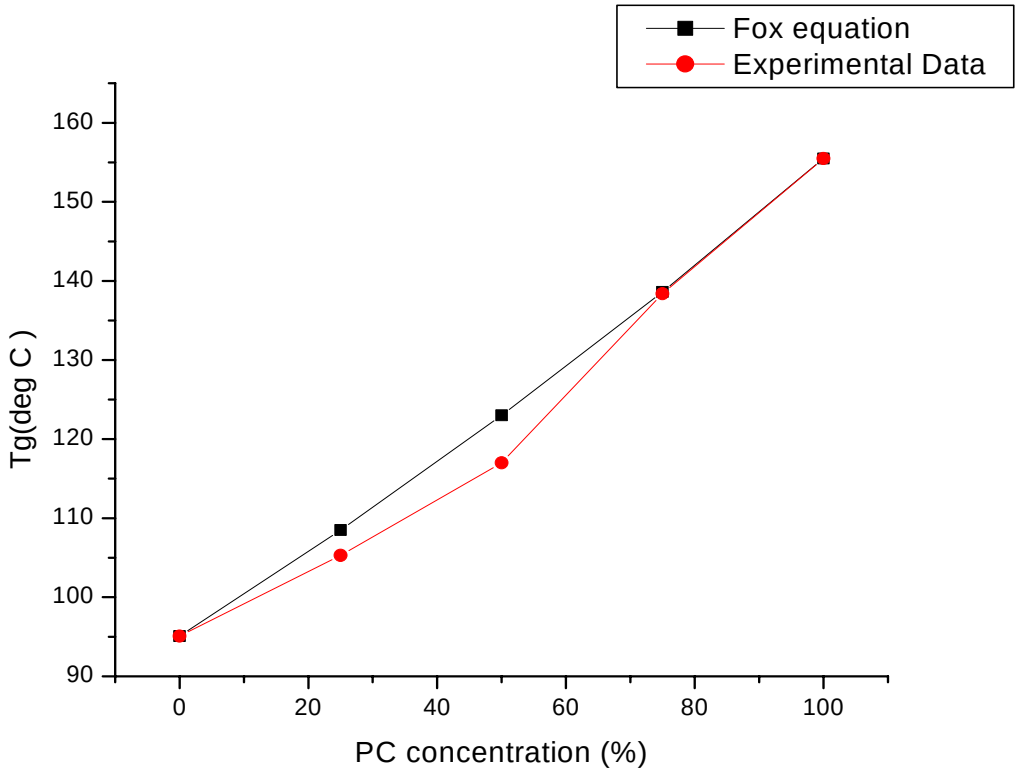

Figure 4.3 Tg vs. PC concentration in polymer blends for experimental DMA data and Fox equation expectation.

It is known that if polymer blends have only one glass transition temperature in DMA test and the Tg is in good accordance to the Fox equation, the polymer blends are miscible at the molecular level. From the DMA data, it is seen that the two polymers in these electrospun nanofibers are homogeneously mixed at the molecular level; the nanofibers have formed a single-phase structure.

In order to determine the effect of the electrospinning process on the phase behavior of the nanofibers produced from PC/PVC blends, a corresponding experiment was performed. The polymer blend solution (PC/PVC 25/75) was kept at room temperature for one day to let the solvents evaporate slowly. The same DMA Dynamic temperature analysis test was performed on the resulting membrane with the same test condition and setup. The Tanδ versus temperature plot is shown in Figure 4.4. From Figure 4.4, two distinct Tanδ peaks are discernible. The higher peak at 100° C was due to the Tg of PVC, while the broader and lower peak at around 160° C was due to the Tg of PVC. In contrast to pure PVC and PC, the Tg of PVC in the blend was a little bit higher and the Tg region of the PC was broader, which suggests that a very small fraction of PVC was miscible with the phase of PC and the interaction between them was very small.

In order to demonstrate the change in tan δ curves induced by phase separation, *in situ* DMA annealing was performed; and the temperature and tan δ data are shown in Figure 4.5 for PC/PVC 25/75. The nanofibers first underwent the same DMA dynamic temperature ramp test as described above with the same test condition. This

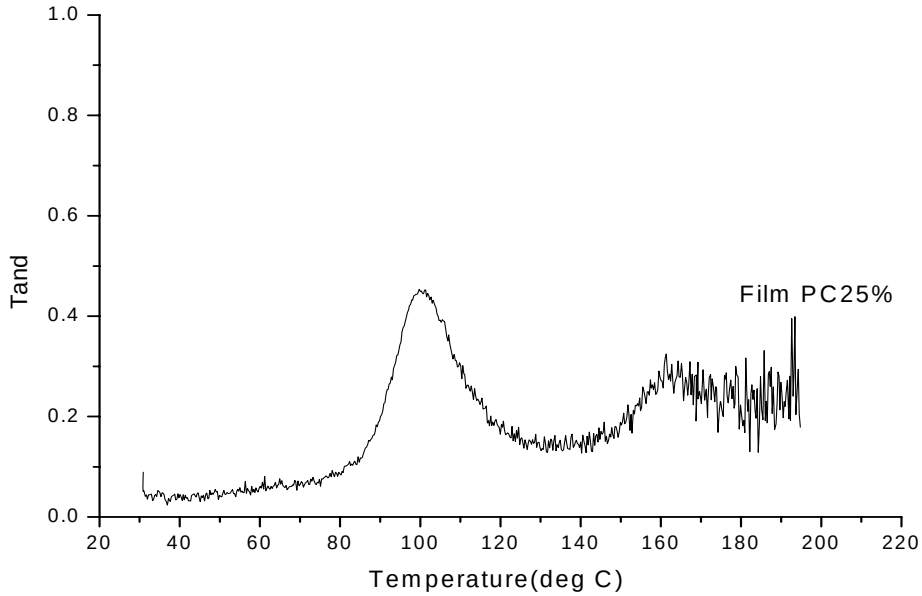

Figure 4.4 Tan δ vs. temperature for membrane from blend solution (PC/PVC 25/75)

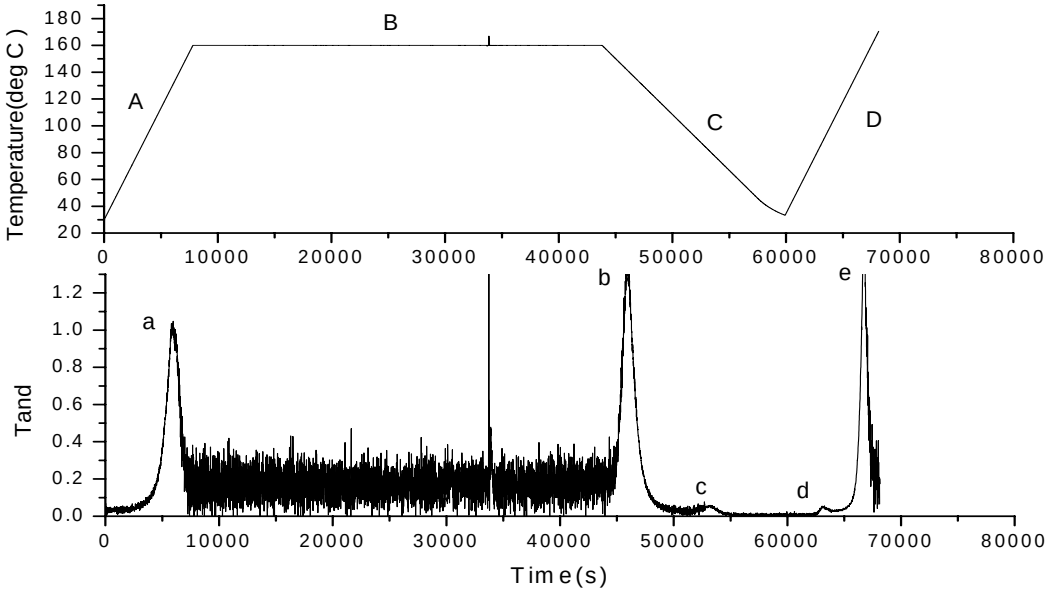

Figure 4.5 DMA test of Tan δ and temperature vs. time for PC/PVC 25/75.

experimental step corresponds to the section A in temperature vs time part of Figure 4.5. After the temperature reached T_g + 50 (160°C), the temperature was kept constant for 8 hours to induce phase separation of the two polymers in the nanofibers. This experimental step corresponds to the section B in temperature vs time part of Figure 4.5. Then the samples were cooled down to room temperature, which is illustrated as section C in Figure 4.5. At last, the nanofibers underwent same DMA dynamic temperature ramp test again as in section A. The final experimental set was shown in section D in Figure 4.5. PC/PVC 50/50 and PC/PVC 75/25 samples were subject to the same in situ DMA annealing, but with different constant temperatures to induce phase separation. The glass transition tanδ peaks for all the samples are illustrated in Figure 4.6 and the corresponding T_gs are listed in Table 4.3. The first heat corresponds to the heating process of experiment step section A in temperature vs time part of Figure 4.5, while the second heat corresponds to the heating process of experiment section D in temperature vs time part of Figure 4.5.

From Figure 4.5, it is very clear that the as-spun fiber has only one peak, shown as point a in tan δ vs time part of Figure 4.5, which means the two polymers were miscible on the molecular level. After heat treatment, the resulting fibers showed two discernible peaks, which means that phase separation occurred during the process. Points b and e correspond to T_g of PC phase in cooling and reheating steps respectively, while points c and d correspond to T_g of PVC phase in cooling and reheating steps respectively.

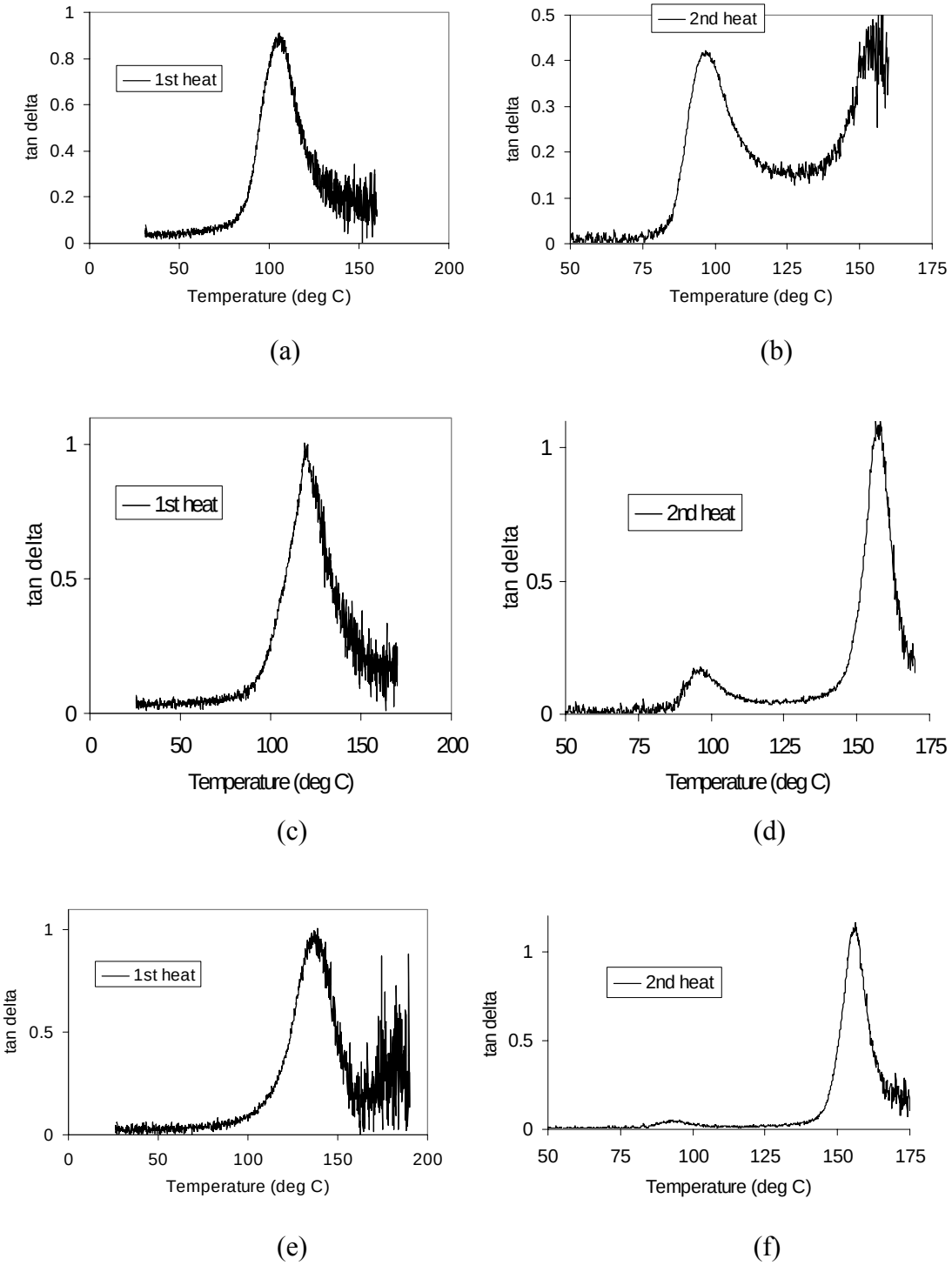

Figure 4.6 Tan delta peak for glass transition for as-spun fibers and fibers underwent heat treatment. (a), (c), (e) are for as-spun fiber PC/PVC 25/75, 50/50,75/25 respectively; (b) for PC/PVC 25/75 annealed at 160 °C (Tg+55) for 8.3hr; (d) for PC/PVC 50/50 annealed at 170°C (Tg+50) for 8.3hr; (f) for PC/PVC 75/25 annealed at 190°C (Tg + 52) for 8.3hr.

Table 4.3 Tgs of PC/PVC samples in first heat and second heat in in situ DMA anneal.

Nanofibers sample	T_g in first heat (°C)	T_{g1} in second heat (°C)	T_{g2} in second heat (°C)
PC/PVC 25/75	105.3	96.8	154.6
PC/PVC 50/50	117	96.2	155.5
PC/PVC 75/25	138.4	95.3	155.5

From Figure 4.6, it is very obvious that after heat treatment, the as-spun fibers underwent phase separation because there are two distinct glass transition peaks. With the decrease of PVC concentration (Figure 4.6 b-d-f), the intensity of PVC glass transition decreases, and the Tg shifts to slightly lower temperature, from 96.8°C to 95.3°C, shown in Table 4.3. The Tg of the PC phase seems unchanged with the decrease of PVC concentration, and the intensity of PC relaxation increases from Figure 4.6 b-d-f. Based on these phenomena, it is reasonable to conclude that after phase separation in the case of PVC/PC 75/25, the PC phase forms discontinuous domains in the PVC continuous domains, while in the case of PVC/PC 25/75, the situation is reversed, with PVC forming discontinuous matrix dispersed in the continuous matrix of PC phase. PC/PVC 50/50 may form some intermediate co-continuous structure. Since the PC and PVC discontinuous phases have minor contribution to the modulus in a DMA test, the intensity of PVC Tg peak decreases from b-d-f as PVC concentration decreases. A similar trend happens to PC Tg peak from Figure 4.6 f-d-b as PC concentration decreases. It is also reasonable to suggest that PC phase is slightly soluble in PVC phase, while PVC phase is not soluble in PC phase.

Therefore, the interaction between the two phases has stronger influence on PVC phase than on PC phase, resulting in a constant PC Tg with the increase of PVC concentration (Figure 4.6 f-d-b). The cause of the shift to lower temperature in PVC Tg with the increase of PC concentration (Figure 4.6 b-d-f) is not fully understood at this moment, it may be due to the solvent residue.

4.1.4 TEM observation on annealed nanofibers

In order to study morphology development during annealing, the as-spun fibers were heated to T_g + 40 °C for 1, 8, 16, 48 hours respectively. After that, the fibers were stained by ruthenium tetroxide to selectively stain PC phase due to its ability to stain aromatic polyesters, in particular PC and PET [**72**]. Transmission electron microscopy (TEM) was used to observe the morphology of the stained fibers. The observed morphology of the fibers is shown in Figure 4.7 (PC/PVC 25/75), which clearly reveals the biphasic morphology in which PC phase appeared dark and the PVC phase appeared lighter. In Figure 4.7, it is obvious that the dark PC domains seem to elongate to form elliptical particles and these particles are aligned along the fiber axis. The dimensions of those domains grow larger from a-c, and the number of the PC domains grows much larger from c-d, though every individual domain size may become small. Also, in c and d, the dark PC domains lie on the surface of the fiber. The PC domain dimensions in Figure 4.7 are listed in Table 4.4. For each figure, 5-10 PC elliptical particles were measured. The length of the long axis and the short axis of the ellipse was taken. The average values

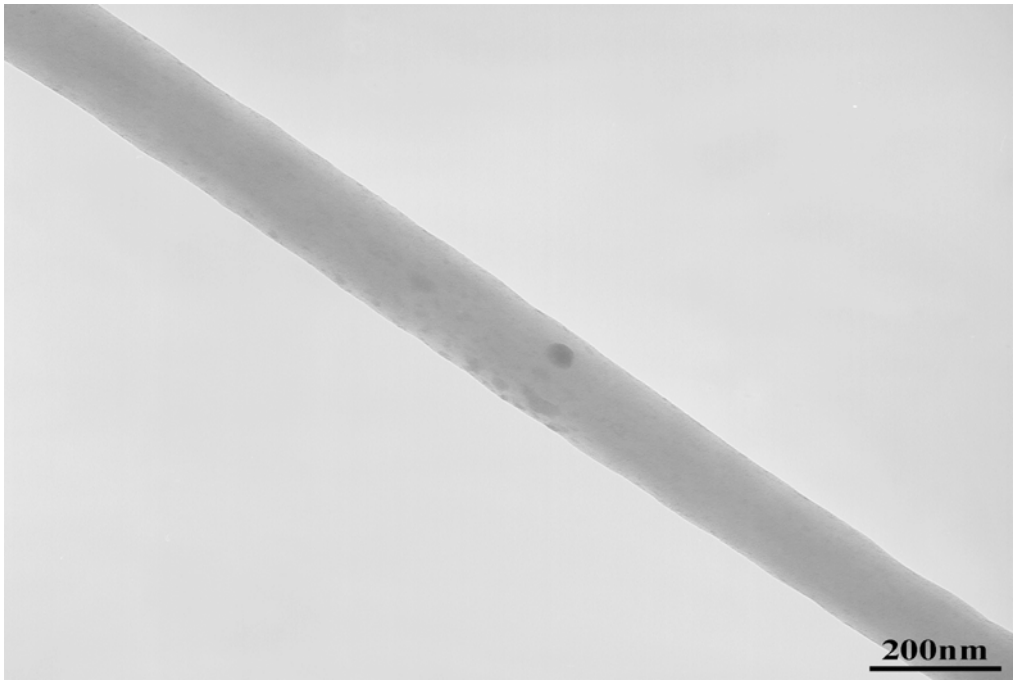

(a)

(b)

Figure 4.7 TEM images of annealed PC/PVC 25/75 blend after staining by RuO_4 for 1 hour. The annealing temperature is T_g +30 °C for sample a, T_g +40 °C for sample b-d. The annealing times: (a) 16 hours (b) 8 hours (c) 16 hours (d) 48 hours

(c)

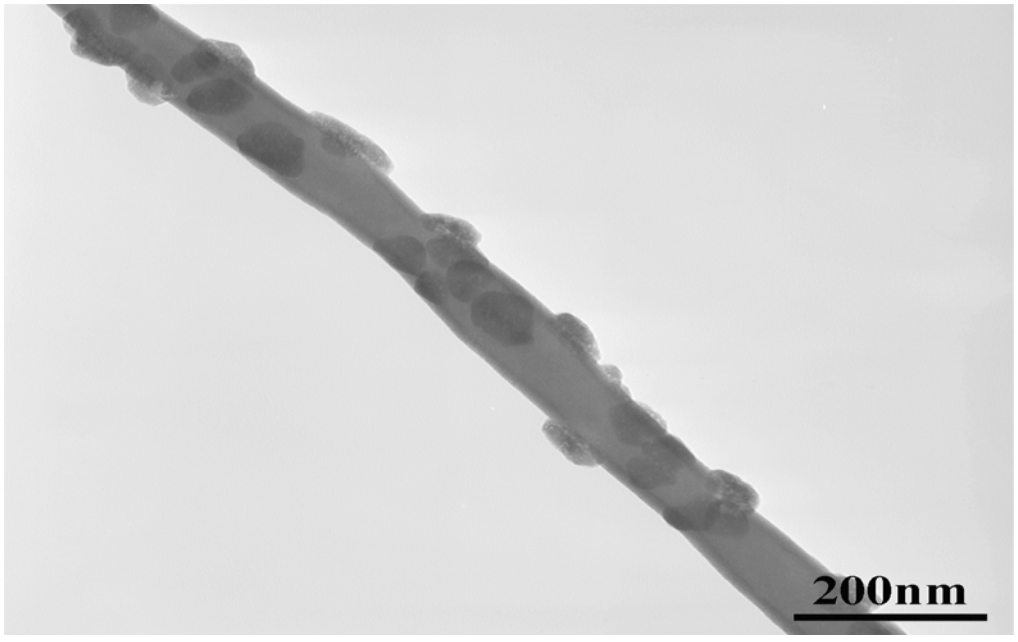

(d)

Figure 4.7 continued

Table 4.4 PC domains sizes in TEM figures.

Time (hr)	Temp (°C)	Major Axis length (nm)	Minor Axis length (nm)
1	Tg+40	38.3±10.0	20.0±9.8
8	Tg+40	83.3±56.2	50.8±34.1
16	Tg+40	120.6±40.8	66.7±32.7
48	Tg+40	74.8±21.0	48.9±10.0

and standard deviations were calculated. Since PC and PVC are both amorphous polymers and the annealing temperatures are all under T_g +50 °C, Figure 4.7 a's annealing condition, T_g +30 °C for 16 hours can be converted T_g +40 °C in a different time scale according to the Williams-Landel-Ferry (WLF) equation for comparison. [**73**]

$$\text{Log } a_{T1} = C_1(T-Ts)/C_2+(T-Ts)$$

$$\text{Log}a_{T2} = \text{Log}(a_{T1/}\, a_{T2}) = C_1(T_1-Ts)/C_2+(T_1-Ts)-C_1(T_2-Ts)/C_2+(T_2-Ts)$$

$$\text{log}t_2 = \text{log}t_1 + \text{Log}a_{T2}$$

where a_{T1} is the horizontal time shift factor of any temperature within a temperature range of Ts ± 50 °C to the reference temperature Ts; a_{T2} is the time shift factor of temperature T_1 to temperature T_2. C_1 and C_2 are WLF constants for amorphous polymers, taken as universal constants here C_1=17.44, C_2=51.6; Ts is the reference temperature and taken as Tg here. T_1 and T_2 is Tg + 40 °C and Tg + 30 °C respectively. t_1 is the time scale. The relationship between the average major axis and minor axis length of PC phase and the square root of heating time is illustrated in Figure 4.8.

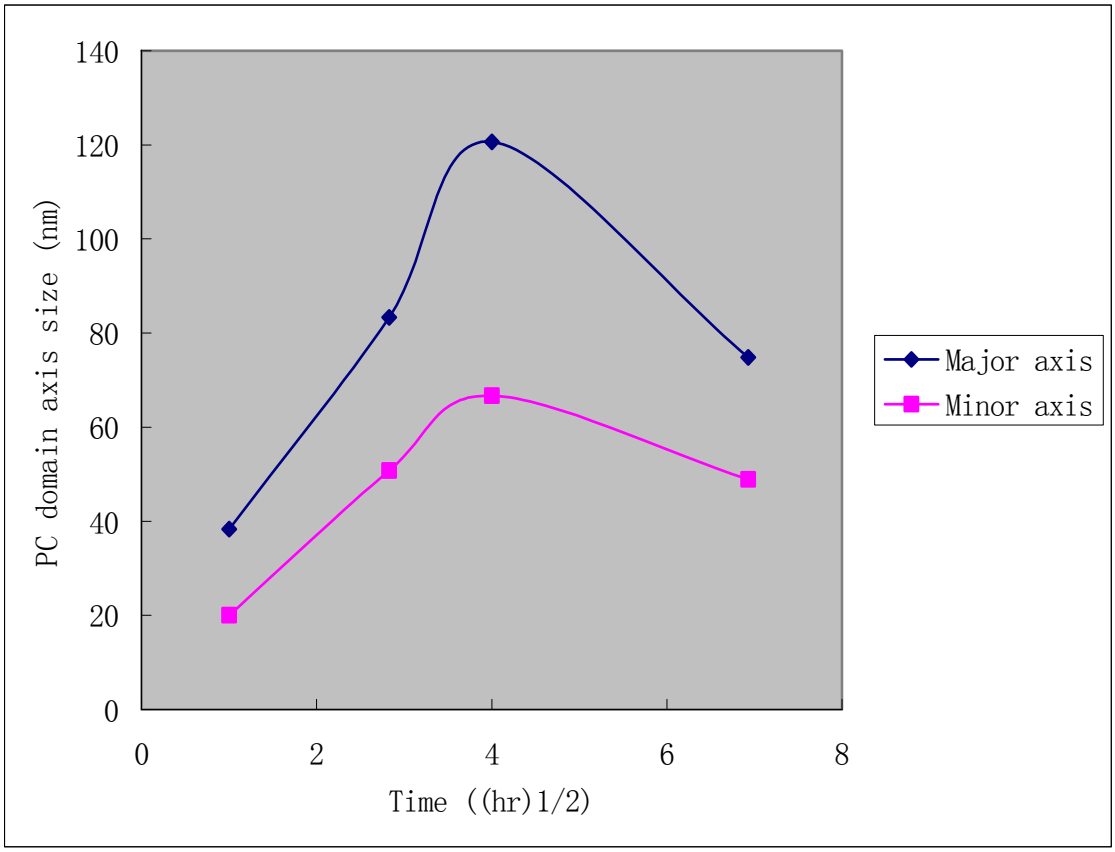

Figure 4.8 PC domain axis growth vs. annealing time square root for PC/PVC 25/75 blend

From the TEM micrographs, it is clear that after heat treatment, which induced phase separation to the once homogeneous blend system, the PC tends to aggregate to form small particles oriented along the fiber axis and dispersed in the PVC matrix. Comparing the figures with different heat treatment time, the phase structure became coarser with the increase of the heat treatment time. The particles of the PC phase became larger in diameter and aggregated together to form even larger domains and the interface between the particles and the matrix became less obscure. From Figure 4.8, it is obvious that the

phase dimension of PC phase grows in a linear way with the square root of time, which is a typical situation in diffusion-controlled coarsening. The linear relationship seems not be followed after 48 hours. It may be due to capillary effect caused by the smaller diameter of the fiber in Figure 4.7 d. However, from Figure 4.7 d, the number of the PC domains is much larger than those in Figure 4.7 a-c.in temperature of T_2 and t_2 is the time scale after temperature converted to temperature T_1. Using these equations, the time scale of sample a converted to T_g + 40 °C is one hour.

4.1.5 Discussion

The phase behavior in polymer blends is very complicated; not only thermodynamic factors but also kinetic factors will affect this process [**24**]. Generally speaking, due to the high molecular weight of polymer molecular chains, the mixing entropy of polymers is very small and usually the mixing process is endothermic. So, usually the Gibbs free energy, ΔGm, is positive; which causes most polymer blends to be two-phased if the system is given enough time to equilibrate. However, that is not always the case in electrospinning process, in which the solvent evaporates and fiber solidifies on a time scale of milliseconds. Such a short period of time may not allow the two polymer components to diffuse to form separated phases before the fiber solidifies, resulting in a one-phase morphology. It has been reported in earlier research of polymer blends electrospinning [**23, 24, 74**] that electrospun polymer blends will show fine phase morphology rather than a coarse one with an expected preference for co-continuous

structure rather than matrix-dispersed one due to the quick solvent evaporation. It was observed that in the present case, not only was the coarsening processing in phase-separation process delayed, but even the whole phase-separation process was suppressed by the electrospinning process. The PC/PVC membrane, which was given enough time to evaporate, showed phase separation behavior, which is evident that the phase separation of the PC/PVC blend is favored thermodynamically, but was hindered kinetically in electrospinning. Because of the solubility parameter difference of the two polymers, the blends were intended to phase separate given enough time, which is the case of the membrane according to DMA data. However, in electrospinning, the solvent evaporates much quicker than the two polymers can diffuse, and the fiber solidification causes the polymer blend to freeze into a one-phase structure, which is the kinetic reason for one-phase structure. Given enough time above T_g, the polymer chains will diffuse fast enough to separate from each other and the one-phase structure will be destroyed to form a two-phase structure. The morphology of the two-phase structure was determined by the annealing temperature and time.

4.2 Study on the relationship between molecular orientation of electrospun nanofibers

For some applications, not only the fiber diameters and their intrinsic properties but also the fiber orientation and the molecular orientation inside nanofibers are important. For tissue engineering, well-aligned nanofibrous scaffold produced by electrospinning will

better support cell culture and improve cell growth because of the fiber orientation. [**64, 65**] For composite reinforcement, carbon nanofibers widely used as fiber fillers can be produced from electrospun PAN precursor fibers, [**75**] and the molecular orientation of the precursor fiber will influence the mechanical properties of the carbon nanofibers and the efficiency of the reinforcement effect. Although orientation has been observed by electrospinning fibers directly onto a rotation drum, [**60, 76, 77**], very few papers have quantified it [**67**]. In these papers dealing with orientation, wide angle X-ray diffraction (WAXD) was normally used, since WAXD is one of the mostly used methods to determine crystal orientation within fibers. However, for polymers that do not crystallize, or have very low crystallinity, WAXD will not be useful to determine the chain orientation within the fibers. In those papers, the orientation measurements were performed on nanofiber non-woven mats. The molecular orientation factors obtained by either FTIR or WAXD is usually the molecular orientation with respect to the fiber winding direction and actually the combination of both fiber orientation and molecular chain orientation within the fibers. In this work, a method is developed to combine FTIR and SEM analysis to eliminate the effect of the fiber orientation and obtain only the molecular orientation within the fibers with respect to the fiber axis. The relationship between two electrospinning process parameters, (applied voltage, polymer molecular weight) and the molecular orientation within the electrospun nanofibers were investigated. The mechanical properties of the nanofibers mats were also studied, which has been barely addressed previously in the literature. [**53, 58, 78, 79**]

4.2.1 Effect of applied voltage on the molecular orientation

Nylon 66 nanofiber mats were directly electrospun onto the metal wheel at nominal test conditions of 10 wt% concentration, 10 cm target distance and at constant rotation frequencies of 20 Hz and 40 Hz. The applied voltages were varied over 15, 17.5, 20, 25 and 30 kV for each rotation frequency. SEM images were taken for each sample, shown in Figure 4.9 and Figure 4.10. Manual measurements were performed on the SEM pictures as discussed in Chapter 3 and the fiber orientations were obtained and demonstrated in Figure 4.11. FTIR scans were also performed on those mats and one of the spectra is shown in Figure 4.12 (nylon 66 electronspun at 20 kV and 40Hz). The overall orientations in those mats were calculated by the dichroism of N-H stretching at 3303 cm^{-1} and are presented in Figure 4.13. The standard deviation is calculated. For both FTIR and Manual measurements, five repetitive measurements were performed to obtain an average value as the final result. By dividing those two orientations, the molecular orientation within nanofibers was obtained and the relationships between it and the applied voltage for two rotation frequencies are demonstrated in Figure 4.14.

From Figure 4.11, it seems the fiber orientation changes in a complicated fashion with the increase of the applied voltage for both rotation frequencies. The orientation factor variation is not much. The variation range for 20 Hz is from 0.67 to 0.74; the range for 40 Hz is from 0.69 to 0.78. From Figure 4.13, it is clear that the overall orientation of both rotation speeds changes in a similar fashion with the increase of the applied voltage, first

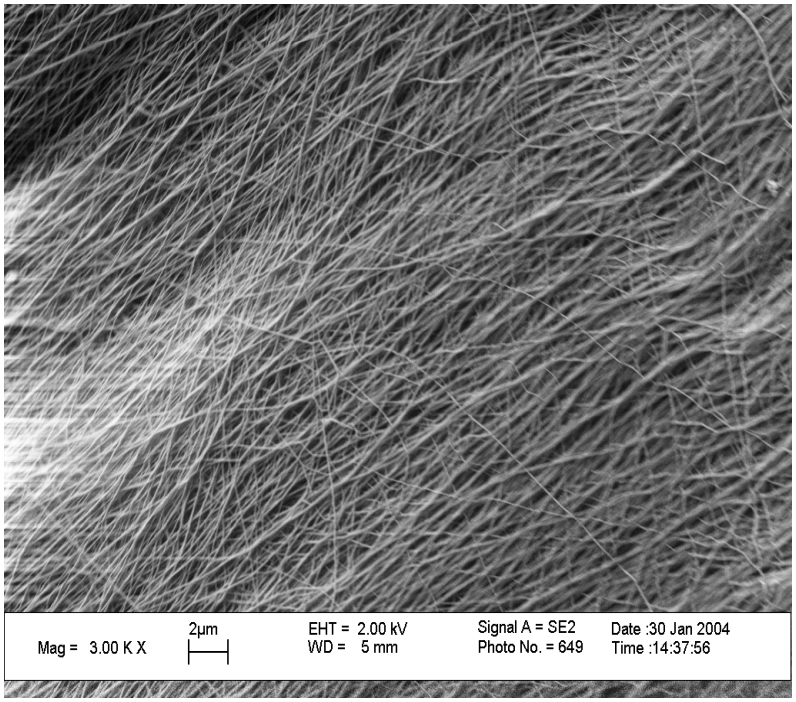

(a)

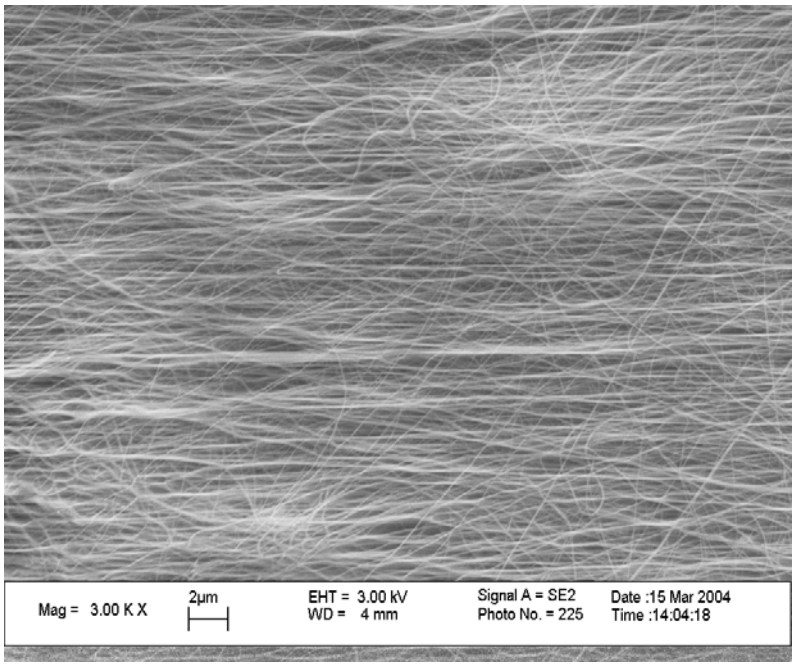

(b)

Figure 4.9 Nylon 66 fibers wound collected at 10 wt% concentration, 10 cm target distance, at a wheel speed of 926 m/min, 20Hz, The applied voltage is 15 Kv for (a); 17.5 kv for (b); 20 kV for (c); 25 kV for (d); 30 kV for (e).

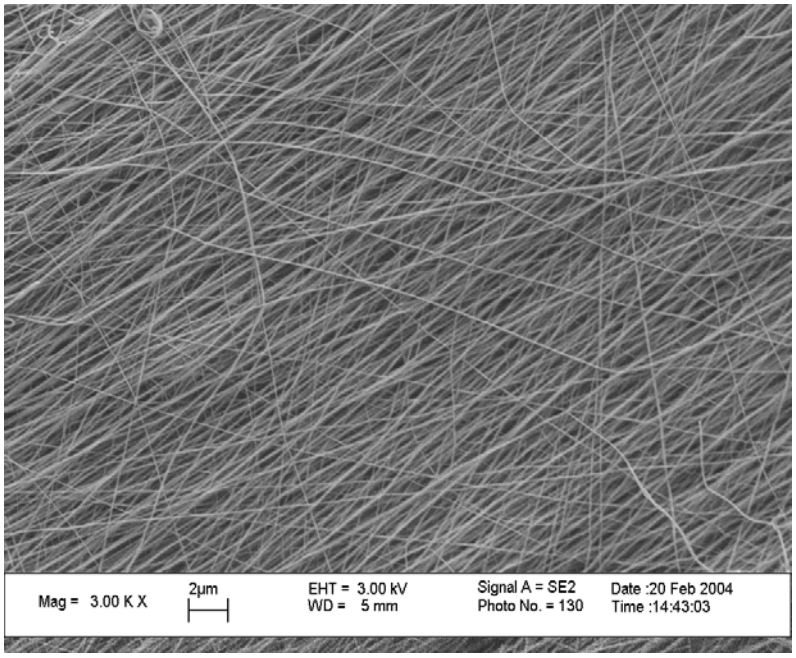

(c)

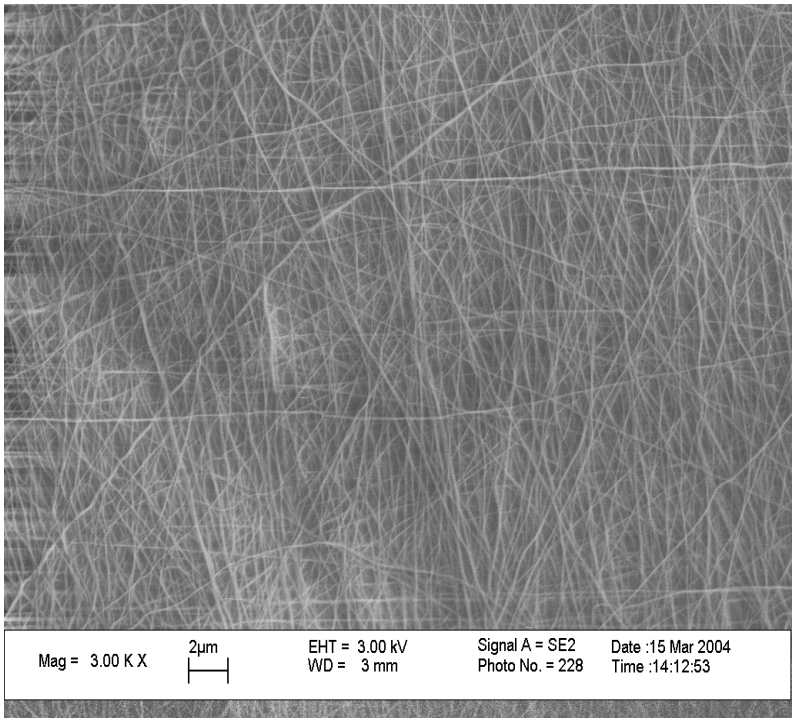

(d)

Figure 4.9 continued

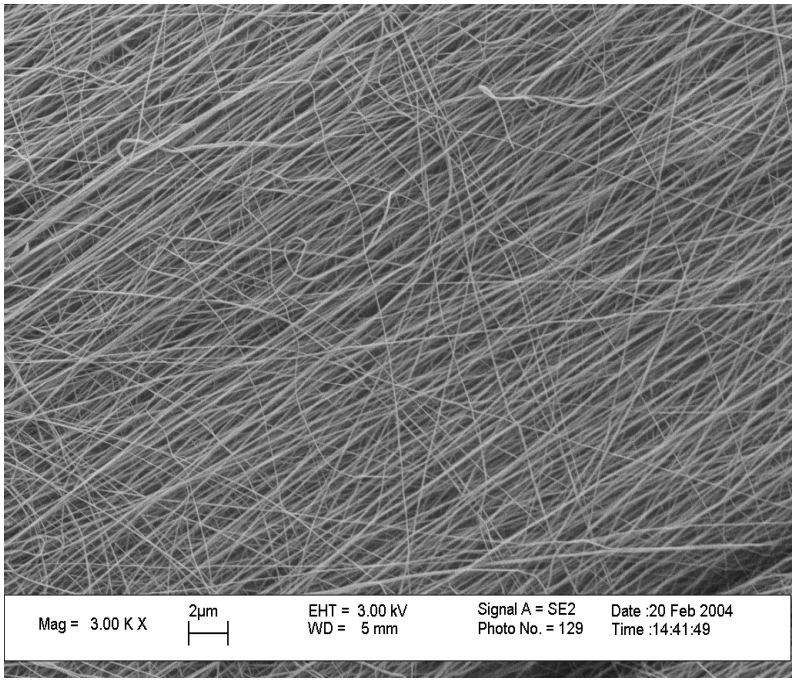

(e)

Figure 4.9 continued

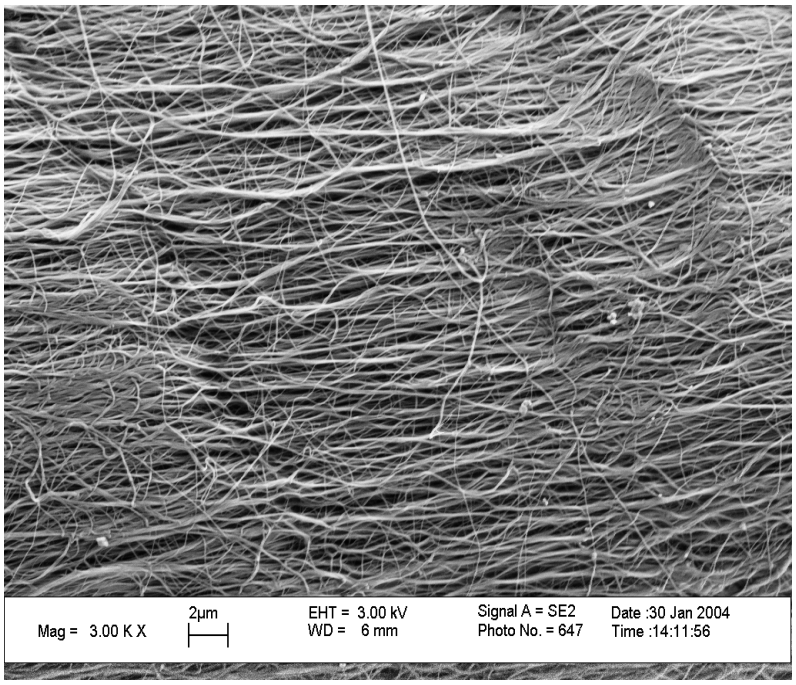

(a)

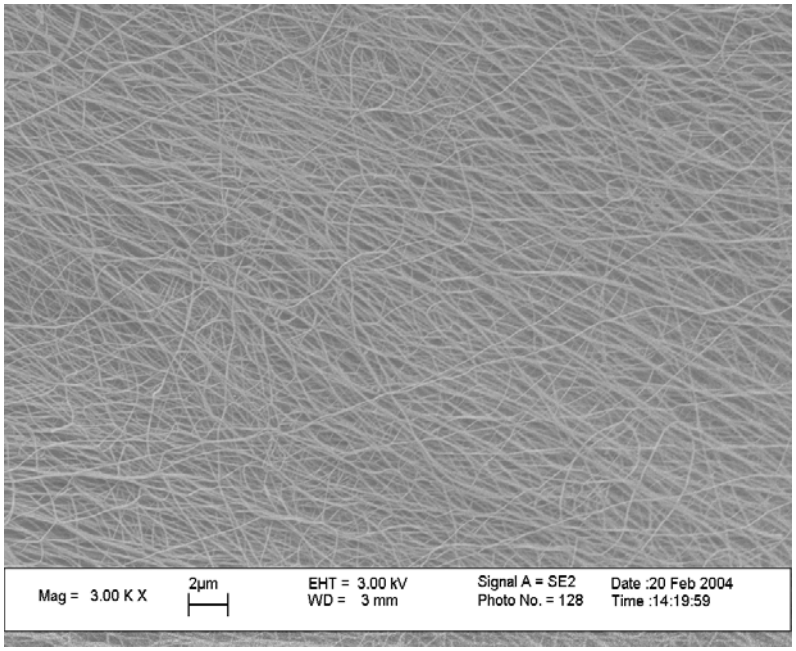

(b)

Figure 4.10 Nylon 66 fibers wound collected at 10 wt% concentration, 10 cm target distance, at a wheel speed of 1868 m/min, 40Hz ((a), (b), (c), (d), (e)). The applied voltage is 15 Kv for (a); 17.5 kv for (b); 20 kV for (c); 25 kV for (d); 30 kV for (e).

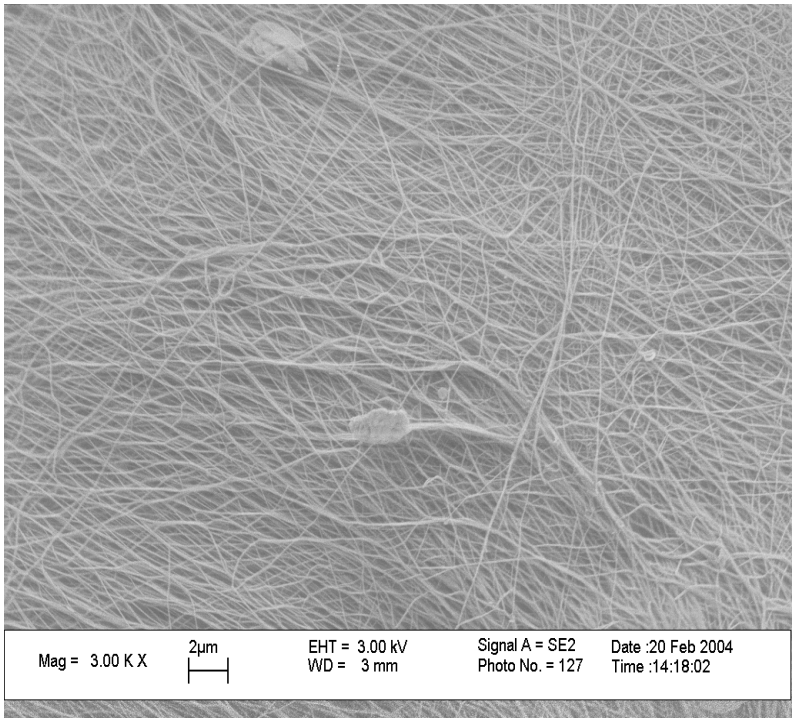

(c)

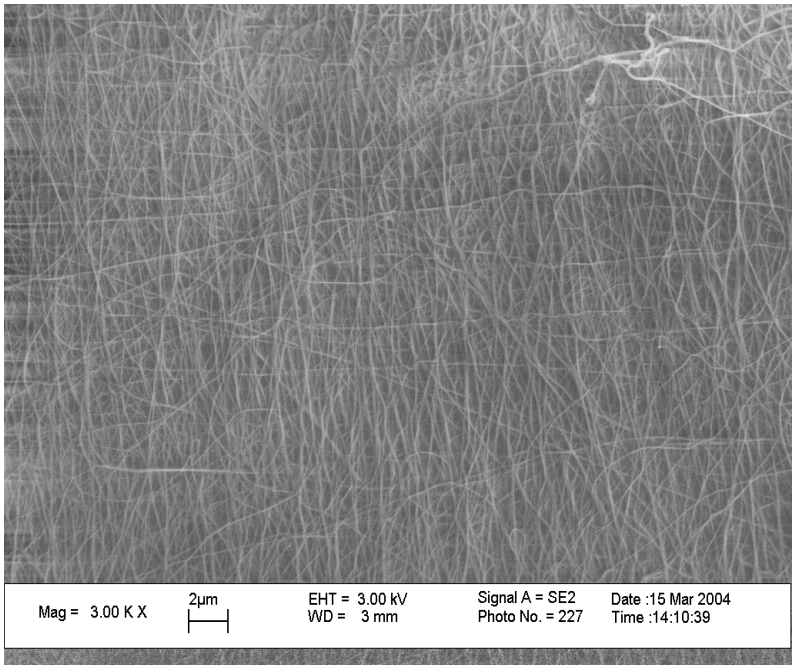

(d)

Figure 4.10 continued

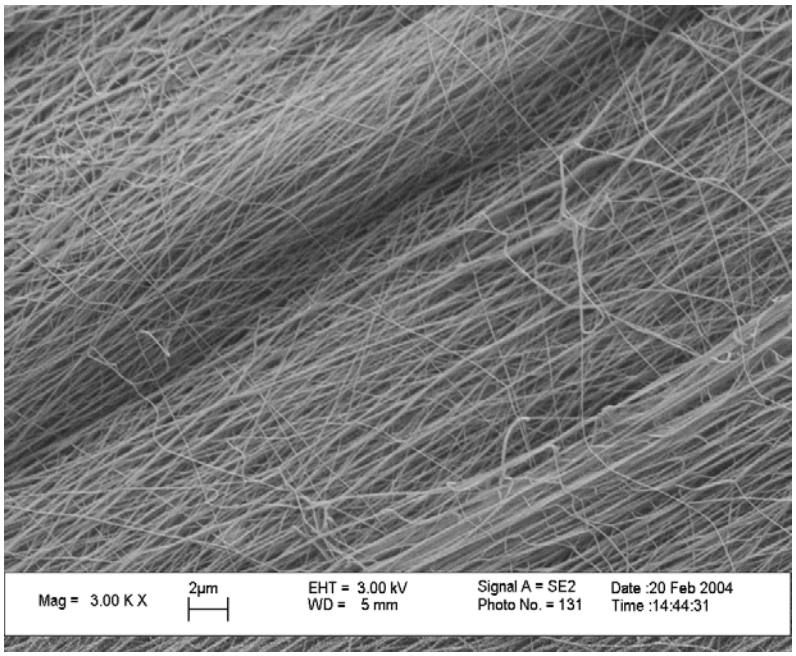

(e)

Figure 4.10 continued

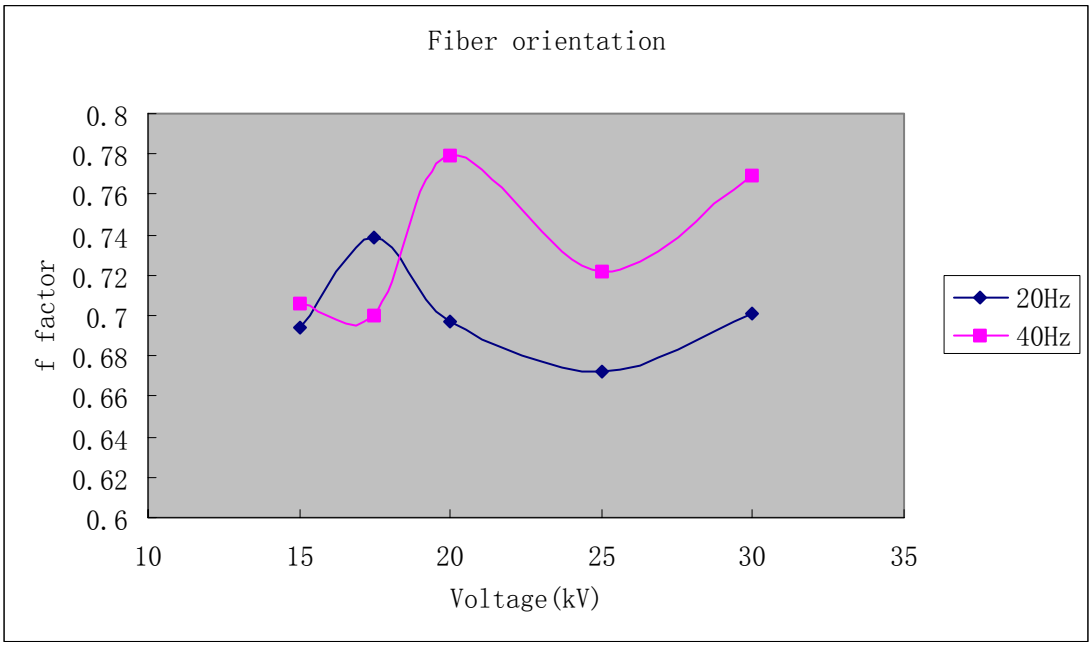

Figure 4.11 Fiber orientation factor vs. applied voltage of nanofiber mats electrospun at wheel rotation frequency of 20 Hz and 40 Hz.

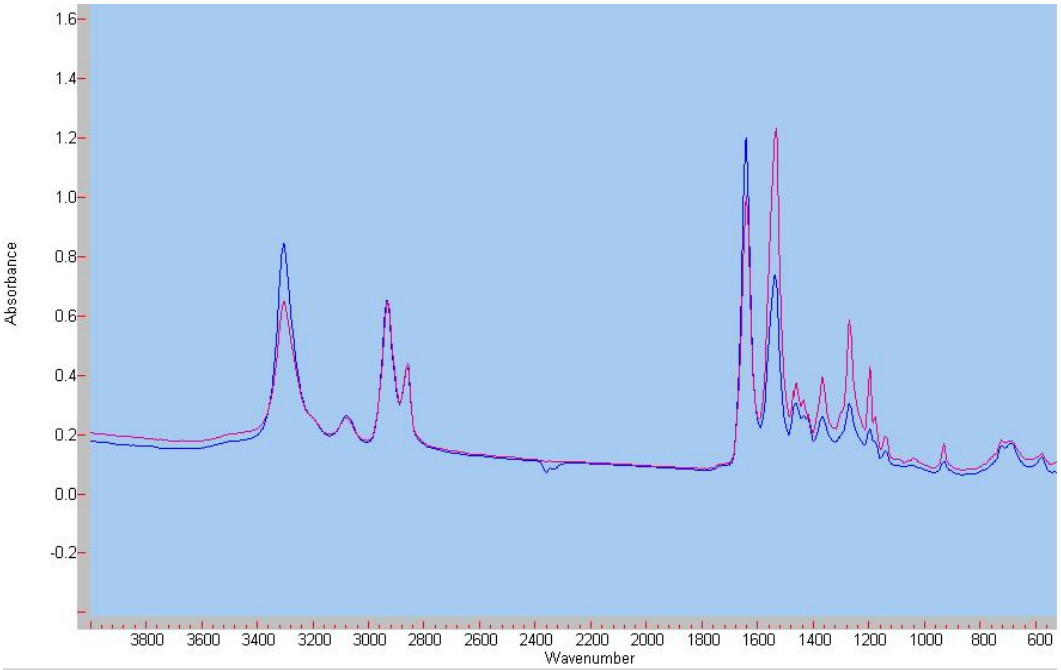

Figure 4.12 FTIR scans of nylon 66 fibers wound at 20kV and 40Hz wheel frequency with direction of IR rays parallel (red) and perpendicular (blue) to direction of winding

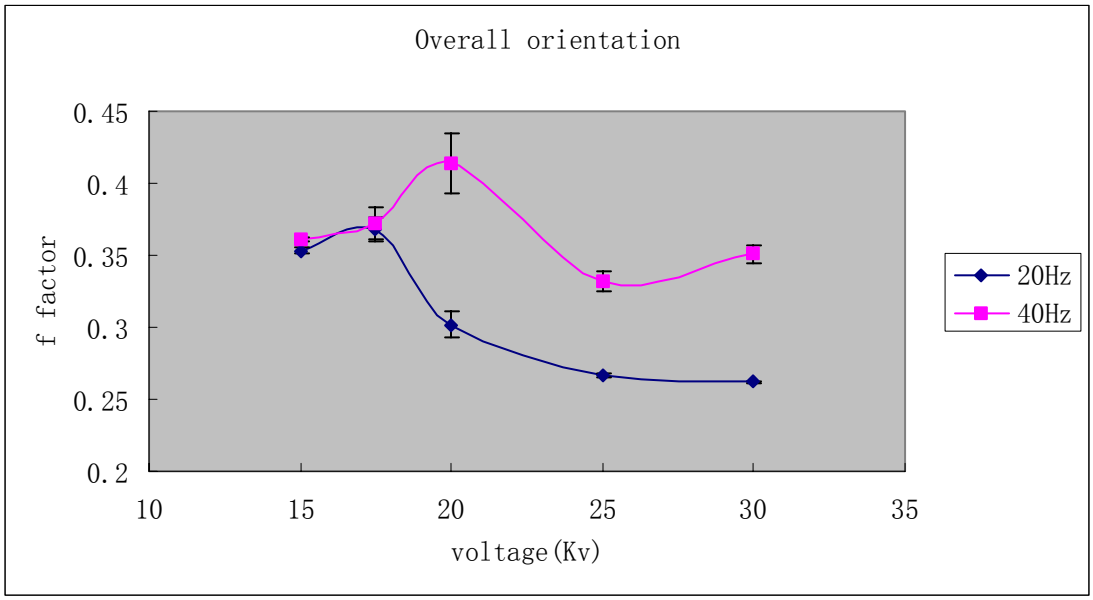

Figure 4.13 Overall orientation factor vs. applied voltage of nylon 66 nanofiber mats electrospun at wheel rotation frequency of 20 Hz and 40 Hz. Error bar is determined by standard deviation.

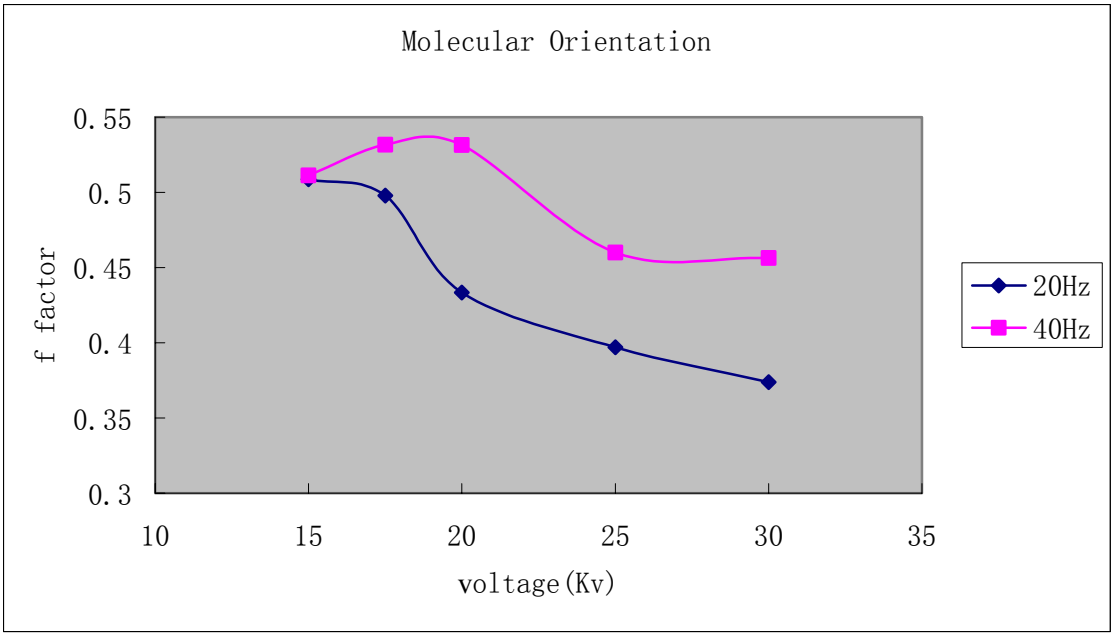

Figure 4.14 Molecular orientation factor with respect to fiber axis vs applied voltage of nylon 66 nanofiber mats electrospun at wheel rotation frequency of 20 Hz and 40 Hz.

increasing to a maximum, then decreasing and remaining nearly constant at last. The difference is in the voltage where the maximum appears. The overall orientation maximum of nanofiber mats electrospun at 20 Hz (0.36) appears at 17.5 kV and the one for 40 Hz (0.42) at 20 kV. From Figure 4.14, the molecular orientation of both rotation frequencies seems to decrease with the applied voltage. For 40 Hz nanofibers, the molecular orientation seems to plateau below 20 kV, and then a sharp decrease occurs at higher voltages. For 20 Hz nanofibers, the molecular orientation decreases in a more steady way. The molecular orientation for 40 Hz is higher than that of 20 Hz at all spinning voltages, which is in agreement with the relationship between the molecular orientation and the wheel rotation speed obtained earlier. It was found that increasing the

wheel rotating frequency, the molecular orientation would increase as is shown in Figure 4.15. [**80**]

Mechanical tests were done on these nanofibers mats electrospun at different applied voltages at 20 Hz and 40 Hz wheel rotation frequencies respectively, and the tangent modulus at 10% strain was calculated. Five repetitive tests were performed to obtain an average value as the results and standard deviation was calculated. The results are shown in Figure 4.16. The modulus of nylon 66 mats at 10% strain is plotted vs. overall orientation factor for different applied voltages in Figure 4.17.

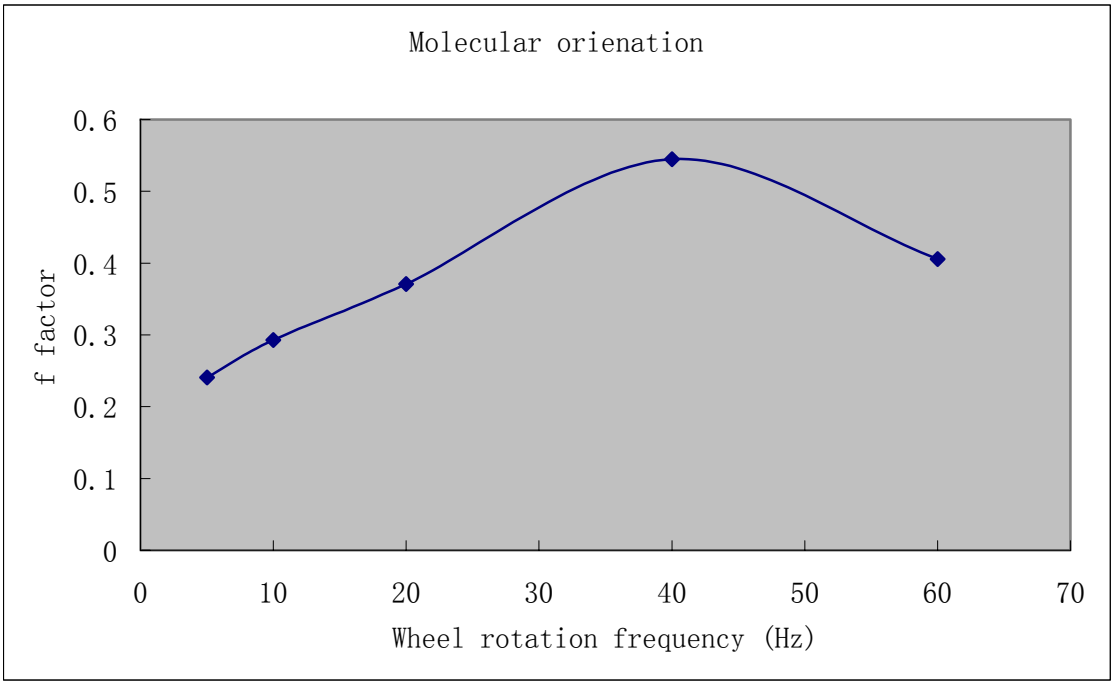

Figure 4.15 Molecular orientation factor with respect to fiber axis vs. wheel rotation frequency [**80**]

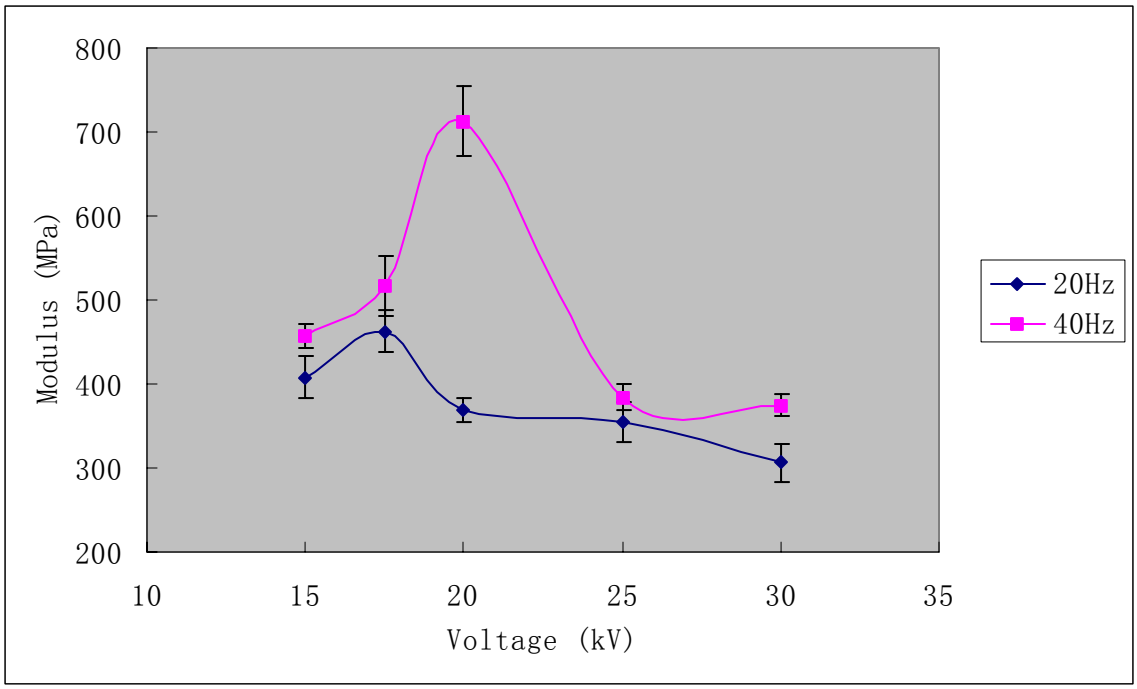

Figure 4.16 Modulus of the nylon 66 nanofiber mats at 10% strain vs. different applied voltages. Error bar is determined by standard deviation.

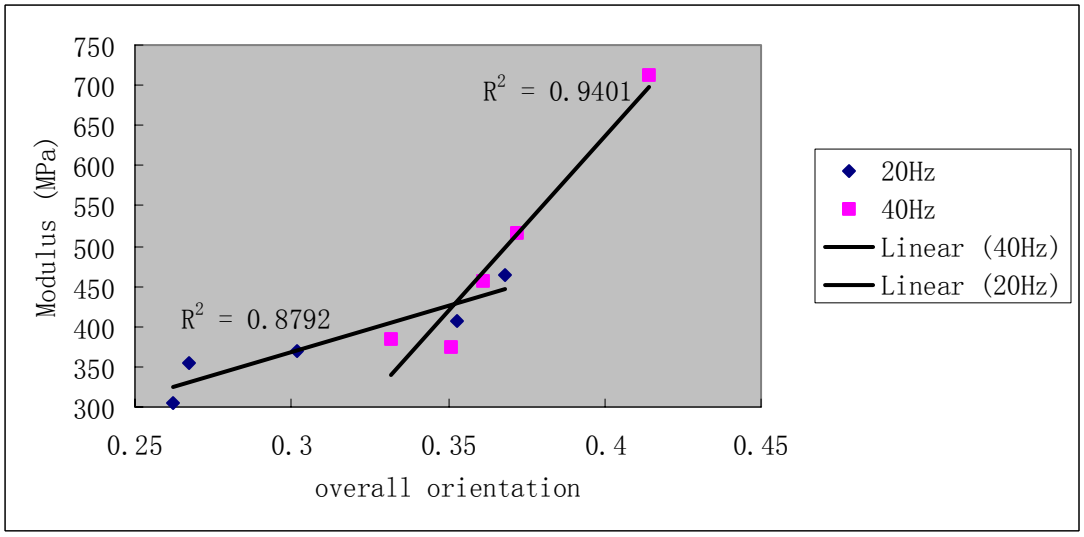

Figure 4.17 Modulus vs. overall orientation factor of the Nylon 66 nanofiber mats at 10% strain.

From Figure 4.16, the modulus changes with the increase of the applied voltage in the same fashion of overall orientation, and the modulus of the nanofiber mats electrospun at 40 Hz is larger than that of the nanofiber mats electrospun at 20 Hz. From Figure 4.17, it is clear that the modulus at 10% increases linearly with the increase of the overall orientation for both nanofiber mats electrospun at 20 Hz and 40 Hz. The slope for 40 Hz is steeper than that of 20 Hz. Thus, it is reasonable to conclude that the modulus is a strong function of overall orientation factor over different applied voltages. The data used to create Figure 4.11-Figure 4.17 are listed in Table 4.5 and Table 4.6. The standard deviations for overall orientation and modulus at 10% strain are also listed in Table 4.5 and Table 4.6.

Table 4.5 Three kinds of orientation and modulus at 10% strain for nanofibers mat electrospun at a rotating wheel frequency of 20 Hz.

Voltage (kV)	Fiber Orientation	Overall orientation	Molecular Orientation	Modulus at 10% strain (MPa)
15	0.694	0.353±0.0023	0.509	408±25.747
17.5	0.739	0.368±0.0085	0.498	463±24.352
20	0.697	0.302±0.0085	0.433	369±13.65
25	0.672	0.267±0.0014	0.397	355±24.427
30	0.700	0.262±0.001	0.374	306±21.825

Table 4.6 Three kinds of orientation and modulus at 10% strain for nanofibers mat electrospun at a rotating wheel frequency of 40 Hz.

Voltage (kV)	Fiber Orientation	Overall orientation	Molecular Orientation	Modulus at 10% strain (Mpa)
15	0.706	0.361±0.001	0.511	457±15.055
17.5	0.700	0.372±0.011	0.532	516±36.002
20	0.779	0.414±0.021	0.531	713±41.992
25	0.722	0.332±0.0064	0.460	384±15.906
30	0.769	0.351±0.0062	0.456	375±13.115

4.2.2 Effect of polymer molecular weight on the molecular orientation

In order to determine the relationship between polymer molecular weight and the molecular orientation within the nanofibers electrospun from polymer solution, PVC (Mw 215000) and a PVC blend (PVC Mw: 215000/ PVC Mw 125,000=55/45 in weight, blend Mw is 172,300 g/mol) were electrospun onto the rotating metal wheel at nominal test conditions of 10 wt% concentration, 10 cm target distance, and a constant applied voltage of 20 kV. The wheel rotation frequencies were varied over 0, 20, 40, and 60 Hz for the two PVC solutions. PVC (Mw 125,000 g/mol) was electrospun alone with the processing conditions, but the fibers had many bead defects and were not suitable for orientation study, so PVC blend was used instead. SEM pictures were taken for each

sample, and are shown in Figure 4.18 and Figure 4.19. Manual fiber angle measurements were performed on the SEM pictures, and the fiber orientations were obtained and demonstrated in Figure 4.20. FTIR dichroism measurements were also performed on those mats. The overall orientation of PVC molecules in those mats was calculated by the dichroism of C-Cl stretching at 615 and 637 $cm^{-1.}$ These two bands corresponds to the C-Cl stretching of isotactic and syndiotactic sequences respectively [**81**] and the areas of the two bands' peaks were added together to calculate dichroism. One of the FTIR scans is shown in Figure 4.21. The results of the overall orientation from dichroism are shown in Figure 4.22. Standard deviation is calculated. For both FTIR and Manual measurements, five repetitive measurements were performed to obtain an average value as the final result. Dividing orientation factor obtained by FTIR by the one obtained by manual measurement of SEM images, the molecular orientation within nanofibers was obtained and the relationships between it and the applied voltage for two rotation frequencies are demonstrated in Figure 4.23.

From Figure 4.20, the fiber orientation of the two PVC increases with the wheel rotation as nylon 66 nanofiber mats do. The fiber orientation of the PVC blend is higher than that of the PVC 215000 except when electrospun onto a stationary target.

From Figure 4.22 and Figure 4.23, it is clear that both the overall orientation and the molecular orientation within the nanofibers follow the same pattern. In both cases, the orientation of the higher molecular weight PVC is higher than that of the lower molecular

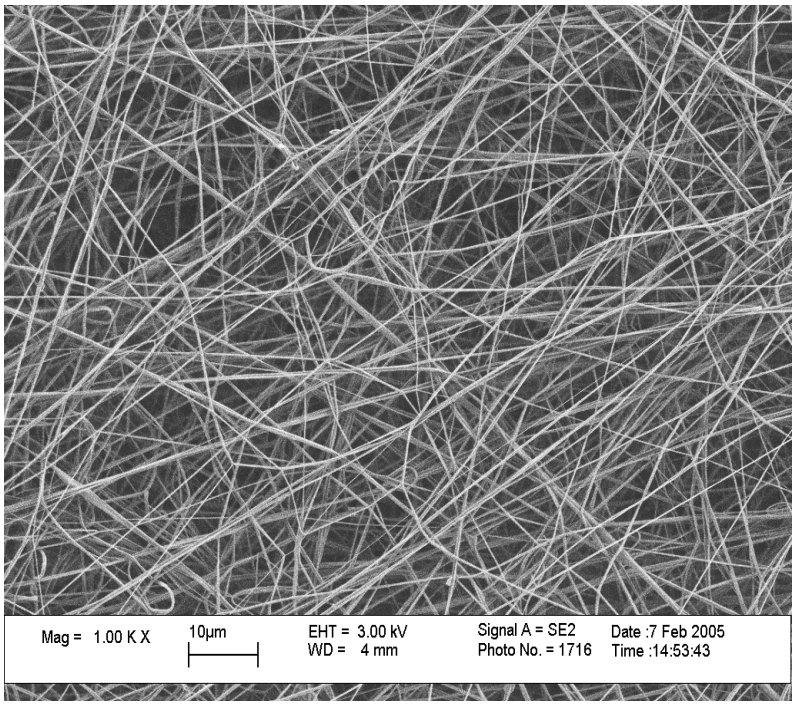

(a)

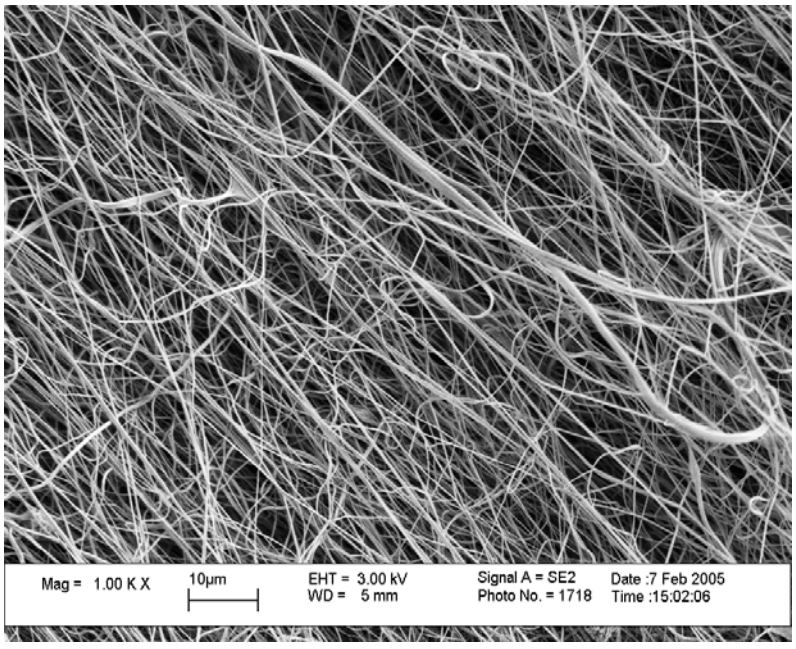

(b)

Figure 4.18 PVC 215000 fibers wound collected at 10 wt% concentration, 10 cm target distance, and 20 kV voltage at a speed of (a) 0m/min, 0Hz; (b): 926 m/min, 20Hz; (c): 1868 m/min, 40Hz and (d): 2833m/min, 60Hz

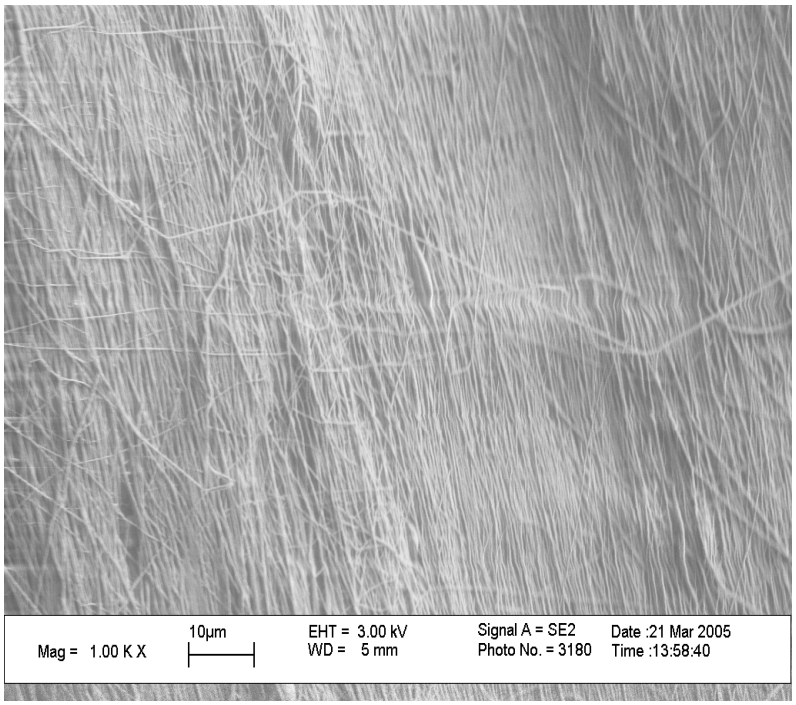

(c)

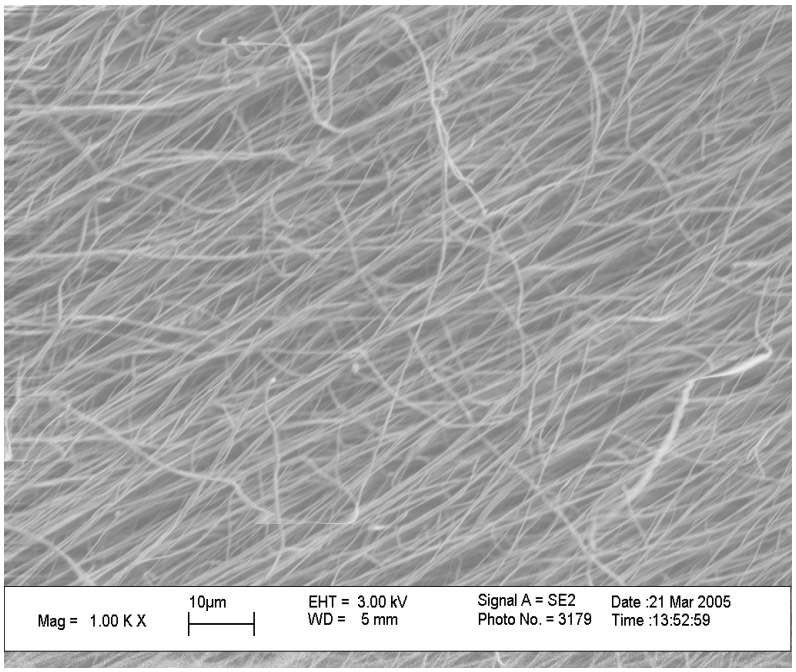

(d)

Figure 4.18 continued

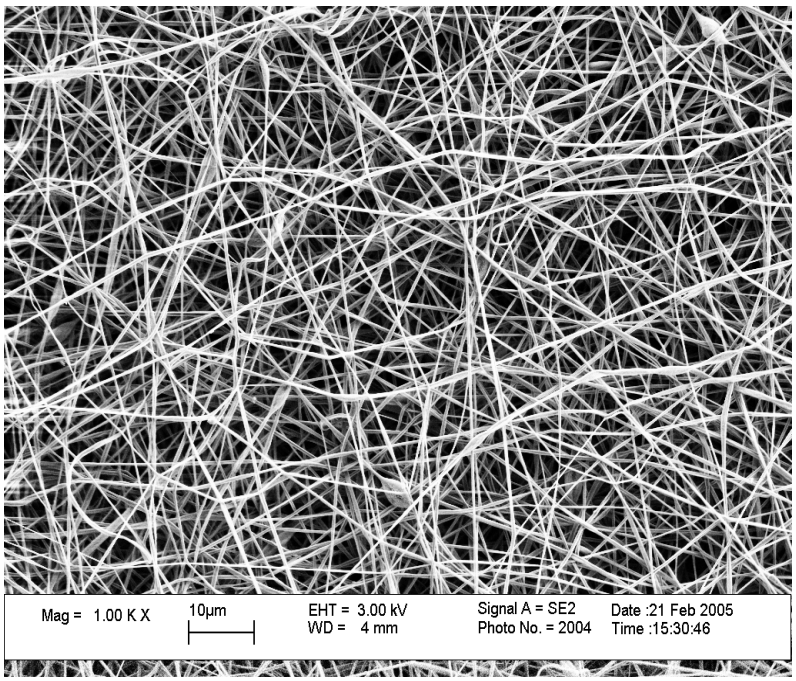

(a)

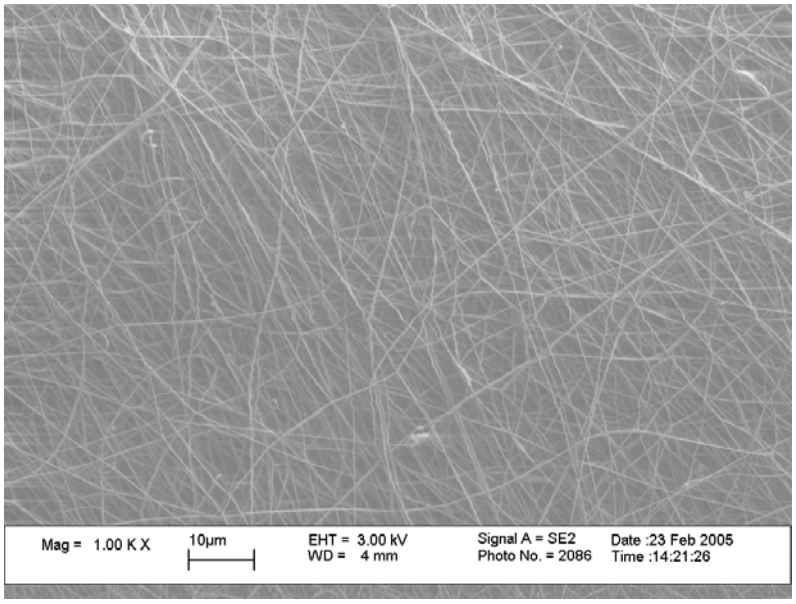

(b)

Figure 4.19 PVC blend 172300 fibers wound collected at 10 wt% concentration, 10 cm target distance, and 20 kV voltage at a speed of (a) 0m/min, 0Hz; (b): 926 m/min, 20Hz; (c): 1868 m/min, 40Hz and (d): 2833m/min, 60Hz

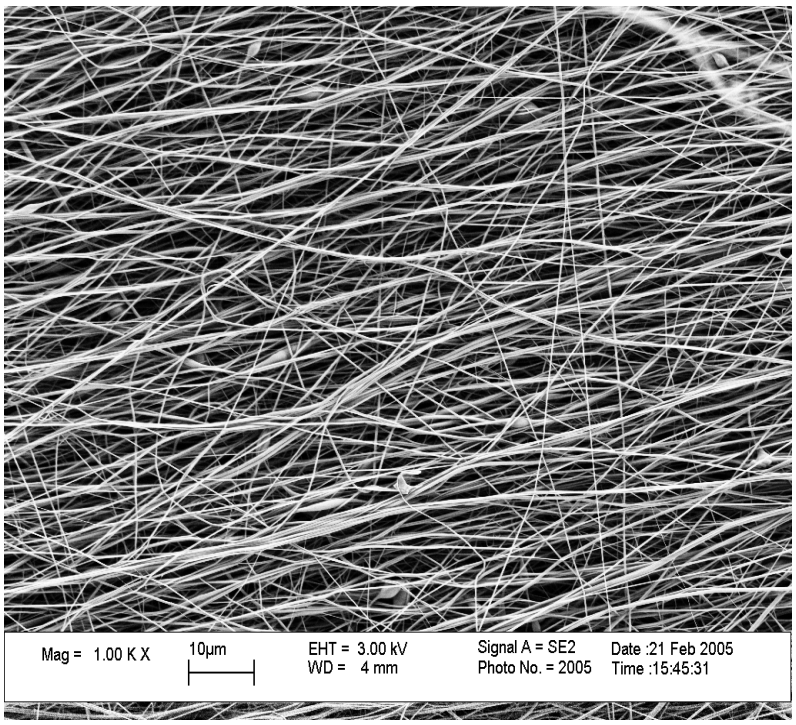

(c)

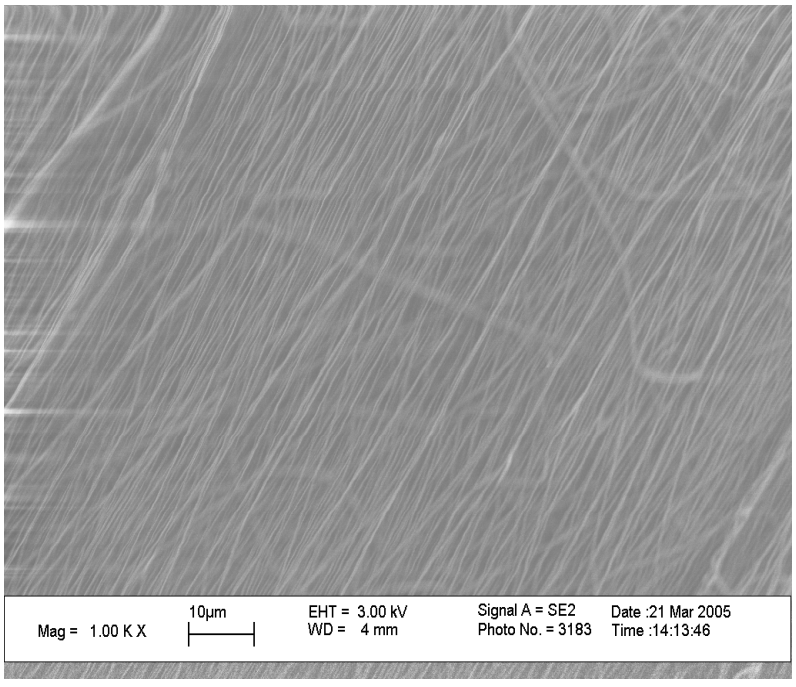

(d)

Figure 4.19 continued

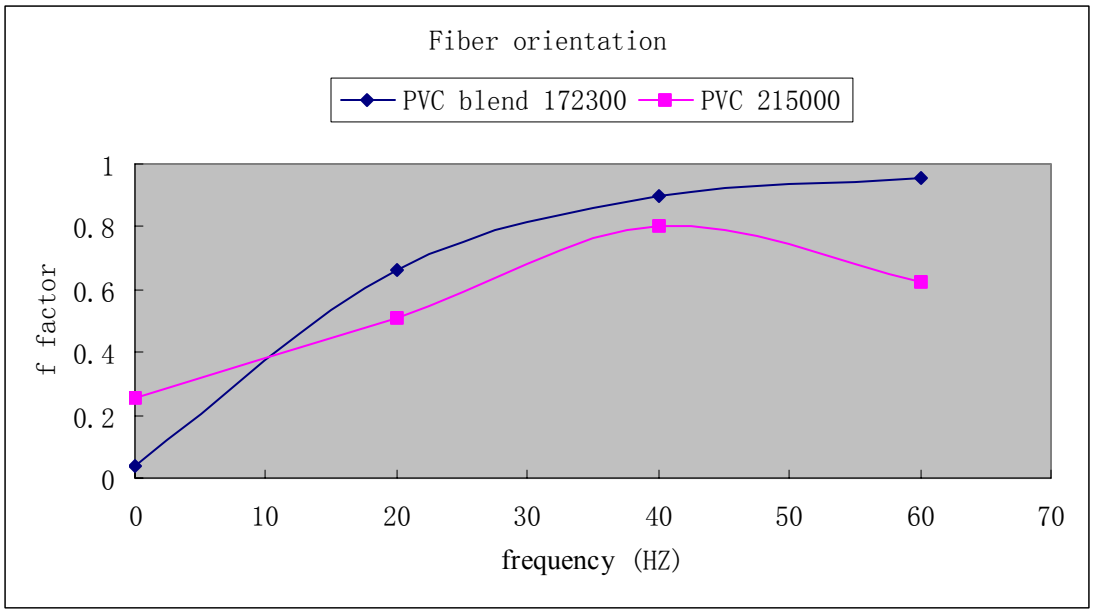

Figure 4.20 Fiber orientation factor vs. wheel speed of nanofiber mats electrospun from PVC 215000 and PVC blend 172300.

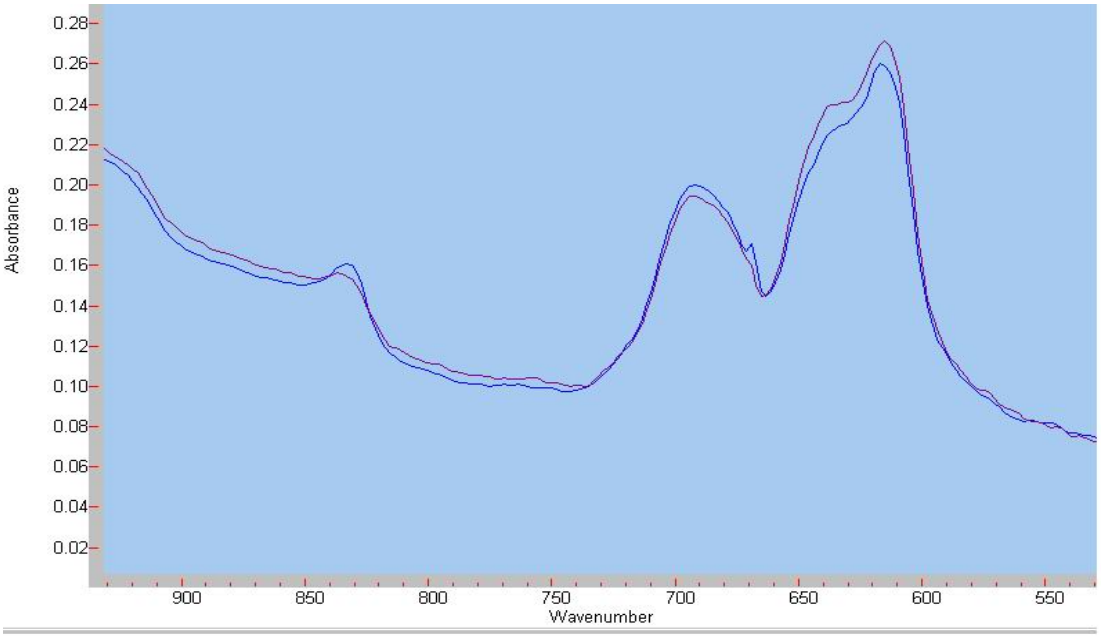

Figure 4.21 FTIR scans of PVC fibers wound at 20kV and 40 Hz with direction of IR rays parallel (blue) and perpendicular (red) to direction of winding

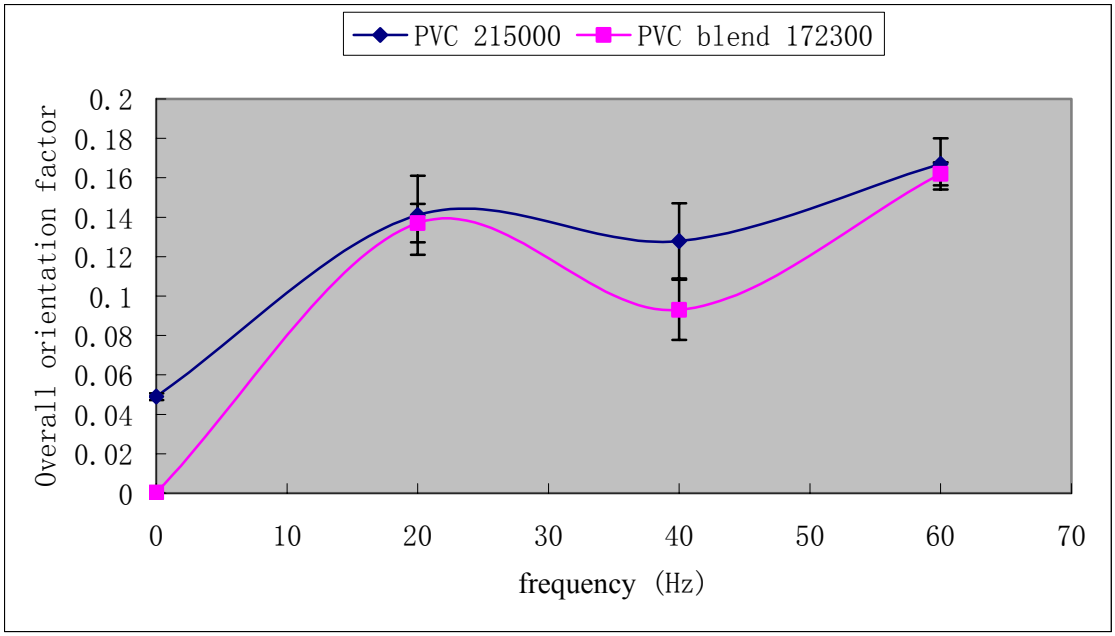

Figure 4.22 Overall orientation factor vs. wheel speed of PVC 215000 and PVC blend 172300 nanofiber mats electrospun at 20 kV. Error bar is determined by standard deviation.

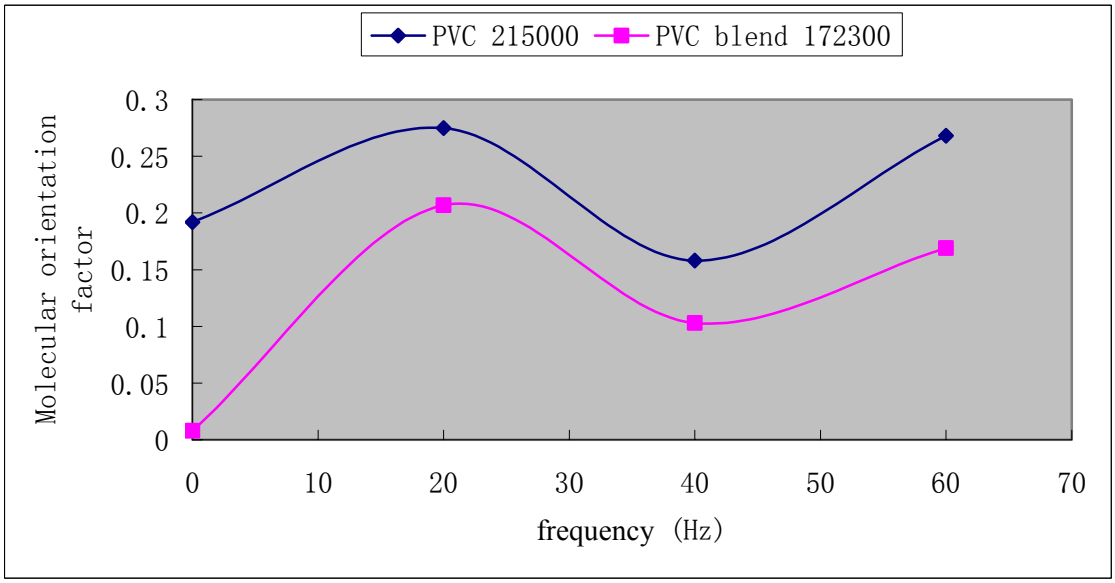

Figure 4.23 Molecular orientation factor with respect to fiber axis vs. wheel speed of PVC 215000 and PVC blend 172300 nanofiber mats electrospun at 20 kV.

weight PVC blend. However, the molecular orientation is much lower than that of the orientation of nylon 66.

Mechanical tests were done on those nanofibers mats electrospun from different molecular weight polymer solution respectively, and the tangent modulus at 10% strain was calculated. Five repetitive tests were performed to get an average value as the results. Standard deviation is calculated. The results are shown in Figure 4.24.

From Figure 4.24, it is obvious that the nanofiber mats electrospun from higher molecular PVC have higher moduli at all wheel rotation frequencies than those from the lower molecular PVC blend. The modulus of both PVC samples increase with the increase of

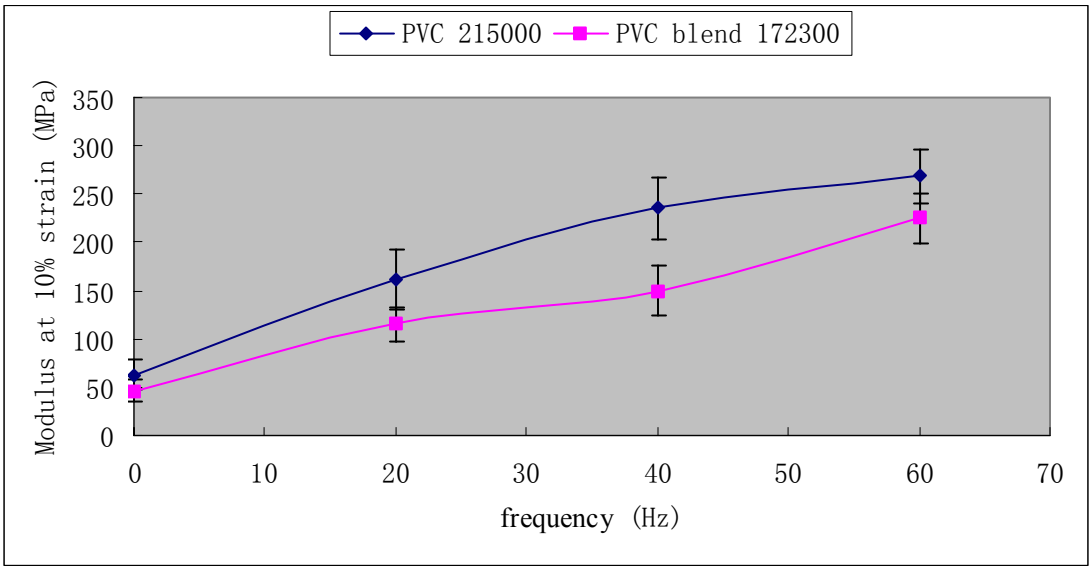

Figure 4.24 Modulus of PVC 215000 and PVC blend 172300 nanofiber mats at 10% strain electrospun at 20 kV vs. different wheel frequencies. Error bar is determined by standard deviation.

the wheel frequencies. The data used to create Figure 4.21-Figure 4.24 are listed in Table 4.7 and Table 4.8. The standard deviations for overall orientation and modulus are also illustrated in Table 4.7 and Table 4.8.

4.2.3 Discussion

The process of electrospinning is complex. When a critical voltage is reached, the charged polymer solution or melt forms cone shape pendent drop at the tip of the needle, which is called "Taylor's cone". [**26**] Once the surface tension of the polymer solution or melt is overcome by the electrical force applied, a charged jet will form from the Taylor's cone. The jets will move straight first and then due to the bending instability will bend and move in a looping and spiraling path, during which the jets elongates reducing the diameter and solvent evaporates. Ultimately, the jets hit the grounded target, solidify and

Table 4.7 Three orientation factors and modulus at 10% strain for nanofiber mats electrospun from PVC 215000.

Wheel frequency (Hz)	Fiber Orientation	Overall orientation	Molecular Orientation	Modulus at 10% strain (MPa)
0	0.257	0.049±0.002	0.192	62.9±16.07
20	0.511	0.141±0.02	0.275	161±31
40	0.806	0.128±0.019	0.158	236+32.02
60	0.625	0.167±0.013	0.268	269+28.02

Table 4.8 Three orientation factors and modulus at 10% strain for nanofiber mats electrospun from PVC blend 172300.

Wheel frequency (Hz)	Fiber Orientation	Overall orientation	Molecular Orientation	Modulus at 10% strain (MPa)
0	0.039	0.0003± 0	0.008	46.4±10.81
20	0.664	0.137±0.01	0.207	115±17.02
40	0.900	0.093±0.015	0.103	150±26.73
60	0.956	0.162±0.006	0.169	225±25.85

form nanofibers on the target. When the target is a rotating metal wheel, the situation is even more complicated. As the fiber hits the wheel surface, it is electrostatically attached to it and will draw the fiber from its spiraling path and orient along the rotation direction. Basically, three factors will work together to determine the final molecular orientation inside the nanofibers produced: electrodynamic force, mechanical tensile drawing force, and relaxation process of the molecular chain. Electrodynamic force induced by applied voltage will determine the natural velocity, which is the speed the jet travels in the spiraling path before the jet reaches the rotating wheel if other parameters like gap distance are kept constant. The natural velocity of nylon 66 electrospun at 15 kV is estimated to be 926-1868 m/min and the natural velocity of nylon 66 electrospun at 20 kV is estimated to be 1868-2833 m/min [**80**]; the mechanical tensile drawing force is

determined by the difference between the fiber natural velocity and the rotation speed of the wheel.

Increasing the voltage and keeping the rotation speed constant acts to decrease the difference between the fiber natural force and the rotation speed, thus decreasing the mechanical tensile drawing. The resulting molecular orientation will decrease as shown in Figure 4.14. However, increasing the applied voltage will increase the electrodynamic forces, which will orient the polymer chains to a degree, so the decrease of the molecular orientation with the increase of the voltage is not linear or exponential, but of a weak function. In these two cases, the relaxation behavior of the polymer are assumed to be the same, but in the case of the effect of the molecular weight, the situation is even more complicated. The relaxation behavior of the polymers is not identical. It is reasonable to assume that the higher molecular weight polymer has a longer relaxation time. Thus, the higher molecular weight polymer can preserve more obtained molecular orientation than lower molecular weight polymer. This may explain why PVC 215000 has higher molecular orientation than PVC blend 172300 shown in Figure 4.23.

The fiber orientation is determined by both the wheel rotation and the charge repulsion. The principle behind it is not clear yet. The relationship between the fiber orientation and the processing parameters does not seem obvious. It changes weakly with the increase of the voltage, but can be regarded as fairly constant since the variation is small. Further research will be carried out in the near future.

The mechanical properties of the nanofiber mats follow the same trend of the overall orientation, not just the molecular orientation within the fibers. With the increase of the applied voltage, the modulus of the mats first increases and reaches a maximum at a certain voltage, then decreases. The modulus of the mats electrospun from higher molecular weight polymer is higher than that of the mats electrospun from lower molecular weight polymer over whole rotating wheel speed range.

Chapter 5 Summary and Conclusions

Electrospinning is a straightforward method to produce polymer nanofibers. The polymers used here for electrospinning are nylon 66, polycarbonate, poly (vinyl chloride), and polycarbonate/poly (vinyl chloride) blends in different solvents.

Nanofibers of PC/PVC blend with fiber diameter ranging from 150 nm to 400 nm can be easily formed by electrospinning. The as-spun fibers demonstrate one-phase morphology that is primarily due to the kinetic factors such as rapid solvent evaporation and rapid fiber solidification. By controlled annealing of the as-spun fibers for different times, specific fiber surface morphologies can be accessed. The phase separated PC domains have an elliptical shape and have major axis lengths ranging from 38.3 nm to 120.6 nm, and minor axis lengths ranging from 20.0 nm to 66.7 nm. From this research, it is clear that electrospinning gives scientists a new way to control the morphology of polymer blends, which will be of great interests for a broad range of applications like filtration, sensors, and medicine research.

Directly electrospinning nanofibers onto a rotating metal wheel can introduce molecular orientation in the nanofibers produced. This molecular orientation with respect to fiber axis is influenced by the electrospinning process parameters. From this research, it was found that with increasing electrospinning voltage, the molecular orientation would decrease. Also by increasing the molecular weight of the polymer, the molecular

orientation will increase. Because of the high aspect ratio, large surface to volume ratio of the electrospun nanofibers and because of the orientation of those nanofibers, the oriented nonwoven nanofiber mats can find great application in composite reinforcement, tissue engineering and carbon fiber production.

5.1 Recommendations for future work

Future work, which will contribute to better understanding of the phase behavior of nanofibers electrospun from polymer blends and orientation of the electrospun nanofibers will include:

1. Annealing of PVC/PC 50/50 and 25/75 nanofiber mats and TEM observation of the phase separation behavior of those samples.
2. Better explanation of the Tg changes of PVC/PC nanofiber mats after *in situ* DMA annealing.
3. Phase behavior of the nanofiber mats electrospun from polymer blends of PVC or PC with other polymers.
4. In addition to wheel speed, applied voltage, molecular weight, the effect of other electrospinning process parameters such as gap distance, solution feed rate on the molecular orientation within the nanofibers.
5. Determination of the effect of processing parameters on the fiber orientation of the electrospun nanofiber mat.

References

References

1. A. Formhals, "Apparatus for producing artificial fibers from fiber-forming liquids by an \"electrical spinning\" method," (Alien Property Custodian). US, 1943.
2. "Artificial threads," (Schreiber-Gastell, Richard). US, 1940.
3. "Apparatus for producing artificial filaments from material such as cellulose acetate," (Schreiber-Gastell, Richard). US, 1934.
4. B. Vonnegut and R. L. Neubauer, *Production of monodisperse liquid particles by electrical atomization*, Journal of Colloid Science **7** (1952), 616-622.
5. V. G. Drozin, *The electrical dispersion of liquids as aerosols*, Journal of Colloid Science **10** (1955), 158-164.
6. H. L. Simons, "Patterned nonwoven fabrics," (Kendall Co.). Application: US, 1966, p. 8 pp.
7. P. K. Baumgarten, *Electrostatic spinning of acrylic microfibers*, Journal of Colloid and Interface Science **36** (1971), no. 1, 71-79.
8. Z.M. Huang, Y. Z. Zhang, M. Kotaki and S. Ramakrishna, *A review on polymer nanofibers by electrospinning and their applications in nanocomposites*, Composites Science and Technology **63** (2003), no. 15, 2223-2253.
9. P. W. Gibson, H. L. Schreuder-Gibson and D. Rivin, *Electrospun fiber mats: Transport properties*, AIChE Journal **45** (1999), no. 1, 190-195.
10. M. M. Bergshoef and G. J. Vancso, *Transparent nanocomposites with ultrathin, electrospun nylon-4,6 fiber reinforcement*, Advanced Materials (Weinheim, Germany) **11** (1999), no. 16, 1362-1365.
11. C. Park, Z. Ounaies, K. A. Watson, K. Pawlowski, S. E. Lowther, J. W. Connell, E. J. Siochi, J. S. Harrison and T. L. St. Clair, *Polymer-single wall carbon nanotube composites for potential spacecraft applications*, Materials Research Society Symposium Proceedings **706** (2002), no. Making Functional Materials with Nanotubes, 91-96.
12. S. J. Kwoun, R. M. Lec, B. Han and F. K. Ko, *A novel polymer nanofiber interface for chemical sensor applications*, Proceedings of the 2000 IEEE/EIA

International Frequency Control Symposium & Exhibition, Kansas City, MO, United States, June 7-9, 2000 (2000), 52-57.

13. X. Wang, C. Drew, S.-H. Lee, K. J. Senecal, J. Kumar and L. A. Samuelson, *Electrospun nanofibrous membranes for highly sensitive optical sensors*, Nano Letters **2** (2002), no. 11, 1273-1275.
14. S.H. Lee, B.-C. Ku, X. Wang, L. A. Samuelson and J. Kumar, *Design, synthesis and electrospinning of a novel fluorescent polymer for optical sensor applications*, Materials Research Society Symposium Proceedings **708** (2002), no. Organic Optoelectronic Materials, Processing and Devices, 403-408.
15. X. Wang, S.-H. Lee, C. Drew, K. J. Senecal, J. Kumar and L. A. Samuelson, *Highly sensitive optical sensors using electrospun polymeric nanofibrous membranes*, Materials Research Society Symposium Proceedings **708** (2002), no. Organic Optoelectronic Materials, Processing and Devices, 397-402.
16. K. J. Senecal, D. P. Ziegler, J. He, R. Mosurkal, H. Schreuder-Gibson and L. A. Samuelson, *Photoelectric response from nanofibrous membranes*, Materials Research Society Symposium Proceedings **708** (2002), no. Organic Optoelectronic Materials, Processing and Devices, 285-289.
17. M. M. Hohman, M. Shin, G. Rutledge and M. P. Brenner, *Electrospinning and electrically forced jets. Ii. Applications*, Physics of Fluids **13** (2001), no. 8, 2221-2236.
18. D. Groitzsch and E. Fahrbach, "Microporous multilayer fabric for medical use and its manufacture," (Freudenberg, Carl, K.-G., Fed. Rep. Ger.). Application: DE, 1986, p. 30 pp.
19. T. V. How and R. M. Clarke, "Artificial vascular grafts," (Johnson and Johnson, USA). Application: BR, 1984, p. 26 pp.
20. G. E. Martin, I. D. Cockshott and F. J. Fildes, "Wound dressing," (Imperial Chemical Industries Ltd., UK). Application: GB, 1978, p. 7 pp.
21. E.R. Kenawy, G. L. Bowlin, K. Mansfield, J. Layman, D. G. Simpson, E. H. Sanders and G. E. Wnek, *Release of tetracycline hydrochloride from electrospun*

poly(ethylene-co-vinylacetate), poly(lactic acid), and a blend, Journal of Controlled Release **81** (2002), no. 1-2, 57-64.

22. C. S. Keyur Desai, *Electrospinning and phase characterization of polyaniline/poly methyl methacrylate blends*, Polymer Preprints **44** (2003), no. 2, 112-113.
23. M. Wei, J. Mead and C. Sung, *Phase morphology of electrospun nanofibers from polybutadiene (pb) /polycarbonate (pc) blends*, Polymer Preprints (American Chemical Society, Division of Polymer Chemistry) **44** (2003), no. 2, 79-80.
24. M. Bognitzki, T. Frese, M. Steinhart, A. Greiner, J. H. Wendorff, A. Schaper and M. Hellwig, *Preparation of fibers with nanoscaled morphologies: Electrospinning of polymer blends*, Polymer Engineering and Science **41** (2001), no. 6, 982-989.
25. T. GI., *Electrically driven jets.*, Proc R Soc London,Ser A **313** (1969), 453-475.
26. G. I. M. Taylor, A.D., *The stability of a horizontal fluid interface in a vertical electric field*, Journal of Fluid Mechanics **22** (1965).
27. J. M. Deitzel, J. D. Kleinmeyer, J. K. Hirvonen and N. C. Beck Tan, *Controlled deposition of electrospun poly(ethylene oxide) fibers*, Polymer **42** (2001), no. 19, 8163-8170.
28. L. Larrondo and R. St. John Manley, *Electrostatic fiber spinning from polymer melts. Iii. Electrostatic deformation of a pendant drop of polymer melt*, Journal of Polymer Science, Polymer Physics Edition **19** (1981), no. 6, 933-940.
29. *Electrostatic fiber spinning from polymer melts. Ii. Examination of the flow field in an electrically driven jet*, Journal of Polymer Science, Polymer Physics Edition **19** (1981), no. 6, 921-932.
30. *Electrostatic fiber spinning from polymer melts. I. Experimental observations on fiber formation and properties*, Journal of Polymer Science, Polymer Physics Edition **19** (1981), no. 6, 909-920.
31. H. L. Schreuder-Gibson, Gibson P, Senecal K, Sennett M, Walker J, Yeomans W, et al., *Protective textile materials based on electrospun nanofibers*, Journal of Advanced Materials **34** (2002), no. 3, 44-55.

32. S. C. Krishnappa RVN, Schreuder-Gibson H., *Electrospinning of polycarbonates and their surface characterization using the sem and tem*, Mat Soc Symp Proc **702** (2002), U6.7.1-0U6.7.6.

33. S.G. H. Tasaia PP, Gibson P., *Different electrostatic methods for making electret filters*, Journal of Electrostatics **54** (2002), 333-341.

34. M. Bognitzki, H. Hou, M. Ishaque, T. Frese, M. Hellwig, C. Schwarte, A. Schaper, J. H. Wendorff and A. Greiner, *Polymer, metal, and hybrid nano- and mesotubes by coating degradable polymer template fibers (tuft process)*, Advanced Materials (Weinheim, Germany) **12** (2000), no. 9, 637-640.

35. S. Megelski, J. S. Stephens, D. B. Chase and J. F. Rabolt, *Micro- and nanostructure surface morphology on electrospun polymer fibers*, Macromolecules **35** (2002), no. 22, 8456-8466.

36. K. H. Lee, H. Y. Kim, Y. M. La, D. R. Lee and N. H. Sung, *Influence of a mixing solvent with tetrahydrofuran and n,n-dimethylformamide on electrospun poly(vinyl chloride) nonwoven mats*, Journal of Polymer Science, Part B: Polymer Physics **40** (2002), no. 19, 2259-2268.

37. R. D. Rangkupan R., *Electrospinning from a polymer melt in a vacuum*, arch Meeting (2000), L36. 059.

38. *Development of electrospinning from molten polymers in vacuum, book of abstracts*, New frontiers in fiber science, Spring Meeting (2001).

39. J.S. Kim and D. S. Lee, *Thermal properties of electrospun polyesters*, Polymer Journal (Tokyo) **32** (2000), no. 7, 616-618.

40. J. Doshi and D. H. Reneker, *Electrospinning process and applications of electrospun fibers*, Journal of Electrostatics **35** (1995), no. 2&3, 151-160.

41. H. Fong, I. Chun and D. H. Reneker, *Beaded nanofibers formed during electrospinning*, Polymer **40** (1999), no. 16, 4585-4592.

42. H. Liu and Y.L. Hsieh, *Ultrafine fibrous cellulose membranes from electrospinning of cellulose acetate*, Journal of Polymer Science, Part B: Polymer Physics **40** (2002), no. 18, 2119-2129.

43. J. M. Deitzel, Kleinmeyer J, Harris D, Tan NCB, *The effect of processing variables on the morphology of electrospun nanofibers and textiles*, Polymer **42** (2001), no. 261-72.

44. M. M. Demir, I. Yilgor, E. Yilgor and B. Erman, *Electrospinning of polyurethane fibers*, Polymer **43** (2002), no. 11, 3303-3309.

45. H. Fong and D. H. Reneker, *Elastomeric nanofibers of styrene-butadiene-styrene triblock copolymer*, Journal of Polymer Science, Part B: Polymer Physics **37** (1999), no. 24, 3488-3493.

46. Y. A. Zussman E, Weiths D., *A micro-aerodynamic decelerator based on permeable surfaces of nanofiber mats*, Experiments in Fluids **33** (2002), 315-320.

47. N. Kattamuri, J. H. Shin, S. E. Park, J. K. Lee and C. Sung, *Doe optimization and tem of polycarbonate nanofibers*, Polymer Preprints (American Chemical Society, Division of Polymer Chemistry) **44** (2003), no. 2, 84-85.

48. I. C. Um, D. Fang, B. S. Hsiao, A. Okamoto and B. Chu, *Electro-spinning and electro-blowing of hyaluronic acid*, Biomacromolecules **5** (2004), no. 4, 1428-1436.

49. C. L. Casper, J. S. Stephens, N. G. Tassi, D. B. Chase and J. F. Rabolt, *Controlling surface morphology of electrospun polystyrene fibers: Effect of humidity and molecular weight in the electrospinning process*, Macromolecules **37** (2004), no. 2, 573-578.

50. P. Gupta and G. L. Wilkes, *Bicomponent fiber electrospinning and the effect of porosity on surface wettability of electrospun mats*, Abstracts of Papers, 226th ACS National Meeting, New York, NY, United States, September 7-11, 2003 (2003), POLY-497.

51. E. H. Sanders, R. Kloefkorn, G. L. Bowlin, D. G. Simpson and G. E. Wnek, *Two-phase electrospinning from a single electrified jet: Microencapsulation of aqueous reservoirs in poly(ethylene-co-vinyl acetate) fibers*, Macromolecules **36** (2003), no. 11, 3803-3805.

52. D. Delimoy, C. Bailly, J. Devaux and R. Legras, *Morphological studies of polycarbonate-poly(butylene terephthalate) blends by transmission electron microscopy*, Polymer Engineering and Science **28** (1988), no. 2, 104-112.

53. K. H. Lee, H. Y. Kim, Y. J. Ryu, K. W. Kim and S. W. Choi, *Mechanical behavior of electro spun fiber mats of poly(vinyl chloride)/polyurethane polyblends*, Journal of Polymer Science, Part B: Polymer Physics **41** (2003), no. 11, 1256-1262.

54. Y.L. H. Yuhong Wang, *Enzyme immobilization via electrospinning of polymer/enzyme blends*, Polymer Preprints **44** (2003), no. 1, 1212-1213.

55. K. H. Lee, H. Kim, K. Kim, C. Kim, W. Kim and S. Pyo, *Mechanical behaviors of electrospun polyblend nonwoven mats through multi-spinneret*, Abstracts of Papers, 228th ACS National Meeting, Philadelphia, PA, United States, August 22-26, 2004 (2004), PMSE-420.

56. B. A., "Production of electrostatically spun products," vol. 4689186, US, 1987.

57. B. JP, U. patent (Editor), vol. 4965110, US, 1990.

58. J. A. Matthews, G. E. Wnek, D. G. Simpson and G. L. Bowlin, *Electrospinning of collagen nanofibers*, Biomacromolecules **3** (2002), no. 2, 232-238.

59. E. D. Boland, G. E. Wnek, D. G. Simpson, K. J. Pawlowski and G. L. Bowlin, *Tailoring tissue engineering scaffolds using electrostatic processing techniques: A study of poly(glycolic acid) electrospinning*, Journal of Macromolecular Science, Pure and Applied Chemistry **A38** (2001), no. 12, 1231-1243.

60. E. Z. A Theron, A L Yarin, *Electrostatic field-assisted alignment of electrospun nanofibres*, Nanotechnology **12** (2001), 384-390.

61. *The temperature dependence of relaxation*, (1955).

62. J. J. Ge, H. Hou, Q. Li, M. J. Graham, A. Greiner, D. H. Reneker, F. W. Harris and S. Z. D. Cheng, *Assembly of well-aligned multiwalled carbon nanotubes in confined polyacrylonitrile environments: Electrospun composite nanofiber sheets*, Journal of the American Chemical Society **126** (2004), no. 48, 15754-15761.

63. J. Kameoka and H. G. Craighead, *Fabrication of oriented polymeric nanofibers on planar surfaces by electrospinning*, Applied Physics Letters **83** (2003), no. 2, 371-373.

64. F. Yang, R. Murugan, S. Wang and S. Ramakrishna, *Electrospinning of nano/micro scale poly(l-lactic acid) aligned fibers and their potential in neural tissue engineering*, Biomaterials **26** (2005), no. 15, 2603-2610.

65. C. Y. Xu, R. Inai, M. Kotaki and S. Ramakrishna, *Aligned biodegradable nanofibrous structure: A potential scaffold for blood vessel engineering*, Biomaterials **25** (2004), no. 5, 877-886.

66. W. Salalha, Y. Dror, R. L. Khalfin, Y. Cohen, A. L. Yarin and E. Zussman, *Single-walled carbon nanotubes embedded in oriented polymeric nanofibers by electrospinning*, Langmuir **20** (2004), no. 22, 9852-9855.

67. S. F. Fennessey and R. J. Farris, *Fabrication of aligned and molecularly oriented electrospun polyacrylonitrile nanofibers and the mechanical behavior of their twisted yarns*, Polymer **45** (2004), no. 12, 4217-4225.

68. R. Dersch, T. Liu, A. K. Schaper, A. Greiner and J. H. Wendorff, *Electro-spun nano-fibers: Internal structure and intrinsic orientation*, Journal of Polymer Science, Part A: Polymer Chemistry **41** (2003), no. 4, 545-553.

69. B. A. Warner SB, Grimler M, Ugbolue SC, Rutledge GC, Shin MY, *A fundamental investigation of the formation and properties of electrospun fibers*, 1999 Annual Report (M98-D01), National Textile Center (1999).

70. G. L. Wilkes, *Measurement of molecular orientation in polymeric solids*, Fortschritte der Hochpolymeren-Forschung **8** (1971), 91-136.

71. S. Y. Hobbs, M. E. J. Dekkers and V. H. Watkins, *Toughened blends of poly(butylene terephthalate) and bpa polycarbonate. Part 1. Morphology*, Journal of Materials Science **23** (1988), no. 4, 1219-1224.

72. J. S. Trent, P. R. Couchman and J. I. Scheinbeim, *Transmission electron microscope studies of polymers stained with ruthenium and osmium tetroxide*, Polymer Science and Technology (Plenum) **22** (1983), no. Struct.-Prop. Relat. Polym. Solids, 205-213.

73. M. L. Williams, R. F. Landel and J. D. Ferry, *The temperature dependence of relaxation mechanisms in amorphous polymers and other glass-forming liquids*, Journal of the American Chemical Society **77** (1955), 3701-3707.

74. K. Desai and C. Sung, *Electrospinning and phase characterization of polyaniline/polymethyl methacrylate blends*, Polymer Preprints (American Chemical Society, Division of Polymer Chemistry) **44** (2003), no. 2, 112-113.

75. C. Kim and K. S. Yang, *Electrochemical properties of carbon nanofiber web as an electrode for supercapacitor prepared by electrospinning*, Applied Physics Letters **83** (2003), no. 6, 1216-1218.

76. P. Katta, M. Alessandro, R. D. Ramsier and G. G. Chase, *Continuous electrospinning of aligned polymer nanofibers onto a wire drum collector*, Nano Letters **4** (2004), no. 11, 2215-2218.

77. N. Vasanthan, S. B. Ruetsch and D. R. Salem, *Structure development of polyamide-66 fibers during drawing and their microstructure characterization*, Journal of Polymer Science, Part B: Polymer Physics **40** (2002), no. 17, 1940-1948.

78. L. C. Li WJ, Caterson EJ, Tuan TS, Ko FK, *Electrospun nanofibrous structure: A novel scaffold for tissue engineering.*, J Biomed Mater Res **60** (2002), no. 4, 613-621.

79. L. Huang, K. Nagapudi, R. P. Apkarian and E. L. Chaikof, *Engineered collagen-peo nanofibers and fabrics*, Journal of Biomaterials Science, Polymer Edition **12** (2001), no. 9, 979-993.

80. S. Jagannathan, "Process-structure-property relationships of electrospun nano fibers," *The university of Tennessee, Knoxville*, August 2003.

81. N. G. a. J.l. Millan, *Irreversibility of stretching-induced local conformational changes as verified through an ftir dichroism study for pvc*, Polym Int **48** (1999), 1108-1112.

VITA

Feng, Kai was born in Shanghai, China on 10th December 1980 to Feng, Guoren and Yao, Yuanyong. He received his Bachelor degree of Science in Macromolecular Science and Engineering from Fudan University, Shanghai, China in the year 2003. He joined the Polymer Engineering program in Department of Material Science and Engineering at University of Tennessee, Knoxville in August 2003 and received the degree of Masters of Science in August 2005.